


# Recent Advances in Nanozymes for Bacteria-Infected Wound Therapy

Fayin Mo<sup>1,2</sup>, Minjun Zhang<sup>1</sup>, Xuewei Duan<sup>1</sup>, Chuyan Lin<sup>1</sup>, Duanping Sun<sup>1,2,3</sup> , Tianhui You<sup>1</sup>

<sup>1</sup>School of Nursing, Guangdong Provincial Key Laboratory of Pharmaceutical Bioactive Substances, Guangdong Pharmaceutical University, Guangzhou, People's Republic of China; <sup>2</sup>Center for Drug Research and Development, Guangdong Provincial Key Laboratory of Pharmaceutical Bioactive Substances, Guangdong Pharmaceutical University, Guangzhou, People's Republic of China; <sup>3</sup>Key Specialty of Clinical Pharmacy, The First Affiliated Hospital of Guangdong Pharmaceutical University, Guangzhou, People's Republic of China

Correspondence: Duanping Sun; Tianhui You, Email [sundp@gdpu.edu.cn](mailto:sundp@gdpu.edu.cn); [youth888cn@aliyun.com](mailto:youth888cn@aliyun.com)

**Abstract:** Bacterial-infected wounds are a serious threat to public health. Bacterial invasion can easily delay the wound healing process and even cause more serious damage. Therefore, effective new methods or drugs are needed to treat wounds. Nanozyme is an artificial enzyme that mimics the activity of a natural enzyme, and a substitute for natural enzymes by mimicking the coordination environment of the catalytic site. Due to the numerous excellent properties of nanozymes, the generation of drug-resistant bacteria can be avoided while treating bacterial infection wounds by catalyzing the sterilization mechanism of generating reactive oxygen species (ROS). Notably, there are still some defects in the nanozyme antibacterial agents, and the design direction is to realize the multifunctionalization and intelligence of a single system. In this review, we first discuss the pathophysiology of bacteria infected wound healing, the formation of bacterial infection wounds, and the strategies for treating bacterially infected wounds. In addition, the antibacterial advantages and mechanism of nanozymes for bacteria-infected wounds are also described. Importantly, a series of nanomaterials based on nanozyme synthesis for the treatment of infected wounds are emphasized. Finally, the challenges and prospects of nanozymes for treating bacterial infection wounds are proposed for future research in this field.

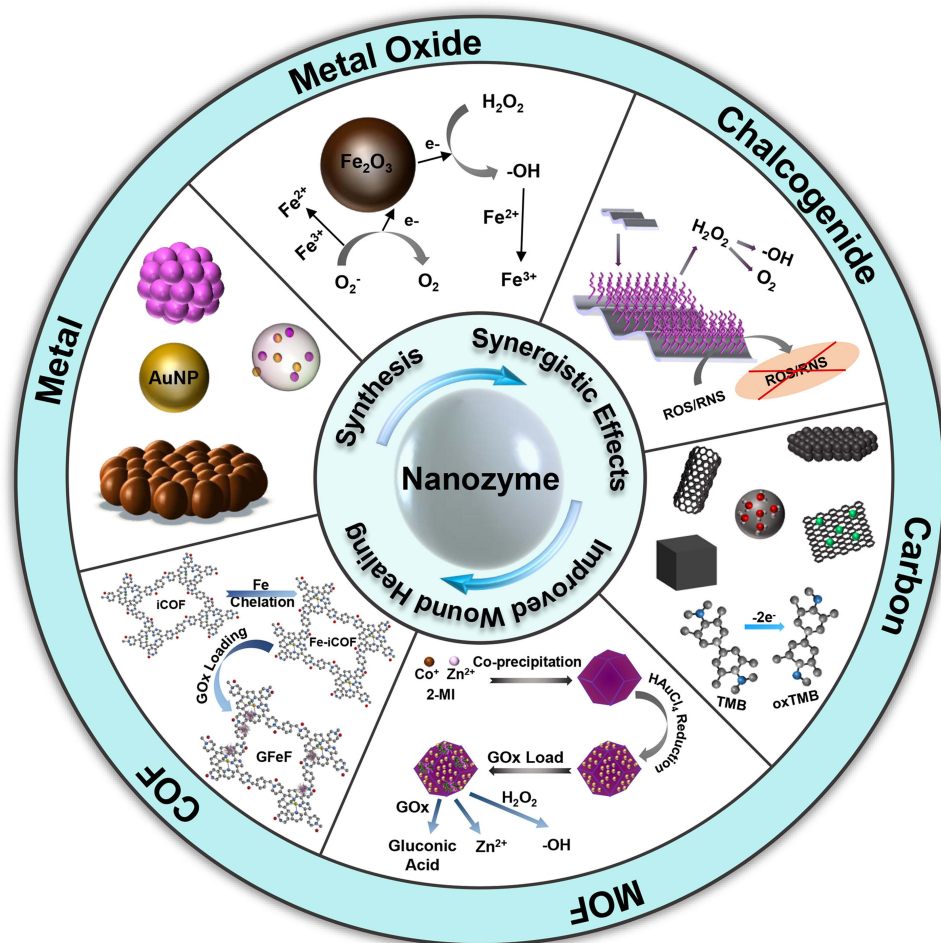
**Keywords:** nanozyme, wound healing, bacterial infections, antibacterial, antibiofilms

## Introduction

Bacteria exist in all corners of the human skin and do not cause infection under normal circumstances. When the skin and mucous barriers are damaged, they invade, grow, reproduce and secrete toxins, which gradually leads to the formation of acute/chronic infectious wounds with the passage of healing time.<sup>1-3</sup> Wound healing is one of the most important biological processes in the human body, and naturally restores the structural integrity of the skin through granulation tissue proliferation and the formation of scar tissue when exposed to external injuries such as cuts, lacerations, and stab wounds.<sup>4,5</sup> It is usually divided into acute trauma and chronic trauma based on recovery time. Acute wounds can complete the repair of anatomical and functional tissues within three weeks, while the healing time of chronic wounds is extended to three months after the formation of the wound. Bacterial infection is one of the important reasons for the formation of chronic wounds.<sup>6,7</sup> All organs and tissues of the body may be infected by bacteria, which can manifest as inflammation,<sup>8</sup> sepsis,<sup>9</sup> etc. In addition, chronic wounds in the form of diabetic ulcers, pressure, and vascular ulcers are common in clinical practice, and they always face the possibility of infectious complications.<sup>10,11</sup> Until the discovery and popularization of antibiotics known as bacterial infection terminating factors, the trend of bacterial infections was effectively controlled.<sup>12,13</sup>

However, decades of overuse and misuse of antibiotics have altered the genes of bacteria, leading to the emergence of drug-resistant strains and even multidrug resistance.<sup>14</sup> Moreover, when bacteria aggregate into biofilms, they acquire drug resistance approximately 10–1000 times that of the corresponding free bacteria due to the protective effect of extracellular polymers, which constitute the main component of biofilms.<sup>15</sup> Currently, approximately 700,000 people die each year due to drug-resistant bacterial infections, and this number is expected to rise to 10 million by 2050, with a resource cost of 100 trillion dollars.<sup>16</sup> Therefore, there is an urgent need to develop new antibacterial agents to address the growing problem of bacterial infections. The

## Graphical Abstract



development of nanotechnology has brought feasible ways for this. Most of the various nanoplateforms that have been developed at present show certain bactericidal properties, but they also have limitations such as a narrow antibacterial spectrum, low efficiency, high toxicity, and short-term effects (silver nanomaterials).<sup>17–19</sup>

Enzymes are biomaterials with excellent catalytic efficiency, substrate specificity, and environmental friendliness.<sup>20,21</sup> After the neutrophils of the human immune system engulf bacteria, their myeloperoxidase can catalyze hydrogen peroxide ( $H_2O_2$ ) to generate highly toxic ROS to attack the bacterial cell membrane.<sup>22</sup> In practical applications, natural enzymes are subject to many limitations. Inspired by natural enzymes, researchers have focused on how to construct artificial nanozymes with enzyme-like activity to kill bacteria or disrupt biofilms.<sup>23,24</sup> As a substitute for natural enzymes, nanozymes can be applied in more fields due to their high surface energy and good photoelectron transport ability.<sup>25</sup> Excitingly, due to the excellent physicochemical properties of most nanomaterials, design adjustments can be made according to practical needs,<sup>26</sup> such as surface modification to improve biocompatibility,<sup>27–29</sup> and control of synthesis conditions to tune the catalytic efficiency.<sup>30</sup> Moreover, it usually has more robust stability and robustness in extreme environments.<sup>31,32</sup> In practical applications, artificial nanozymes have more advantages than natural enzymes, consisting of low cost, high stability, mass production, etc.<sup>33</sup>

Bacterial infection not only easily delays the wound healing process, but also easily causes severe tissue and cell damage, and even threatens life. In recent years, among the known nanomaterials researched, there are currently more researched metal nanoparticles (Au, Ag, Pd, and Cu),<sup>34–37</sup> nanoalloys (gold silver, gold copper, and iron platinum),<sup>38–40</sup>

compounds (cerium oxide, iron oxide, silicon dioxide, and cadmium selenide),<sup>41–45</sup> carbon-based materials (graphene, carbon nanotubes, fullerenes),<sup>46–48</sup> etc. Different materials are used for the development of nanozyme antibacterial agents, which tend to be multifunctional and intelligent in a single system. In this review, we aim to highlight the significant advances of nanozymes for improving bacterial-infected wound healing. First, we briefly describe the pathophysiology and information of bacteria infected wound healing. Second, cover the treatment strategies for bacterially infected wounds of nanozymes. The application of nanozymes in infected wounds is mainly reviewed. Finally, the future challenges and prospects of nanozymes in bacterially infected wounds are also discussed.

## Bacteria-Infected Wound Healing and Treatment

Bacteria-infected wound healing is common in daily life and in the occurrence of diseases, and many factors affect wound healing.<sup>49</sup> Wound types are divided into acute wounds and chronic wounds according to the length of healing time. Although both types of wounds go through the same repair process, the former can take longer to heal than three months to develop into a chronic wound that may be accompanied by pathological changes involving infection or increased protease activity.<sup>50,51</sup> Acute wounds are common in cuts, lacerations, abrasions, burns, and incisions caused by surgery or accidental injury. All stages of wound healing are completed within a certain time frame, but infection may occur.<sup>52,53</sup> Chronic wounds are often caused by chronic diseases and complications caused by their care, and even acute wounds caused by improper treatment or infection (such as diabetic foot ulcers, acute orthopedic wounds, venous leg ulcers, ischemic ulcers, pressure ulcers, etc.).<sup>54–57</sup>

In chronic wounds, common features are usually depicted compared with normal wound healing, including nonmigrating epidermis, unresolved inflammation, fibrosis, presence of infection, and biofilm formation (Figure 1). Although there is an increase in neutrophils and macrophages, not all are properly functioning. Some fibroblasts become senescent

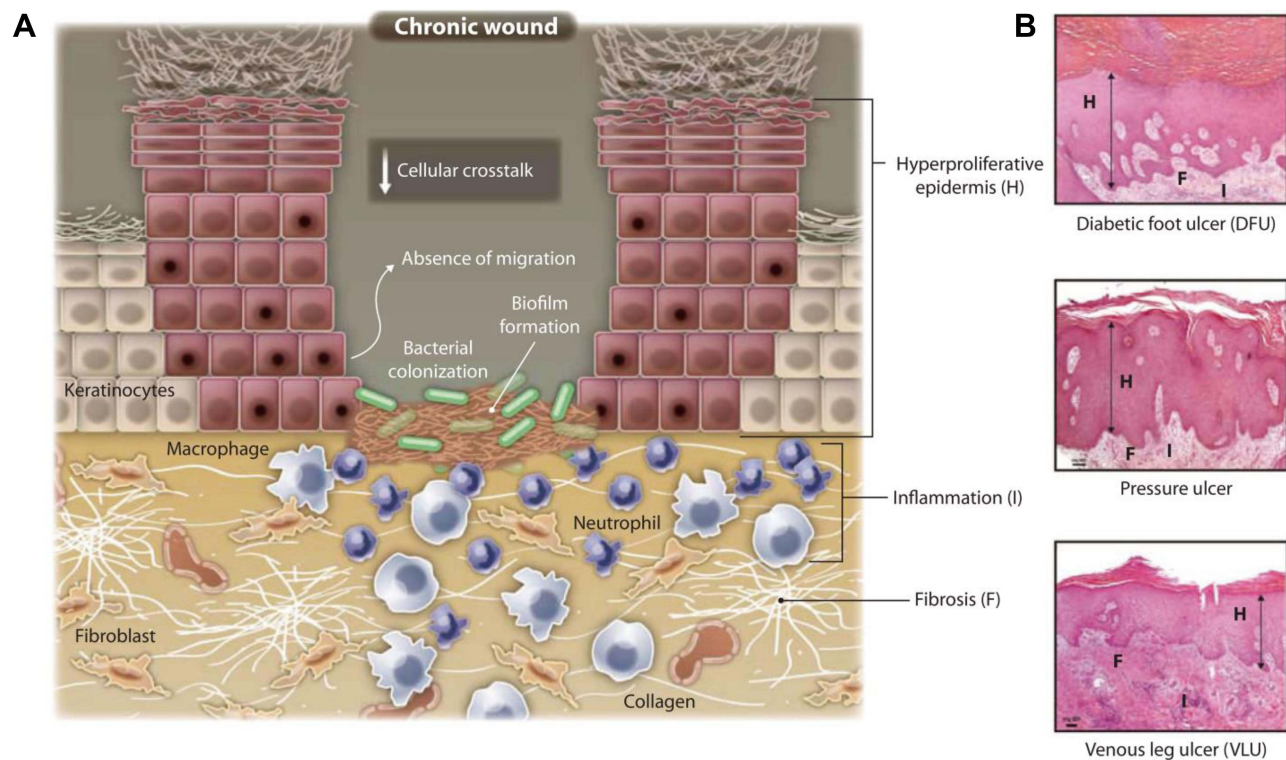


**Figure 1** Molecular pathology of chronic wounds. Illustrations show molecular and cellular mechanisms that are impaired in chronic wounds. **(A)** Chronic wounds show hyperproliferative and nonmigratory epidermis, unresolved inflammation, presence of infection, and biofilm formation. **(B)** Histologies represent characteristics of a diabetic foot (DFU), venous stasis (VLU), and pressure ulcers. Although different in etiology, these chronic wounds show common cellular features: H, hyperproliferative epidermis; F, fibrosis; I, increased cellular infiltrate (inflammation). Reprinted from Eming SA, Martin P, Tomic-Canic M. Wound repair and regeneration: mechanisms, signaling, and translation. *Sci. Transl. Med.* 2014;6(265):265sr6. Copyright 2014, Wiley. Reprinted with permission from AAAS.<sup>60</sup>

and uncontrolled proteases interfere with essential repair mechanisms. Then, the healing time is gradually prolonged, eventually leading to the formation of a chronic wound.<sup>58,59</sup>

## Pathophysiology and Formation of Bacteria-Infected Wounds

### Pathophysiology of Bacteria-Infected Wound Healing

Wounds are most commonly colonized by a variety of microorganisms, including many potentially pathogenic microorganisms.<sup>61,62</sup> Therefore, wounds have a high risk of infection during the healing process. For normal wounds, the healing process is a succession and overlap of several multidimensional phases of hemostasis, inflammation, proliferation, and remodeling (Figure 2A).<sup>63,64</sup> In the dynamic process of wound healing, once the wound is formed, the damaged blood vessels rapidly constrict to initiate hemostasis.<sup>65</sup> Then, the platelets are activated upon contact with the subendothelial matrix, rapidly recruiting and secreting growth factors and chemokines to promote the recruitment of inflammatory cells, forming a blood clot as a temporary barrier to protect the wound (Figure 2B). Blood clots can also store cytokines and growth factors and provide a scaffold for the entry of immune cells, which are released as platelets activate, leading to early wound repair.<sup>66</sup>

The inflammatory phase represents the second stage of wound healing. During this phase, the accumulation of macrophages, lymphocytes, monocytes, mast cells, and polymorphonuclear neutrophils (PMNs) leads to inflammation.<sup>67,68</sup> Among them, macrophages are generally considered to be the predominant inflammatory cells in wound healing, and they play a role in phagocytosis of microorganisms, stimulation of granulation tissue and vascular formation, and gradually take over 3–5 days after wound formation.<sup>69</sup> Immune cells such as mast cells are also activated early in inflammation to recruit neutrophils by releasing histamine, which is beneficial for wound healing.<sup>70,71</sup> Moreover, PMNs play a central role in delayed wound healing. In healthy individuals, PMNs flow freely in a resting state, called the dormant state. After wound infection, the activation of inflammatory mediators and complement released by various cells induces changes in the endothelial properties of the blood vessels. The endothelium sends signals to PMNs to migrate across the endothelial barrier toward the site of infection along a gradient of inflammatory factors and chemotactic agents (tumor necrosis factor- $\alpha$ , interleukin 8, platelet activating factor, leukotriene B4, and bacterial chemotactic peptides).<sup>72,73</sup> Upon exposure to pathogens, PMNs first recognize “pathogen-associated molecular patterns” that are widespread in microorganisms through cell surface pattern recognition receptors (Toll-like receptors).<sup>74</sup> Then, it binds and phagocytoses the pathogen. Phagocytosis triggers the PMN activation program by activating nicotinamide adenine dinucleotide phosphate oxidase (NADPH), leading to the release of superoxide anions, antimicrobial peptides, myeloperoxidases, and proteases.<sup>75,76</sup> This process is called “respiratory burst” (Figure 3). However, bacterial infection leads to excessive ROS production continuously and the wound remains in the inflammatory phase for a long time. Therefore, the prolonged healing time does not allow smooth entry into the proliferative and remodeling phases.<sup>77</sup>

Primary functions of normal intact skin, include control of microbial populations living on the skin surface and prevention of colonization and invasion of underlying tissues by potential pathogens.<sup>78</sup> Because the deep dermis is less repaired than the functioning epidermis in the later stages of healing, improperly healed wounds may lead to ulcerative skin abnormalities or excessive scar formation.<sup>60</sup> Ultimately, prolonged barrier defects may provide warm, moist, and nutritious conditions for bacteria to invade the underlying tissues of the skin, especially resistant bacteria that can further render antibiotics ineffective or even ineffective by forming biofilms, altering numbers and virulence, such as *Staphylococcus aureus* (*S. aureus*) and *Pseudomonas aeruginosa* (*P. aeruginosa*).<sup>79</sup> In addition, factors affecting infected wound healing include age, sex hormones, oxygenation, comorbidities (diabetes, obesity, nutrition), medication use (nonsteroidal anti-inflammatory drugs, steroids, anti-rejection drugs), lifestyle (alcoholism, smoking), and tumor treatment (chemotherapy, radiotherapy).<sup>80,81</sup> Meanwhile, different wound care methods and techniques can lead to different event outcomes.<sup>11</sup>

### Formation of Bacterial Infection Wounds

Bacteria are ubiquitous in nature and in the human body, and colonize different body parts, such as the skin, gut, stomach, mouth, lungs, reproductive tract, and conjunctiva.<sup>82</sup> The bacterial microbiome plays a crucial role in human health, such as nutrient acquisition, control of cell proliferation and differentiation, molecular metabolism, and

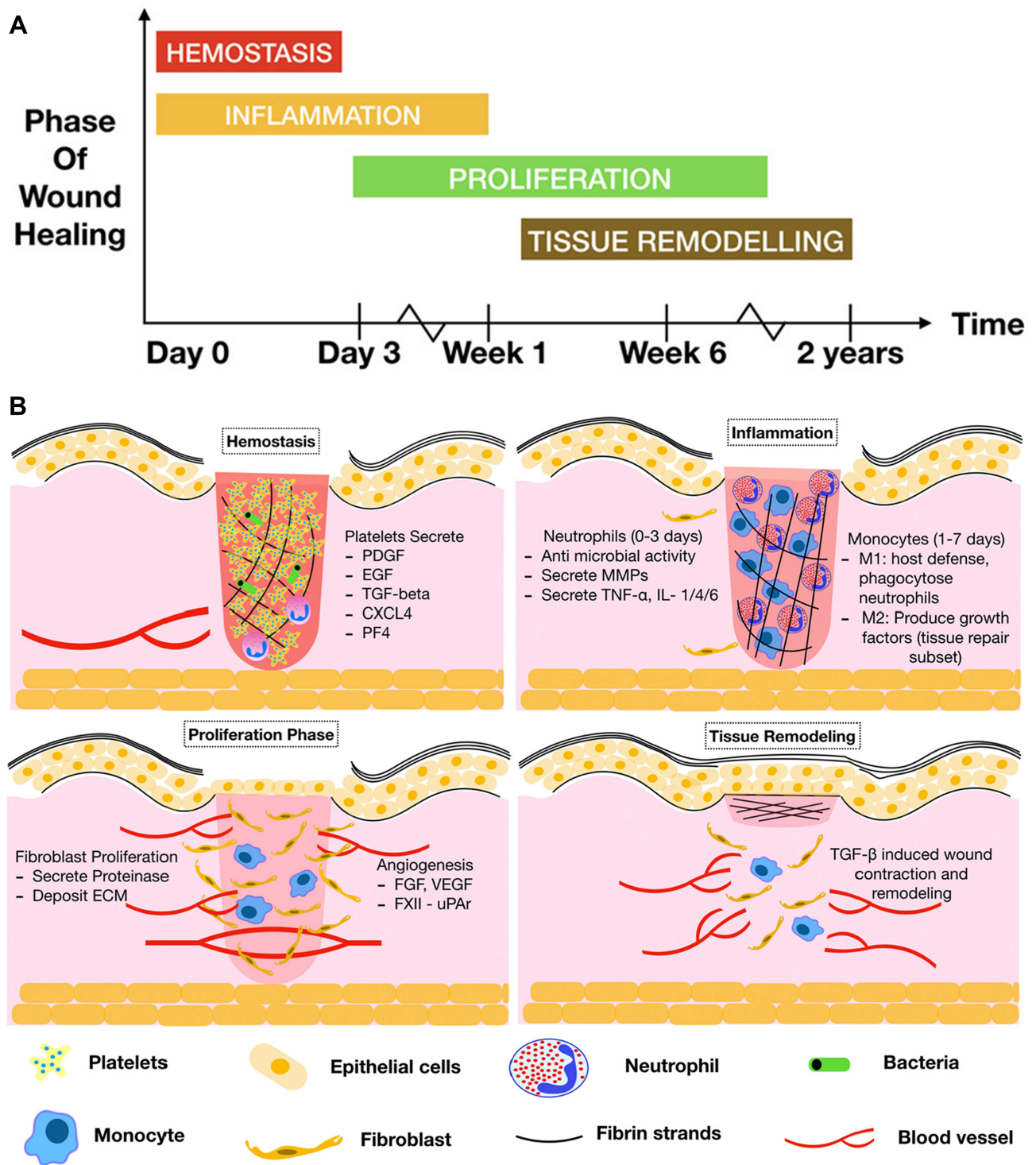


**Figure 2 (A)** Phases of wound healing. Timeline depicting the sequential yet overlapping phases of wound healing namely, hemostasis (red), inflammation (yellow), keratinocyte proliferation, angiogenesis (green) and tissue remodeling (brown). **(B)** Contribution of hematopoietic cells to wound healing. Reprinted from *Thromb. Res.* 179. pnej A, Kapoor S, Stavrou EX. Contribution of platelets, the coagulation and fibrinolytic systems to cutaneous wound healing. 179:56–63. Copyright 2019, with permission from Elsevier.<sup>64</sup>

**Abbreviations:** CXCL4, CXC chemokine ligand 4; ECM, extracellular matrix; EGF, epidermal growth factor; FGF, fibroblast growth factor; IL, interleukin; MMP, matrix metalloproteinase; PDGF, platelet derived growth factor; PF4, platelet factor 4; TGF- $\beta$ , transforming growth factor- $\beta$ ; TNF- $\alpha$ , tumor necrosis factor- $\alpha$ ; uPAR, urokinase plasminogen activator receptor; VEGF, vascular endothelial growth factor.

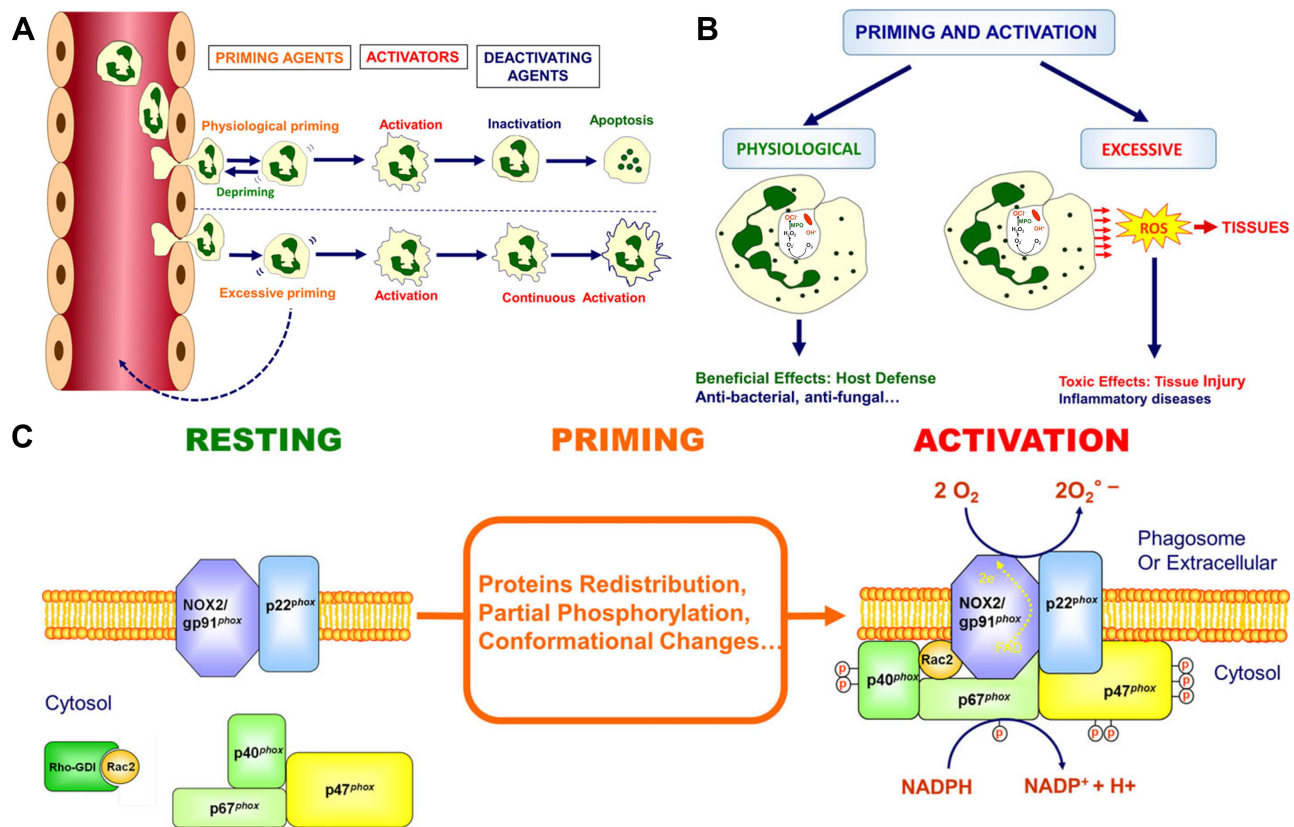


**Figure 3** (A) Neutrophils from the circulation to the inflammation site. (B) Role of priming and activation of neutrophils in host defense and inflammation. (C) The NADPH oxidase in resting, primed and activated neutrophils. Reprinted with permission from J. El-Benna, M. Hurtado-Nedelec, V. Marzaoli, et al. Priming of the neutrophil respiratory burst: role in host defense and inflammation. *Immunol. Rev.* 2016;273(1):180–193. Copyright 2016, Wiley.<sup>74</sup>

development of the immune system.<sup>3</sup> However, when the living environment of the microbiome changes due to diet, low immunity, and the use of antibiotics, the diversity of the microbiome will be out of balance, thereby becoming opportunistic pathogens and leading to serious infections.<sup>83,84</sup> The skin, which is the organ with the second-highest number of microorganisms, is also at risk of infection if its integrity is compromised.<sup>82</sup>

The outcomes of wound healing may be related to the diversity of bacterial species.<sup>85</sup> Low levels of bacterial colonization do not affect wound healing; in contrast, high levels of colonization play a significant role in the formation of infectious chronic wounds.<sup>86,87</sup> Certain specific pathogenic microorganisms such as *S. aureus*, *P. aeruginosa*, and Group A Streptococcus are common types of infection. Bacterial infection wounds are formed due to their resistance to antibiotics and the formation of bacterial biofilms while secreting toxins and enzymes to aggravate wound damage.<sup>88</sup> Generally, bacterial biofilm is a viscous structure of polysaccharide matrix formed by autocrine after bacterial aggregation in a specific microenvironment. Most are produced in adversity, such as antibiotic use, and nutritional deficiencies.<sup>89</sup> Biofilms can be composed of single or multiple bacterial species.<sup>90</sup> Once biofilms are formed, it is difficult for immune cells to engulf them, which reduces the effectiveness of this type of infection.<sup>91,92</sup> Furthermore, biofilms are approximately 1000 times more resistant to fungicides than planktonic cells.<sup>93</sup>

The persistence of biofilms can cause an excessive inflammatory state, in which inflammatory cells produce oxidative free radicals and enzymes that further damage surrounding collateral tissue cells and are the main cause of bacterial infection wound formation.<sup>94,95</sup> After invading wounds, pathogenic microorganisms suppress the adaptive immunity of wound healing through quorum sensing (QS) signaling, making them unable to fully activate dendritic cells and macrophages.<sup>96</sup> It can also prevent the expression of endogenous antimicrobial peptides (AMPs) in wounds in innate immunity. AMPs can respond to trauma by macrophages, infiltrating granulocytes, and keratinocytes, and are part of the skin's innate immune response to defend against infection. For instance, S100A8/A9 is not expressed in human venous

chronic leg ulcers, but is expressed in actively healing wounds.<sup>97–99</sup> Moreover, some components of biofilms, such as rhamnolipids in *P. aeruginosa* biofilms, cause neutrophil death and cell necrosis.<sup>100,101</sup> Another possible underlying mechanism is that biofilms block the recognition of bacterial infections in the body through the Toll-like-receptor pathway. This results in reduced oxidative burst activity of neutrophils in wounds, insufficient stimulation of cytokines, and markedly slowed wound epithelialization.<sup>102</sup>

## Treatment Strategies for Bacterially Infected Wounds

### Traditional Strategies

The skin is a multilayered organ barrier that prevents the human body from dehydrating and invading pathogenic microorganisms. Repair after injury is a significant and complex biological process in the human body.<sup>103,104</sup> Due to the widespread use and even abuse of antibiotics, bacterial resistance is rising year by year.<sup>105</sup> Currently, to promote the rapid healing of wounds and avoid the formation of chronic wounds caused by infection, traditional treatments, and new application methods are researched and developed, and new modern treatments are also sought.

Traditional treatment strategies have a long history of development in developing countries such as Asia, Africa, Australia, and Latin America.<sup>106</sup> Common materials include herbs, plant extracts, compounds of animal origin, organisms, silver, and traditional dressings.<sup>107–109</sup> There are many kinds of plant extracts, such as sea buckthorn,<sup>110,111</sup> aloe,<sup>112–114</sup> angelica,<sup>115</sup> and periwinkle,<sup>116</sup> containing a wide variety of Bioactive compounds,<sup>117,118</sup> which have good antibacterial activities and anti-inflammatory effects in the treatment of wound healing. Frogskin and its secretions,<sup>119,120</sup> honey, and propolis<sup>121,122</sup> are products of animal origin; and are generally used as ointments or temporary dressings. In addition, leech therapy also has numerous applications in bacterial infection wound healing as an alternative therapy.<sup>123,124</sup> The antimicrobial properties of silver can also help effectively control and prevent wound infections.<sup>125–127</sup> Even at the current frontier of antimicrobial drug development, traditional therapies still have enormous exploratory value.

Numerous advanced therapies have been investigated to meet the care needs of bacteria-infected wounds. Modern treatments are more demanding and functionally diverse, including modern dressings, stem cells, growth factors, and skin replacement therapies.<sup>128–132</sup> The main goal is to improve the antibacterial activity of the material so that it can be fully developed and made harmless to the human body. The combination of traditional therapy with modern technology is a new approach, for example, the use of honey combined with gelatin and chitosan (CS) to construct a hydrogel dressing for the treatment of burns, which has significant antibacterial activity and biosecurity against *Escherichia coli* (*E. coli*) and *S. aureus*.<sup>133</sup> In addition, there are also hydrogel dressings loaded with bacteriophages for research against certain drug-resistant infections.<sup>134</sup> Negative pressure wound therapy has changed the way acute and chronic wounds are treated, especially in the management of infected wounds, it can shrink wound edges, remove inflammatory and infectious Substances, reduce edema and promote the formation of blood vessels and granulation tissue.<sup>135</sup> Hyperbaric oxygen therapy utilizes the binding mechanism of oxygen and hemoglobin to improve the oxygen content of ischemic tissue, enhance the activity of fibroblasts, promote angiogenesis and the clearance of some bacteria, downregulate inflammatory factors, and upregulate growth factors, and is generally used to treat intractable or complex ulcers.<sup>136–138</sup>

Traditional dry gauze dressings used in the clinic have difficulty creating an environment of low oxygen tension, which is not conducive to the activation of hypoxia-inducible factors and the accelerated rate of re-epithelialization.<sup>139,140</sup> Therefore, many new dressings have been developed to promote wound tissue regeneration by improving the micro-environment of the wound. The materials used include the antioxidants polyurethane, collagen, bacterial cellulose, CS, silica gel, HA, alginate, etc.<sup>141–148</sup> In recent years, studies have found that lasers and tissue-engineered alternatives can shorten the healing time of leg ulcers, pressure ulcers, diabetes, and wounds at high risk of infection.<sup>15</sup>

Compared with traditional treatment methods, modern treatment methods have solved the problems of dosage, safety, formulation, cost, production method, batch, and efficacy to a certain extent.<sup>106,149,150</sup> For instance, honey is one of the representative natural substances in traditional remedies. Differences in antibacterial activity are affected by differences in ingredients, with an incomplete understanding of the mechanism of action of active ingredients and lack of standardization of antibacterial activity being the main reasons for its limitation.<sup>121,151,152</sup> Moreover, while various treatment methods promote wound healing, they also have side effects that cannot be ignored. Including glucocorticoids

with powerful anti-inflammatory effects, long-term use can lead to osteoporosis, muscle atrophy, eye diseases, central nervous system diseases, hyperglycemia, etc.<sup>153</sup> Worryingly, new antibiotics are always effective initially, but inevitably develop resistance over time into clinical use, which means that limited shelf life needs to be extended by the continuous development of new drugs and strategies.<sup>154</sup>

## Nanozyme Strategies

Nanozymes as emerging materials have more advantages than traditional antibacterial agents. Currently, the synthetic route of nanozymes is mainly chemical synthesis, and manual intervention is the basis for the realization of the controllable design. The advantages of nanozymes mainly include the following aspects (Figure 4): (1) They are less susceptible to drug resistance than other materials. For instance, antibiotics target the basic cellular functions of bacteria, and bacteria can acquire compensatory mutations in adverse environments to reduce the adverse effects of resistance mutations.<sup>155</sup> Resistant plasmids and gene cassettes accumulate continuously and gradually form multiple drug resistance through self-transmission among bacteria, manifested as inactivated enzymes or changes in cell membrane permeability, making it difficult for drugs to bind to bacteria.<sup>156</sup> However, the bactericidal mechanism of nanozymes is mainly to catalyze the substrate through its oxidoreductase activity to generate highly toxic ROS, while it is difficult for bacteria to deal with the damage caused by ROS. (2) Enables the construction of nanozymes with targeting capabilities. Even though the selectivity of the nanozyme itself is relatively weak, its structural advantage enables it to form other components (aptamers, peptides, nucleic acid probes, antibodies, antibiotics) to achieve selective antibacterial effects. For instance, through the surface-binding properties and endocytosis of ROS, nanozymes selectively act on bacteria rather than normal tissue cells.<sup>157</sup> In addition, a selective antigram system was constructed based on photoacid molecules and MoS<sub>2</sub> for the differences in the structural composition of the cell walls of different bacteria. Charge switching is regulated by controlling the duration of UV light irradiation, with shorter durations focusing on Gram-positive bacteria and longer durations on Gram-negative bacteria.<sup>158</sup> (3) Nanozymes can modulate catalytic performance by changing various conditions. The catalytic performance of nanozymes is affected by ambient temperature, pH, light, activators, and inhibitors, therefore, ROS generation can be indirectly regulated by controlling the influencing factors.<sup>159</sup> In addition, size, morphology, components, and surface modification will also directly affect the catalytic activity of nanozymes.<sup>160–162</sup> (4) Multifunctional antimicrobial agent design is a future trend. Nanozymes in monotherapy mode are often ineffective in practical applications. In addition to enzyme-like catalytic activity, nanozymes can also combine photodynamic, physical cleavage, magnetic, fluorescence, and other capabilities at the same time, or construct multienzyme systems.<sup>163–165</sup> The synergy of multiple functions enables nanozymes to remove bacteria and biofilms more efficiently. (5) Furthermore, most of the preparation methods of nanozymes are relatively simple chemical syntheses, with obvious cost advantages and excellent stability, so they are suitable for mass production and in line with clinical application research.<sup>166</sup>

There are many types of nanozymes, and there have been many studies on different types of materials, such as metal-based nanozymes, metal oxide-based nanozymes, carbon-based nanozymes, and metal-organic framework (MOF) @covalent-organic framework (COF)-based nanozymes. In general, the antibacterial design of nanozymes mainly revolves around two aspects: first, how to destroy the biofilm so that it can come into contact with bacteria, and then how to ensure the effectiveness and maintenance of antibacterial ingredients after contact with bacteria. Most nanozymes utilize intrinsic enzyme-like and physicochemical activities, such as common peroxidase (POD)-like and oxidase (OXD)-like activities, to catalyze the production of abundant highly toxic free radicals in a short time, and regulate the level of ROS to achieve antibacterial activity.<sup>167</sup> Nanozymes mainly carry out antibacterial activity in the following ways.

ROS possess a powerful oxidative capacity and play a crucial role in the body's defense against pathogen invasion (Figure 5). Redox nanozymes can exhibit an intrinsic ROS generation ability to kill bacteria. For instance, a nanomaterial with POD-like activity can convert H<sub>2</sub>O<sub>2</sub> to hydroxyl radicals (-OH), which inactivate the biological components of bacteria and biofilms (such as proteins, nucleic acids, lipids, and polysaccharides) (Figure 6A).<sup>168</sup> Namely, increasing ROS levels can lead to genetic and structural damage to bacteria and biofilms, making it difficult to develop drug resistance.<sup>169</sup>

In general, elevated concentrations (1–6%) are required to exert the antibacterial effect of H<sub>2</sub>O<sub>2</sub>, which can cause damage to healthy tissue surrounding an infected wound.<sup>170</sup> For instance, nanomaterials mimic vanadium chloroperoxidase, when halide ions and H<sub>2</sub>O<sub>2</sub> coexist, the catalytic reaction produces abundant singlet oxygen (<sup>1</sup>O<sub>2</sub>) and hypochlorous acid to destroy



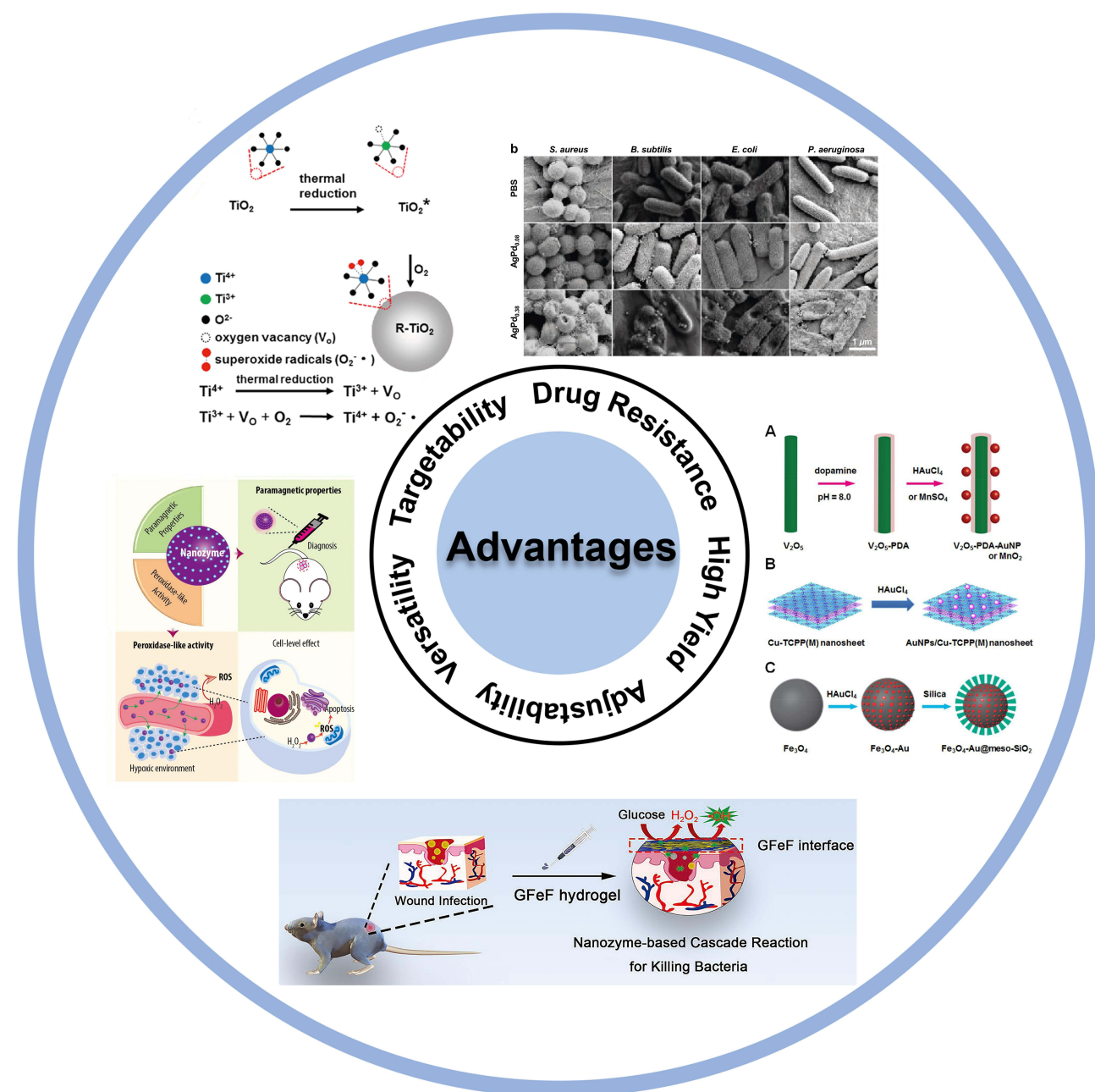


**Figure 4** Schematic diagram of the antibacterial advantages of nanozymes. Reprinted with permissions from Liu X, Gao Y, Chandrawati R, et al. Therapeutic applications of multifunctional nanozymes. *Nanoscale*. 2019;11(44):21046–21060. Copyright 2019, The Royal Society of Chemistry, permission conveyed through Copyright Clearance Center, Inc.<sup>165</sup> Wu J, Li S, Wei H. Integrated nanozymes: facile preparation and biomedical applications. *Chem. Commun. (Camb)*. 2018;54(50):6520–6530. Copyright 2018, The Royal Society of Chemistry.<sup>166</sup> Li Y, Wang L, Liu H, et al. Ionic Covalent-Organic Framework Nanozyme as Effective Cascade Catalyst against Bacterial Wound Infection. *Small*. 2021;17(32):e2100756. © 2021 Wiley-VCH GmbH.<sup>364</sup> And F. Gao, T. Shao, Y. Yu, et al. Surface-bound reactive oxygen species generating nanozymes for selective antibacterial action. *Nat. Commun.* 2021;12(1):745. Creative Commons license and disclaimer available from: <https://doi.org/10.1038/s41467-021-20965-3>.<sup>157</sup>

bacteria and biofilms.<sup>171</sup> However, nanozymes are mostly pH-dependent, and relatively high doses of ROS may cause unnecessary damage. Therefore, one study encapsulated glucose oxidase (GOx) in MOF. Gluconic acid is produced by consuming glucose in the wound by GOx, which regulates the pH microenvironment suitable for the antimicrobial activity of the nanozyme and achieves a glucose-H<sub>2</sub>O<sub>2</sub>-hydroxyl radical cascade catalytic reaction (Figure 6B).<sup>172</sup>

The ROS generation performance of some nanozymes sensitive to external stimuli can be enhanced with additional light. For instance, TiO<sub>2</sub> nanotubes and black phosphorus are candidates for photoactivated enhancement therapy due to their excellent electron transportability and electronic band structure.<sup>173,174</sup> The composite material composed of these

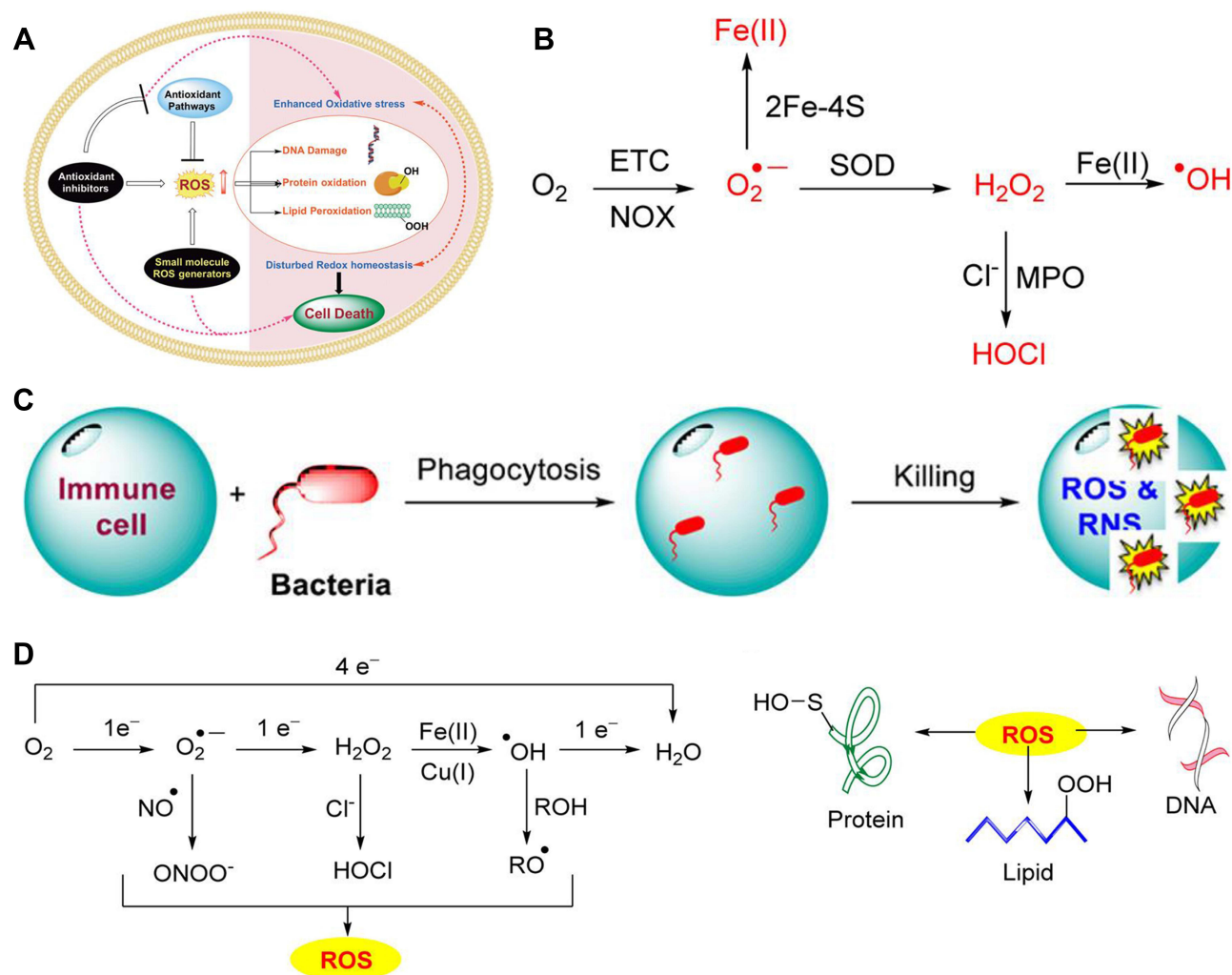


**Figure 5** (A) Schematic illustration of ROS causing cell death. (B) ROS generation is induced by cellular enzymes. (C) Phagocytosis of bacteria during immune response in cells. (D) General scheme for ROS production and damaging effects of ROS to biomacromolecules. Reprinted with permission from Dharmaraja AT. Role of Reactive Oxygen Species (ROS) in Therapeutics and Drug Resistance in Cancer and Bacteria. *J. Med. Chem.* 2017;60(8):3221–3240. Copyright 2017, American Chemical Society.<sup>169</sup>

materials can actively catalyze the generation of ROS under light irradiation, and enhance the original enzyme-like activity of the binding component.<sup>175</sup> A modality of synergistic energy conversion to stimulate therapy can more precisely control the course of treatment and reduce the probability of resistance to a single antibacterial modality.<sup>176,177</sup>

Biofilms are a barrier to the effective functioning of antibacterial agents, in which environmental DNA (eDNA) is believed to play a Key role in maintaining membrane integrity. According to reports, some nanozymes with deoxyribonuclease (DNase)-like enzymes can hydrolyze eDNA to destroy biofilms.<sup>178</sup> In addition, hydroperoxidase-like nanozymes can block bacterial QS, impeding biofilm formation by inhibiting autoinduction such as N-acyl homoserine lactones.<sup>179</sup> The biofilm microenvironment (BME) has also received increasing attention from scholars in recent years. Utilizing the characteristics of the BME: (negative charge, low pH, and high concentration of reduced glutathione (GSH)), pH or GSH-dependent nanozyme design was carried out, and these characteristics were used to assist high-efficiency antibacterials.<sup>180,181</sup>

## Nanozyme-Based Treating for Bacterial Infection Wounds

With the rapid development in nanotechnology and computer science, many synthetic methods have been proposed for the fabrication of new nanozymes, and possible catalytic mechanisms can be revealed through theoretical calculations. Benefiting from the advantages of materials synthesis, it is possible to modify the structure, morphology and size to

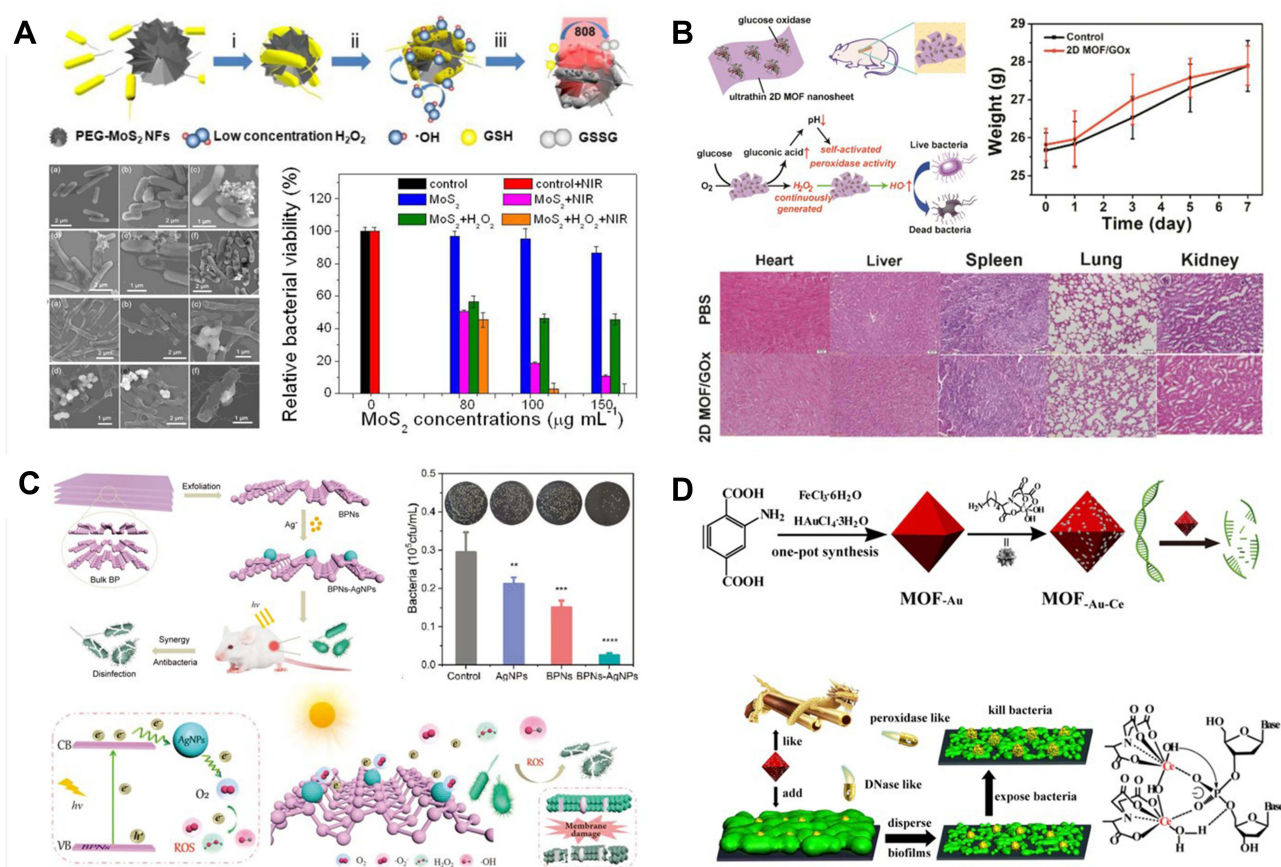


**Figure 6** (A) Schematic illustration of PEG-MoS<sub>2</sub> as a combined system for POD catalyst-photothermal synergistic eliminating of bacteria. (i) PEG-MoS<sub>2</sub> was captured by bacteria; (ii) PEG-MoS<sub>2</sub> catalyze decomposition low concentrated H<sub>2</sub>O<sub>2</sub> to generate OH to damage the cell walls integrity; (iii) 808 nm laser irradiation causes hyperthermia, which accelerates GSH oxidation. Reprinted with permission from Yin W, Yu J, Lv F, et al. Functionalized Nano-MoS(2) with Peroxidase Catalytic and Near-Infrared Photothermal Activities for Safe and Synergetic Wound Antibacterial Applications. *ACS nano*. 2016;10(12):11000–11011. Copyright 2016, American Chemical Society.<sup>168</sup> (B) GOx encapsulation in MOF to construct a Band-Aid dressing and its toxicity test. Scale bars: 50 μm. Reprinted with permission from Liu X, Yan Z, Zhang Y, et al. Two-Dimensional Metal-Organic Framework/Enzyme Hybrid Nanocatalyst as a Benign and Self-Activated Cascade Reagent for in Vivo Wound Healing. *ACS nano*. 2019;13(5):5222–5230. Copyright 2019, American Chemical Society.<sup>172</sup> (C) Preparation of silver-loaded black phosphorus nanosheets (BPN-AgNPs) by facile BPN-mediated reduction of Ag<sup>+</sup> precursors and their antibacterial effect under light irradiation. Reprinted with permission from Wiley, Liang M, Zhang M, Yu S, et al. Silver-Laden Black Phosphorus Nanosheets for an Efficient In Vivo Antimicrobial Application. *Small*. 2020;16(13):e1905938. © 2020 WILEY-VCH Verlag GmbH & Co. KGaA, Weinheim.<sup>173</sup> (D) Schematic diagram of the synthesis of MOF-Au-Ce by attaching cerium complexes to the surface of MOF-Au, which catalyzes DNA cleavage through DNase-like enzyme activity. Reprinted from *Biomaterials*. 208. Liu Z, Wang F, Ren J, et al. A series of MOF/Ce-based nanozymes with dual enzyme-like activity disrupting biofilms and hindering recolonization of bacteria. 21–31. Copyright 2019, with permission from Elsevier.<sup>178</sup>

confer enzymatic activity to nanomaterials.<sup>182</sup> The well-defined structure facilitates the elucidation of the active catalytic center, and the location of the active site means that it may have different catalytic properties. For example, noble metal nanoparticles, the distribution of active atoms may be located at the edges, corners, and tips. In wound antimicrobial therapy, numerous synthetic strategies have been used to synthesize and design nanomaterials with excellent intrinsic enzymatic activity, such as metals, metal oxides, sulfur generics, carbon-based nanoparticles, MOFs, and covalent metal organic frameworks (Table 1).

## Metal-Based Nanozymes

In recent years, many researchers have made efforts to find new nanozyme antibacterial agents for bacterial infection wound treatment and have achieved important research results (Table 2). Metals are one of the most common constituent materials of nanozymes.<sup>183</sup> Metal nanomaterials have excellent electronic properties, which are derived from their rich charge coverage.<sup>184</sup> In addition, there are characteristics such as facile preparation, high surface energy, and excellent photothermal conversion performance,<sup>185,186</sup> which suggest that relevant adjustments (such as surface modification) can

**Table 1** Summary of the Strategy, Synthesis Methods, Activity, Kinetic Parameters, and Healing Effect of Nanozymes

Strategy	Synthesis Method	Nanozyme	Activity	Substrate, Km (mM), Vmax ( $\mu\text{M s}^{-1}$ )	Wound Healing Days	Ref.
Synthesis and surface modification	Modified Hummers method	GQD	POD	H <sub>2</sub> O <sub>2</sub> (2.288, 0.1563)	3	[272]
	Soft-template strategy	Fe-NC SAzyme	POD	H <sub>2</sub> O <sub>2</sub> (4.48, 0.118)	4	[266]
	AuNPs modification	AuNPs/Cu-MOFNs	POD	H <sub>2</sub> O <sub>2</sub> (0.65, 0.225), TMB (0.29, 0.396)	8	[29]
One-step solvothermal/hydrothermal reaction	“Sequential growth” strategy	NMC <sub>TP-TTA</sub>	POD	H <sub>2</sub> O <sub>2</sub> (0.458, 0.57), TMB (0.291, 0.7351)	5	[369]
	One-step bottom-up ethanol-thermal method	VOx NDs	POD, OXD	H <sub>2</sub> O <sub>2</sub> (0.077, 2.876), TMB (0.21352, 2.669)	6	[226]
	One-pot solvothermal method	MoO <sub>3-x</sub> NDs	POD	H <sub>2</sub> O <sub>2</sub> (0.26, 0.152), TMB (2.65, 0.00152)	6	[227]
	Solvothermal method	nFeS	POD, CAT	H <sub>2</sub> O <sub>2</sub> (172.3, 0.4191), TMB (1.807, 9.113)	6	[241]
	Facile one-pot hydrothermal route	PEG-MoS <sub>2</sub> NFs	POD	H <sub>2</sub> O <sub>2</sub> (2.812, 0.0801), TMB (0.537, 0.0388)	5	[168]
Precipitation	Deposition-precipitation	gC <sub>3</sub> N <sub>4</sub> @AuNPs	POD	H <sub>2</sub> O <sub>2</sub> (0.222, 1.508), TMB (0.295, 0.86)	3	[200]
	Co-precipitation process	GOx-Hb MRs	POD, GOx	GOx (2.6, 0.0294)	/	[300]
Exfoliation	Sonication exfoliation	N-MoS <sub>2</sub> , N-WS <sub>2</sub> NSs	POD	/	8	[247]
Pyrolysis	“Encapsulated-pyrolysis” strategy	SAF NCs	POD	H <sub>2</sub> O <sub>2</sub> (0.01195, 0.234)	13	[263]
	Pyrolysis of colloidal silica/polyaniline assemblies	N-SCSs	POD, OXD, SOD, CAT	H <sub>2</sub> O <sub>2</sub> (81.53, 0.2327), TMB (0.15, 0.2205)	9	[262]
	Mesoporous silica protected pyrolysis strategy	PMCS	POD	H <sub>2</sub> O <sub>2</sub> (40.16, 0.1215), TMB (0.224, 0.1066)	6	[25]
	Pyrolysis	PEG@Zn/Pt-CN	POD	H <sub>2</sub> O <sub>2</sub> (0.067, 0.0511)	12	[325]
Reduction	In situ reduction of AgNPs by TA	TA-Ag	POD	H <sub>2</sub> O <sub>2</sub> (180.53, /), TMB (2.28, /)	21	[216]
	Via in situ reduction	UsAuNPs/MOFs	POD	H <sub>2</sub> O <sub>2</sub> (7.94, /), TMB (0.101, /)	5	[310]
Others	A solution-based approach	CuO NRs	POD	H <sub>2</sub> O <sub>2</sub> (3.4, 0.109), ABTS (0.04, 0.111)	/	[224]
	1, Ice bath	UNMS NCs	POD	H <sub>2</sub> O <sub>2</sub> (0.23, 0.157), TMB (2.35, 0.00157)	5	[375]
	2, Vacuum drying					
	1, Fe chelation	GFeF	POD, GOx	H <sub>2</sub> O <sub>2</sub> (3.35, 0.588), GOx (20, 0.01136)	9	[364]
	2, GOx loading					

**Table 2** Metal-Based Nanozymes and Metal Oxide-Based Nanozymes for Improving Bacterial Infectious Wound Healing

Type	Materials	Substrate	Synthesis Procedure	Microbial Type	Antibacterial Mechanism	Antimicrobial Activity	Special Characteristics	Ref.
Metal-based	gC <sub>3</sub> N <sub>4</sub> @AuNPs	H <sub>2</sub> O <sub>2</sub> (100 μM)	Deposition-precipitation	<i>S. aureus</i> , <i>E. coli</i>	Generates ROS, AuNPs stabilize -OH through partial electron exchange interactions, damage biofilm	>97% inactive bacteria in the presence of 20 μg/mL, SEM: Bacterial surface roughening and wrinkling	Avoid the injury caused by the use of high concentration H <sub>2</sub> O <sub>2</sub> and maintain high activity in the pH (5.0–7.4) environment of the wound	[200]
	Cu-HCSs and CuO-HCSs	H <sub>2</sub> O <sub>2</sub> (Gram-positive: 10 mM, Gram-negative: 1 mM)	Thermal decomposition	<i>Sphingomonas typhimurium</i> ( <i>S. typhimurium</i> ), <i>P. aeruginosa</i> , <i>Streptococcus mutans</i> ( <i>S. mutans</i> ), <i>E. coli</i> and <i>S. aureus</i>	Releases Cu ions and generates ROS, leading to membrane damage, enzymatic inhibition and possible DNA degradation	Sterilization decreased logarithmically	Kill bacteria and inhibit inflammation effectively, exhibited copper state-dependent peroxidase, catalase, and superoxide dismutase-like activities	[204]
	AgPd <sub>0.38</sub>	O <sub>2</sub>	1, Electro-displacement reaction 2, An ice-water bath	<i>S. aureus</i> , <i>B. subtilis</i> , <i>E. coli</i> and <i>P. aeruginosa</i>	Destroys the cell wall and cytoplasmic membrane	MBC = 4–64 μg/mL	ROS production is material dose-dependent, independent of pH, temperature and buffers, surface binding properties, inhibits biofilm formation	[157]
	TA-Ag	H <sub>2</sub> O <sub>2</sub> (1 mM)	In situ reduction of AgNPs by TA	<i>Staphylococcus epidermidis</i> ( <i>S. epidermidis</i> ), <i>E. coli</i>	Electron transfer between Ag NPs and TA maintains the dynamic redox balance of phenol-quinone, high POD-like activity	In the presence of H <sub>2</sub> O <sub>2</sub> , the bacteriostatic rate within 2 hours: <i>S. epidermidis</i> (90%), <i>E. coli</i> (89%)	Rapid ROS production, bacterial adhesion, repeatability	[216]

(Continued)

Table 2 (Continued).

Type	Materials	Substrate	Synthesis Procedure	Microbial Type	Antibacterial Mechanism	Antimicrobial Activity	Special Characteristics	Ref.
Metal oxide-based	CuO NRs	H <sub>2</sub> O <sub>2</sub> (under visible light)	A solution-based facile approach under ambient conditions	<i>E. coli</i>	Generates ROS, CuO photoexcite the charge carriers to enhance the generation of -OH radicals, POD-like activity	Reduction of viability = 92% (pH 6.0 and visible light), TEM: Bacterial surface roughening and wrinkling	Sterilization; H <sub>2</sub> O <sub>2</sub> production rate increased by 20 times under visible light, ~60% of the activity is retained at pH 6 and ~80% of the activity is retained at 37 °C	[224]
	CeO <sub>2</sub> /BG	H <sub>2</sub> O <sub>2</sub> (50 mM)	1, Liquid-feed flame spray pyrolysis 2, One-step synthesis	<i>S. aureus</i> , <i>E. coli</i> , and <i>Candida albicans</i>	Promotes intracellular ROS	Reduction of viability = ~ 90%	Antioxidant protection cell, synthesis controllable, different antibacterial activities of materials containing Ce <sup>4+</sup> or Ce <sup>3+</sup> in different phosphate environments	[225]
	ZnO/graphene oxide	/	Solution precipitation	<i>B. subtilis</i> , <i>Enterococcus faecalis</i> ( <i>E. faecalis</i> ), <i>E. coli</i> and <i>S. typhimurium</i>	Oxidizes cellular lipids and damages cell membranes, generates ROS	MIC = 6.25 µg/mL ( <i>E. coli</i> and <i>S. typhimurium</i> ), MIC = 12.5 µg/mL ( <i>B. subtilis</i> ) MIC = 25 µg/mL ( <i>E. faecalis</i> )	ZnO particles and graphene oxide complement each other to enhance antibacterial properties, simple and fast synthesis	[230]
	Fe <sub>3</sub> O <sub>4</sub> MNPs	H <sub>2</sub> O <sub>2</sub> , DNA, BSA	One-step in a solvothermal system	<i>E. coli</i> , <i>P. aeruginosa</i>	Oxidative cleavage of nucleic acids, proteins and oligosaccharides, generates ROS	98% inactive bacteria in the presence of 0.01% H <sub>2</sub> O <sub>2</sub> and 20 µg /mL MNP	Wide pH range (4.5–9), significant biofilm cleavage ability	[231]
	VO <sub>x</sub> NDs	H <sub>2</sub> O <sub>2</sub> (50 µM), O <sub>2</sub>	One-step bottom-up ethanol-thermal method	Extended spectrum β-lactamases producing (ESBL-producing) <i>E. coli</i> , MRSA, kanamycin-resistant <i>E. coli</i>	Oxidizes cellular lipids and damages cell membranes, generates ROS	SEM: Bacterial surface roughening and wrinkling	Bienzymatic synergism, concentration of H <sub>2</sub> O <sub>2</sub> decreased by about 2–4 orders, broad-spectrum antibacterial	[226]
	MoO <sub>3-x</sub> NDs	H <sub>2</sub> O <sub>2</sub> (100 µM)	One-pot solvothermal method	ESBL-producing <i>E. coli</i> , MRSA	Generates ROS, photothermal effect, damage biofilm	SEM: Bacterial surface roughening and wrinkling	POD/PTT/Photodynamic triple-therapy, broad-spectrum antibacterial, steady	[227]

be made according to practical applications. For instance, increasing the biocompatibility or changing the catalytic efficiency; is expected to be extended in biomedical applications.<sup>27</sup> Certainly, metals such as silver, cobalt, and copper have certain toxicity in the antibacterial treatment of infected wounds, and metal nanozymes face the challenge of how to enhance selectivity and improve biosafety.<sup>187,188</sup>

The morphology of nanoparticles is one of the parameters affecting catalytic performance. For example, gold nanozymes have excellent and stable catalytic, optical, electronic, supramolecular, and biological properties, manifested in different sizes and shapes (spheres, cubes, stars, prisms, etc.).<sup>189</sup> In general, smaller gold nanoparticles have better catalytic activity due to the higher number of angular sites.<sup>190</sup> However, the size dependence of the catalytic performance is not applicable to different shapes of gold nanoparticles.<sup>191</sup> McVey et al observed that smaller AuNSs (14 nm diameter) showed higher catalytic efficiency.<sup>192</sup> However, Biswa et al found that gold nanorods (AuNRs) with an aspect ratio of 2.8 were slightly more efficient than 34 nm gold nanorods (AuNSs) for the oxidation of 3,3',5,5'-tetramethylbenzidine.<sup>193</sup> Gold nanozymes are able to catalyze the production of ROS through POD activity for application in infected wounds. Ultrathin graphitic carbon nitride (gC<sub>3</sub>N<sub>4</sub>) is a nontoxic conjugated polymer with good thermal stability, chemical stability, and natural enzyme-like catalytic activity.<sup>194,195</sup> It has a wide range of applications in photocatalysis, sensors, biomedicine, and other fields. Although gC<sub>3</sub>N<sub>4</sub> alone cannot be directly used for wound anti-infection, the use of gC<sub>3</sub>N<sub>4</sub> combined with other antibacterial materials provides the possibility for the treatment of wound infection.<sup>196–199</sup> Wang et al prepared a g-C<sub>3</sub>N<sub>4</sub>@AuNPs (CNA) nanocomposite by a deposition-precipitation method.<sup>200</sup> AuNPs stabilize the -OH generated by CNA catalyzed by H<sub>2</sub>O<sub>2</sub> through the interaction of electron exchange, and the two work synergistically. CNAs are capable of POD-like catalysis in the presence of ultralow concentrations of H<sub>2</sub>O<sub>2</sub> (10 μM) to generate highly toxic -OH to destroy biofilms and even kill individual bacteria shed on biofilms. It not only avoids tissue damage and persistent inflammation caused by the use of high concentrations of H<sub>2</sub>O<sub>2</sub>, but also maintains high activity in the pH environment in the wound. Animal experiments showed that CNA could efficiently decompose gram-positive bacteria and gram-negative bacteria. In addition, it can also inhibit the formation of new biofilms and reduce the inflammation of lung infections caused by methicillin-resistant *S. aureus* (MRSA). These characteristics indicate that CNA can be used in clinical research. In addition, Zhang et al combined gold nanoparticles with α-FeOOH/porous carbon as an enzyme-Fenton bionanocatalyst.<sup>201</sup> The GOx activity of gold nanoparticles catalyzes the generation of gluconic acid from glucose and regulates the pH while inducing the reaction of H<sub>2</sub>O<sub>2</sub> with Fe<sup>2+</sup> to produce -OH. Crucially, the above synergy can achieve the target sterilization effect at near physiological concentrations of H<sub>2</sub>O<sub>2</sub>. Despite the lack of further studies to exploring different shapes to obtain empirical information, as a general rule, higher surface-to-volume ratios are expected to show enhanced catalytic performance.

The activity of nanozymes is related to their composition and structure.<sup>202,203</sup> Some metal-based nanozymes exhibit metal valence-dependent catalytic activity, and materials with different sterilization mechanisms are often designed by adjusting the metal valence. For instance, Xi et al compared two copper/carbon nanozymes (Cu-HCSs and CuO-HCSs) with metal valence states of Cu<sup>0</sup> and Cu<sup>2+</sup>, respectively (Figure 7A–E).<sup>204</sup> Interestingly, the two nanozymes have completely different antibacterial mechanisms. The Cu-modified copper/carbon nanozyme catalyzes the generation of ROS for sterilization through POD activity, while the CuO-modified copper/carbon nanozyme directly releases Cu<sup>2+</sup>. The experimental results show, that although both enzymes have significant antibacterial effects, the enzyme-like activity of Cu<sup>0</sup> is higher than that of Cu<sup>2+</sup>.

The variable particle size of metal-based nanozymes makes it possible to further explore. The endocytosis of mammalian cells is not possessed by bacteria, and the internalized substances are captured in endocytic vesicles in the cytoplasm. Due to the abundance of endocytic vesicles, partial disruption does not necessarily lead to cell death.<sup>205</sup> Developing antibacterial agents that target bacteria without damaging normal cells has always been a challenge. Gao et al designed silver-palladium bimetallic alloy nanocages AgPd, which can be catalyzed by the oxidase activity possessed by Pd to generate highly toxic <sup>1</sup>O<sub>2</sub> (Figure 7F–K).<sup>157</sup> The material exploits clathrin-mediated endocytosis in mammalian cells to protect cells from AgPd<sub>0.38</sub> and the surface-bound nature of ROS to preferentially target bacteria. Biosafety and antibacterial experiments also show that it can effectively kill gram-positive and gram-negative bacteria by destroying cell walls and cytoplasmic membranes while maintaining low toxicity, even for MRSA. In contrast, AgPd<sub>0.08</sub> does not have the antibacterial properties of AgPd<sub>0.38</sub>. In addition, AgPd<sub>0.38</sub> is stable at different pH values and temperatures, and

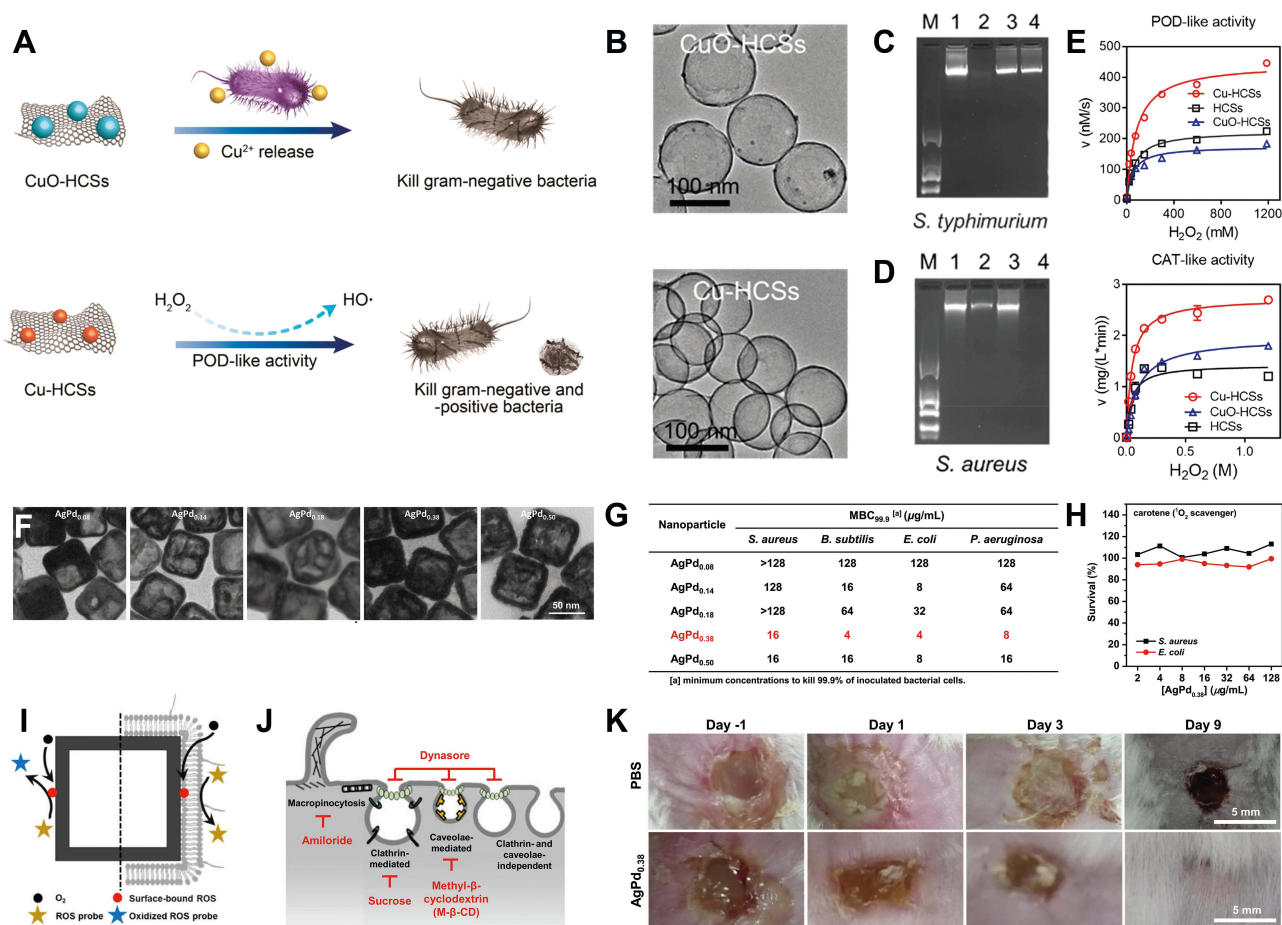


**Figure 7** Metal-based nanozymes. (A) Schematic representation of antibacterial activity of CuO-HCSs and Cu-HCSs. (B) TEM images of copper/carbon nanozymes. (C) Genomic DNA degradation of treated with copper/carbon nanozymes. M, DNA marker; 1, control; 2, CuO-HCSs; 3, Cu-HCSs; 4, HCSs. (D) Genomic DNA degradation of *S. aureus* treated with Cu-HCSs and H<sub>2</sub>O<sub>2</sub>. M, DNA marker; 1, control; 2, Cu-HCSs; 3, H<sub>2</sub>O<sub>2</sub>; 4, Cu-HCSs/H<sub>2</sub>O<sub>2</sub>. (E) Steady-state kinetic assay of POD-like activity and CAT-like activity of copper/carbon nanozymes with varied [H<sub>2</sub>O<sub>2</sub>], respectively. Reprinted with permission from Xi J, Wei G, An L, et al. Copper/Carbon Hybrid Nanozyme: Tuning Catalytic Activity by the Copper State for Antibacterial Therapy. *Nano letters*. 2019;19(11):7645–7654. Copyright 2019, American Chemical Society.<sup>204</sup> (F) Transmission electron microscopy (TEM) images of AgPd nanocages with different Pd content. (G) In vitro antibacterial potentials of AgPd nanocages. (H) Plate-killing assays of AgPd<sub>0.38</sub> in the presence of carotene. (I) Schematic illustration of the strikingly suppressed oxidation of ROS probes in the bulk solution by AgPd<sub>0.38</sub>@lipid, as compared to that by AgPd<sub>0.38</sub>, indicative of effective separation of the ROS generated by AgPd<sub>0.38</sub> from the ROS probes in the bulk solution due to the presence of the lipid bilayer coating, suggesting that the ROS on AgPd<sub>0.38</sub> is surface-bound. (J) Schematic illustration of endocytosis pathways and their respective inhibitors. (K) Photographs of wounds from the two treatment groups throughout the observation window. Reprinted with permission from Gao F, Shao T, Yu Y, et al. Surface-bound reactive oxygen species generating nanozymes for selective antibacterial action. *Nat. Commun.* 2021;12(1):745. Creative Commons license and disclaimer available from: <https://doi.org/10.1038/s41467-021-20965-3>.<sup>157</sup>

when used as a coating additive, it can enable inert substrates to inhibit biofilm formation, which may be an antigenetically encoded and phenotypic antimicrobial resistance. The size of the endocytosed substances has a certain range, which can be considered for the improvement of nanozymes with low toxicity, high antibacterial, and high metabolic properties.<sup>206</sup>

Toxicity is an unavoidable primary challenge for metal nanomaterials. Excessive use of AgNPs can lead to the danger of poisoning and even death, and exposed AgNPs are prone to aggregation after contact with bacteria, thereby reducing the antibacterial efficiency and biocompatibility.<sup>207,208</sup> Liang et al used the binding affinity of phosphorus and metal atoms to load AgNPs into ultrathin two-dimensional (2D) black phosphorus nanosheets (BPNs) to form nanohybrids (BPN-AgNPs).<sup>173</sup> As new ideal photocatalysts, BPNs not only possess tunable bandgaps and high carrier mobility, but also possess unique in-plane anisotropy, which provides a significant stable scaffold. The advantage of hybrid materials lies in the use of BPNs to ensure the slow release of Ag ions and reduce toxicity. In addition, the addition of AgNPs as



electron acceptors solves the problem that the photocatalytic activity of BPNs is limited by light-induced electron-hole recombination and the narrow spectrum of light absorption.

Dressings are powerful candidates as carriers, providing a stable platform for metal nanozymes to function. Hydrogels are 3D hydrophilic polymer networks that retain and absorb water, creating a moist environment suitable for wound healing.<sup>209</sup> In recent years, the construction of stable and effective nanobiocomposites based on hydrogels (carboxymethyl cellulose, lignin-agarose, sodium alginate, CS, etc.) has received extensive attention.<sup>210–215</sup> Jia et al simulated the viscosity of mussel secretions and reduced tannic acid (TA) on Ag nanoparticles in situ to construct an ultra-small self-coagulating hydrogel nanozyme with POD-like activity.<sup>216</sup> The resulting nanozymes are rich in phenolic hydroxyl groups, which not only support the long-term reproducible existence of adhesion, but also enable the nanozymes to be uniformly distributed in the hydrogel to improve mechanical properties and electrical conductivity, and shorten the distance for free radicals to reach bacteria. The POD-like activity can catalyze  $H_2O_2$  in the wound to generate  $-OH$ , and synergize with the inherent antibacterial properties of Ag to kill bacteria. In the antibacterial experiment with *E. coli* as the target strain, the hydrogel achieved an excellent bactericidal effect, and promoted the formation of granulation tissue and collagen deposition. In addition, there are others such as supramolecular-based adhesives, lignin-based hydrogels, and topologically adhesive hydrogels that are also under development, which may be potential candidates for wound antimicrobial therapy delivery platforms.<sup>217–219</sup>

## Metal Oxide-Based Nanozymes

Metal oxide nanomaterials have unique redox and optoelectronic properties.<sup>220</sup> Compared with antibacterial agents such as traditional antibiotics, quaternary ammonium ions, and metal ions, metal oxide nanozymes, like other artificial enzymes, can use enzyme-like activity to catalyze  $H_2O_2$  to exert an antibacterial effect.<sup>171,221</sup> Nanozymes based on metal oxides such as  $Fe_3O_4$ ,<sup>222,223</sup>  $CuO$ ,<sup>224</sup>  $CeO_2$ ,<sup>225</sup>  $VCl_3$ ,<sup>226</sup>  $MoCl_3$ ,<sup>227</sup>  $V_2O_5$ ,<sup>228</sup>  $Tb_4O_7$ ,<sup>229</sup> and  $ZnO$ <sup>230</sup> have been studied in antibacterial aspects, and the construction of multifunctional antibacterial agents from multiple perspectives (Table 2).

The ROS that catalyzes the production of  $H_2O_2$  can effectively decompose the protein, polysaccharide, and nucleic acid components of bacterial biofilms.<sup>22</sup> It has been studied to decompose  $H_2O_2$  by the POD-like activity of  $Fe_3O_4$  metal nanoparticles (MNPs) for cleaning and disinfection.<sup>231</sup> However, in practical applications, ROS are not specific to bacteria, and the survival cycle of ROS is very short. Therefore, shortening the time required for ROS to reach bacteria is a feasible means to improve sterilization efficiency. Ji et al utilized  $Fe_3O_4$  MNPs as catalysts and HA-encapsulated graphene-mesoporous silica nanosheets (GS) as drug carriers to constitute a targeted “on-demand” prodrug ascorbic acid (AA) delivery material (AA@GS@HA-MNPs).<sup>223</sup> The choice of AA as the prodrug is based on the characteristics of non-toxicity and anti-oxidation, which can avoid the generation of free radicals and destroy itself at the same time. Additionally, the light absorption ability brought by GS is used to synergize with the ROS catalyzed by  $Fe_3O_4$  nanoparticles for effective sterilization. The material can effectively destroy the biofilm in situ, significantly shorten the action distance of ROS, and solve the problem of massive inactivation of ROS during the transfer process.

For the infected wound environment, it is a more precise method to adjust the external conditions to activate nanozymes to control the action process, such as light and pH, which can also enhance the activity of some light and nanozymes suitable for acidic conditions.<sup>232,233</sup> Karim et al used visible light as a trigger for semiconducting  $CuO$  nanorods (NRs) with POD-like activity (Figure 8).<sup>224</sup> Experiments showed that the affinity of  $CuO$  NRs for  $H_2O_2$  under visible light irradiation was increased by 4 times compared with the nonirradiated condition, and the further result was that the rate of ROS generation was increased by 20 times. Therefore, the antibacterial efficiency of  $CuO$  NRs triggered by visible light against *E. coli* can be enhanced even at ultralow  $H_2O_2$  concentrations. Studies have demonstrated that the catalytic activity of nanozymes is pH-dependent, which limits their application in infected wounds. Vallabani et al took advantage of the fact that adenosine triphosphate (ATP) can interact with Fe ions,<sup>234</sup> using ATP as a modulator to improve the enzymatic activity of citrate-modified  $Fe_3O_4$  nanozymes.<sup>235</sup> The experimental results show that the nanozyme can catalyze  $H_2O_2$  in a neutral pH environment under the regulation of ATP, and the killing effect on *E. coli* and *Bacillus subtilis* (*B. subtilis*) is improved.

Adjusting the internal conditions of nanozymes is an effective way to control their activity. Martin et al controlled the oxidation state during the synthesis of cerium oxide nanomaterials by liquid feed flame spray pyrolysis, and then

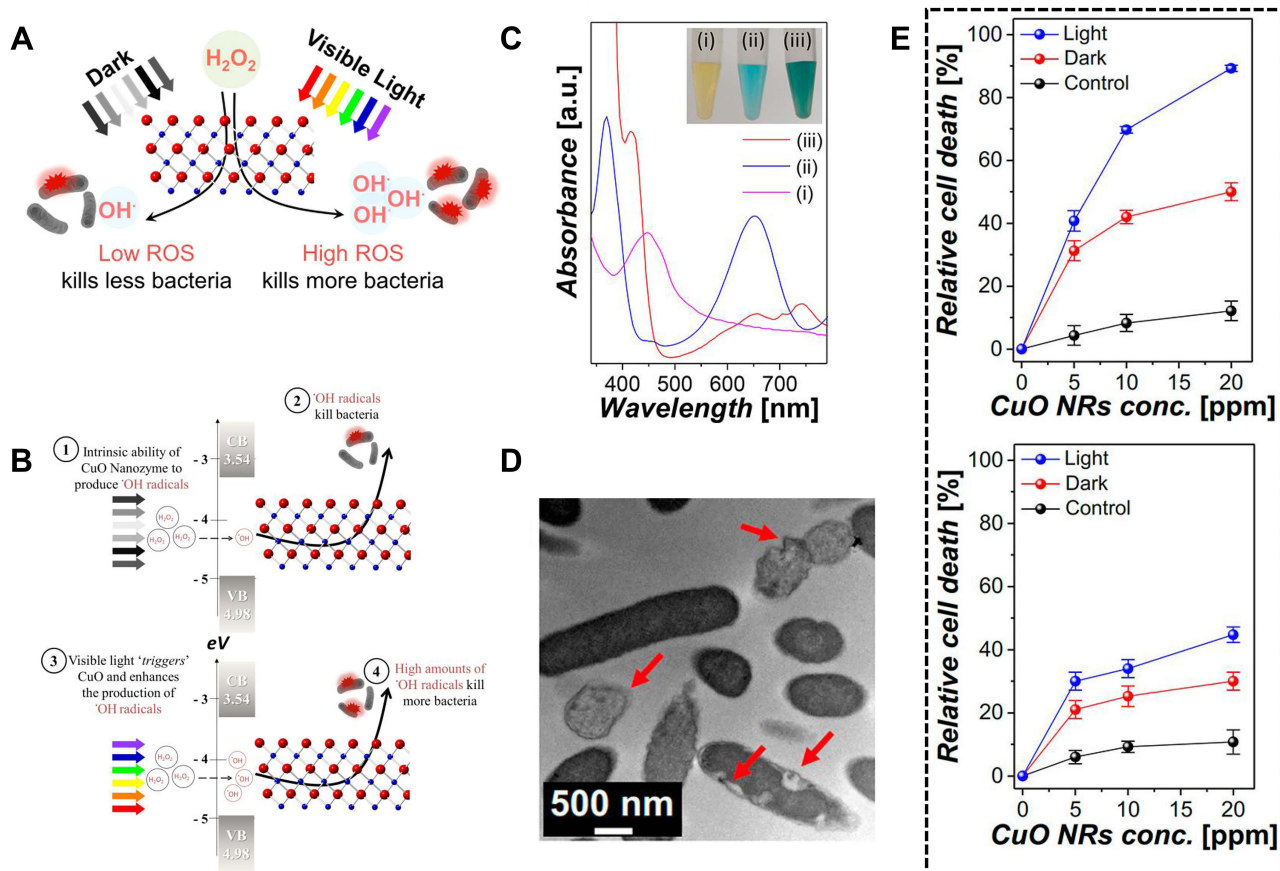


**Figure 8** Metal oxide-based nanozymes. **(A)** Schematic diagram of the action of CuO nanorods (NRs) under dark and visible light illumination. **(B)** Mechanism of Nanozyme-catalysed antibacterial performance of CuO NRs. **(C)** UV-visible absorbance spectra of different peroxidase substrates using CuO NRs in the presence of  $H_2O_2$ : (i) OPD, (ii) TMB, and (iii) ABTS. Insets show the color of post-reaction solutions. **(D)** CuO NRs +  $H_2O_2$  with visible light irradiation. Red arrows showed physical damage of ROS to bacterial cells. **(E)** Light triggered antibacterial performance of CuO NRs at pH 6.0 and pH 7.0, respectively. Reprinted with permission from Karim MN, Singh M, Weerathung P, et al. Visible-Light-Triggered Reactive-Oxygen-Species-Mediated Antibacterial Activity of Peroxidase-Mimic CuO Nanorods. *ACS Appl. Nano Mater.* 2018;1(4):1694–1704. Copyright 2018, American Chemical Society.<sup>224</sup>

combined them with bioglass to form  $CeO_2$ /bioglass hybrid nanozymes.<sup>225</sup> Attempts were made to control the size, oxidation state, and  $Ce^{3+}/Ce^{4+}$  ratio of the nanoparticles, thereby directly changing the catalytic activity of the nanozyme and balancing the antioxidative and antibacterial behavior of the nanozyme. Antibacterial experiments show that  $CeO_2$  rich in  $Ce^{3+}$  has higher antibacterial activity than  $CeO_2$  rich in  $Ce^{4+}$  in a phosphorus-poor environment, but the opposite is true in a phosphorus-rich environment. Therefore, the property that the ratio of metal oxidation states in metal oxide nanozymes affects the enzymatic activity can be a feasible way to design nanozymes adapted to the wound environment.

A single enzyme-like activity is easily limited to the infectious wound microenvironment, and the multifunctional construction of nanozymes is an effective means to improve antibacterial efficiency. Ma et al prepared dual-enzyme active vanadium oxide nanodots ( $VO_x$ NDs) by a one-step ethanol thermal method using  $VCl_3$  as a precursor, which exhibited significant performance against both nonresistant and drug-resistant *S. aureus* and *E. coli*.<sup>226</sup> The POD-like and oxidase-like activities act synergistically in the presence of 50  $\mu M$   $H_2O_2$ , the former induces the decomposition of external  $H_2O_2$  to generate  $\cdot OH$ , and the latter decomposes  $O_2$  to generate superoxide anion radical ( $O_2^{\cdot -}$ ). Compared with the  $H_2O_2$  concentration with the same effect, the  $H_2O_2$  concentration catalyzed by  $VO_x$ NDs was reduced by four orders of magnitude. The material has excellent biocompatibility and can be applied to the research of infected wounds. In addition, combining multiple therapies is also an important means to prevent drug-resistant bacteria and promote wound healing. For instance, photothermal therapy (PTT) can be used to adjust the temperature, and photodynamic therapy (PDT) can be used to increase ROS generation.<sup>236,237</sup> Zhang et al constructed  $MoO_3$ -xND nanozymes by a one-pot hydrothermal method using  $MoCl_3$  as a precursor with POD-like catalysis, photodynamic and photothermal adsorption

capabilities.<sup>227</sup> During the antibacterial process, the enzyme-like activity decomposes  $\text{H}_2\text{O}_2$ , the photodynamic effect mediated by negative ions induces the generation of ROS, and the photothermal effect stimulated by photothermal adsorption adjusts the temperature of the material to  $50\text{ }^\circ\text{C}$  (the optimal enzymatic temperature). Experiments show that  $\text{MoO}_3$ -xNDs have excellent broad-spectrum antibacterial properties and can play a role in low concentrations of  $\text{H}_2\text{O}_2$  ( $100\text{ }\mu\text{M}$ ).

## Chalcogenide-Based Nanozymes

Nanomaterials constructed from metal sulfides offer considerable advantages in electron optics, physicochemistry, functional structure, and fabrication cost. When an enzyme-like active material is constructed, it can synergistically exert its excellent photodynamic properties, providing a feasible way for efficient and highly safe antibacterial materials.<sup>238</sup> For instance, 2D nanomaterials of metal sulfides are more environmentally and biosafety friendly than metals and metal oxides. Although most forms of sulfur are not toxic, the main safety issues of sulfide 2D nanomaterials focus on sulfide metal dissolution and concomitant heavy metal formation.<sup>239</sup> Therefore, it is necessary to pay attention to the detection of stability and safety in the application research of infected wounds. At present,  $\text{MoS}_2$ ,  $\text{CuS}$ , and  $\text{FeS}_2$  nanomaterials have been widely studied due to their intrinsic enzyme-like catalytic activity.<sup>240,241</sup> This section introduces the antimicrobial wound application of chalcogenide-based nanozymes (Table 3).

Because the enzyme-like catalytic activity of chalcogenide itself is not enough for the antibacterial treatment of wounds, most studies focus on how to improve its catalytic performance or synergize with other means. In situ photodynamic sterilization is an efficient antibacterial method, and the inherent optical properties of metal sulfides can exert excellent photocatalytic or photothermal properties.<sup>242</sup> Yi et al prepared polyethylene glycol functionalized molybdenum disulfide nanoflowers (PEG- $\text{MoS}_2$  NFs) with good biocompatibility by a one-pot hydrothermal method, and the antibacterial mechanism was to utilize POD activity to catalyze the generation of  $-\text{OH}$  to enhance the effect of PTT.<sup>168</sup> The POD activity decomposes the low concentration of  $\text{H}_2\text{O}_2$  in the wound to generate  $-\text{OH}$ , and after the bacterial cell wall is destroyed, the permeability and thermal sensitivity are improved. When combined with the thermal effect of PEG- $\text{MoS}_2$  NFs under 808 nm laser induction, the treatment time is shortened. Compared with the separate use of the two antibacterial methods, the synergistic effect appears to be fast and efficient. Notably, the affinity of PEG- $\text{MoS}_2$  for  $\text{H}_2\text{O}_2$  was better than that of horseradish peroxidase (HRP). X-ray photoelectron spectroscopy (XPS) and X-ray near-edge absorption spectra spectrum analysis proved that under the high temperature of light induction, nanozymes can promote the oxidation of GSH to destroy the cell defense system. It showed the ability to quickly kill ampicillin-resistant *E. coli* and endospore *B. subtilis*. Similarly, nanocomposites (UNMS NCs) synthesized by MOF-modified  $\text{MoS}_2$  by Liao et al also possess the ability to promote GSH oxidation under photothermal conditions.<sup>243</sup> UNMS NCs can synergistically sterilize the three antibacterial abilities of photothermal, photodynamic, and POD activity in the presence of 808 nm near-infrared radiation.

Contrary to the above, Yu et al synthesized a photo catalytically enhanced enzyme-like activity nanomaterial  $\text{TiO}_2\text{NTs}@MoS_2$ .<sup>174</sup>  $\text{MoS}_2$  nanoflowers serve as a coating for  $\text{TiO}_2$  nanotubes, which have a high specific surface area and excellent electron transport ability,<sup>244</sup> and the layered structure of  $\text{MoS}_2$  reduces the bandgap of  $\text{TiO}_2$  from 3.2 eV to 2.97 eV, which undoubtedly extends the photoresponse scope. The combination of  $\text{TiO}_2$  greatly improves the POD-like activity of  $\text{MoS}_2$ , and the two components work synergistically to generate abundant ROS for antibacterial treatment under visible light conditions. Meanwhile, bacterial experiments show that  $\text{TiO}_2\text{NTs}@MoS_2$  has a good broad-spectrum antibacterial effect. Alleviating the hypoxia and inflammatory response of wound tissue plays a crucial role in promoting the healing of infected wounds. Thus, Yang et al immobilized TA-chelated Fe-modified molybdenum disulfide nanosheets ( $\text{MoS}_2@TA/\text{Fe}$  NSs) on multifunctional hydrogels, which exhibited excellent antibacterial properties.<sup>245</sup> This is due to the catalase (CAT) activity brought about by the TA/Fe complex, which can decompose  $\text{H}_2\text{O}_2$  into  $\text{O}_2$  in a neutral pH environment, thereby alleviating tissue hypoxia. The photothermal effect and POD-like activity are derived from  $\text{MoS}_2$  NSs, which can catalyze the generation of  $-\text{OH}$  in an acidic environment. The combination of the two materials enables the hydrogel to acquire antioxidant capacity, and the hydrogel inhibits the release of inflammatory factors, which can effectively remove excess ROS and reactive nitrogen species to alleviate the inflammatory response. The phenolic hydroxyl group retained by TA chelation makes

**Table 3** Chalcogenide-Based Nanozymes and Carbon-Based Nanozymes for Improving Bacterial Infectious Wound Healing

Type	Materials	Substrate	Synthesis Procedure	Microbial Type	Antibacterial Mechanism	Antimicrobial Activity	Special Characteristics	Ref.
Chalcogenide-based	nFeS	H <sub>2</sub> O <sub>2</sub> (50 mM)	Solvothermal method	<i>S. mutans</i> , <i>E. coli</i> , <i>P. aeruginosa</i> , <i>S. enteritidis</i> , <i>S. aureus</i> and multidrug-resistant (MDR) <i>S. aureus</i>	Nano-iron sulfides accelerate the release of hydrogen polysulfanes to inhibit enzyme activity, degrade DNA, and accelerate ROS generation	Kill bacteria with 3-log reduction of viability (from 10 <sup>7</sup> to 10 <sup>4</sup> CFU mL <sup>-1</sup> ) within 10 min	The main antibacterial ingredient is polysulfane, H <sub>2</sub> O <sub>2</sub> improves release, broad-spectrum antibacterial	[241]
	PEG-MoS <sub>2</sub> NFs	H <sub>2</sub> O <sub>2</sub> (100 mM), GSH	Facile one-pot hydrothermal route	Ampicillin-resistant ( <i>Ampr</i> ) <i>E. coli</i> , <i>B. subtilis</i>	Accelerates GSH oxidation to destroy cell protection system, generates ROS	Exposure to the 808 nm laser for 10 min, the bacteria inactivation percentages are 97% ( <i>Ampr E. coli</i> ) and 100% ( <i>B. subtilis</i> ), the statistical loss of GSH after 6h is 73.4%	Synergistic treatment of POD and PTT, low concentration H <sub>2</sub> O <sub>2</sub> , controllable	[168]
	UNMS NCs	H <sub>2</sub> O <sub>2</sub> (140 μM)	1, Ice bath 2, Vacuum drying	<i>Ampr E. coli</i> , MRSA	Generates ROS, induce membrane stress and damage cell integrity, accelerate GSH oxidation	The capture efficiency of UNMS NCs was about 22.8% (AREC) and 35.4% (MRSA), in the presence of H <sub>2</sub> O <sub>2</sub> , reduce bacterial viability: AREC (99.7%), MRSA (96.7%)	Positive charge trapping, POD/PTT/ Photodynamic triple-therapy	[243]
	MoS <sub>2</sub> @TA/Fe	H <sub>2</sub> O <sub>2</sub> (100 μM)	Temperature requirement: 220 °C	<i>S. aureus</i> , <i>E. coli</i>	Generates ROS, accelerates GSH oxidation, alleviates hypoxia removes excess ROS and reactive nitrogen species (RNS)	Reduction of survival = ~ 100% ( <i>S. aureus</i> and <i>E. coli</i> ), SEM: Bacterial surface roughening and wrinkling	Combine PTT, GSH loss, and POD/CAT-like activity, anti-inflammatory	[245]
	R-CMs	H <sub>2</sub> O <sub>2</sub> (100 μM)	One-pot hydrothermal method	<i>S. aureus</i> , <i>E. coli</i>	Surface-adhering bacteria, generates ROS	SEM: Bacterial surface roughening and wrinkling	Rough surface increases the adhesion to bacteria, POD-like activity, PTT	[246]

Carbon-based	C-dots	O <sub>2</sub>	1, Heating 2, Column chromatography	<i>E. coli</i> , <i>S. enteritidis</i>	Generates ROS	Inhibition efficiency: 92% ( <i>E. coli</i> ), 86% ( <i>S. enteritidis</i> )	Synthetic controllability, excellent water solubility, PDT POD-like activity and PTT synergy	[260]
	SAF NCs	H <sub>2</sub> O <sub>2</sub> (100 × 10 <sup>-6</sup> M)	“Encapsulated- pyrolysis” strategy	<i>S. aureus</i> , <i>E. coli</i>	Generates ROS, thermal effect	MIC = 62.5 µg mL <sup>-1</sup> (SAF NCs)		[263]
	N-SCSs	H <sub>2</sub> O <sub>2</sub> (10 mM)	Pyrolysis of colloidal silica/ polyaniline assemblies	<i>S. aureus</i> , <i>E. coli</i> , MDR <i>S. aureus</i>	Generates ROS, disrupted cell membranes	SEM: Bacterial surface roughening and wrinkling	Larger surface area, good bacterial adsorption, photoexcitation, lower dose of H <sub>2</sub> O <sub>2</sub> , multienzyme activity	[262]
	o-CNTs	H <sub>2</sub> O <sub>2</sub> (10 mM)	One-pot nitric- acid-assisted reflux method	<i>Ampr E. coli</i> , MRSA	“Competitive inhibition” effect of oxygen-containing groups weakens non-catalytic sites, generates ROS	SEM: Bacterial surface roughening and wrinkling	Synthetic adjustable, POD-like activity, competitive inhibitory effect	[268]
	GQD	H <sub>2</sub> O <sub>2</sub> (1 mM: <i>E. coli</i> , 10 mM: <i>S. aureus</i> )	Modified Hummers method	<i>S. aureus</i> , <i>E. coli</i>	Generates ROS, oxidative lysis of biofilms	Inhibition efficiency = ~ 90%, SEM: Bacterial surface roughening and wrinkling	Lower dose of H <sub>2</sub> O <sub>2</sub> , best catalytic performance = 4 (pH), applied to antibacterial band-aid	[272]

the hydrogel highly viscous, which can fill the wound defect and make close contact with it. Simultaneously, it can also promote the oxidation of GSH, and experiments show that the material has excellent clinical application value.

The roughness of the material surface can improve the adhesion of bacteria, thereby improving the antibacterial efficiency. Cao et al proposed a strategy to construct rough surfaces to expose more active sites and adhere to bacteria.<sup>246</sup> MoS<sub>2</sub> and Cu NWs were composited to construct nanozymes to destroy bacteria by enhancing the affinity for the cell wall and exposing the active site to increase the amount of -OH generation. Similar to the mechanism of action, Wang et al used an ultrasonic exfoliation strategy to fabricate defect-rich N-doped transition metal dichalcogenide nanosheets.<sup>247</sup> Both N-MoS<sub>2</sub> and N-WS<sub>2</sub> NSs exhibited enhanced enzyme-like activity in experiments.

Although natural organosulfur compounds have been used for the prevention of bacterial diseases for a long time, their poor water solubility and difficulty in mass production limit their biomedical applications.<sup>248</sup> Xu et al converted natural organosulfur compounds to inorganic sulfur compounds by a solvothermal method (Figure 9A), and the obtained nanomaterial (nFeS) has more than 500 times higher antibacterial ability than garlic-derived organosulfur compounds.<sup>241</sup> Synthetic nanozymes exhibit universal antimicrobial activity against Gram-positive and Gram-negative bacteria. The POD-like and CAT-like activities of nFeS are better than those of Fe<sub>3</sub>O<sub>4</sub>. The antibacterial activity comes from the rapid oxidation of the nFeS surface under the condition of H<sub>2</sub>O<sub>2</sub>, which accelerates the release of free sulfide (hydropoly-sulfane). In addition, CuS is also a common material for the sulfide construction of nanozymes. Nain et al prepared copper sulfide nanocrystals (BSA-CuS NCs) by heating an alkaline solution containing Cu<sup>2+</sup> and bovine serum albumin (BSA), a facile method that does not require the addition of an additional sulfur source (Figure 9B).<sup>249</sup> BSA-CuS NCs possess abundant surface-active sites and can catalyze H<sub>2</sub>O<sub>2</sub> in situ to generate <sup>1</sup>O<sub>2</sub> and -OH. Moreover, under near infrared (NIR) laser irradiation, BSA-CuS NCs could eradicate 99% of bacteria in MASA-infected wounds within one minute, a more than 60-fold enhanced antibacterial response compared to nonirradiated conditions. Good biocompatibility is also one of the basic elements that BSA-CuS NCs are expected to be used in the clinic. In summary, nanozyme treatment platforms based on metal sulfides have many advantages. In addition to improving enzyme-like activity, the combination of other efficient antibacterial methods also brings more possibilities for wound treatment.<sup>250</sup>

## Carbon-Based Nanozymes

Carbon-based nanomaterials, including carbon dots (CDs), carbon nanotubes, carbon nitride, fullerenes, and graphene, have been widely reported for nanozyme catalytic applications.<sup>251,252</sup> Due to their good biocompatibility, catalytic

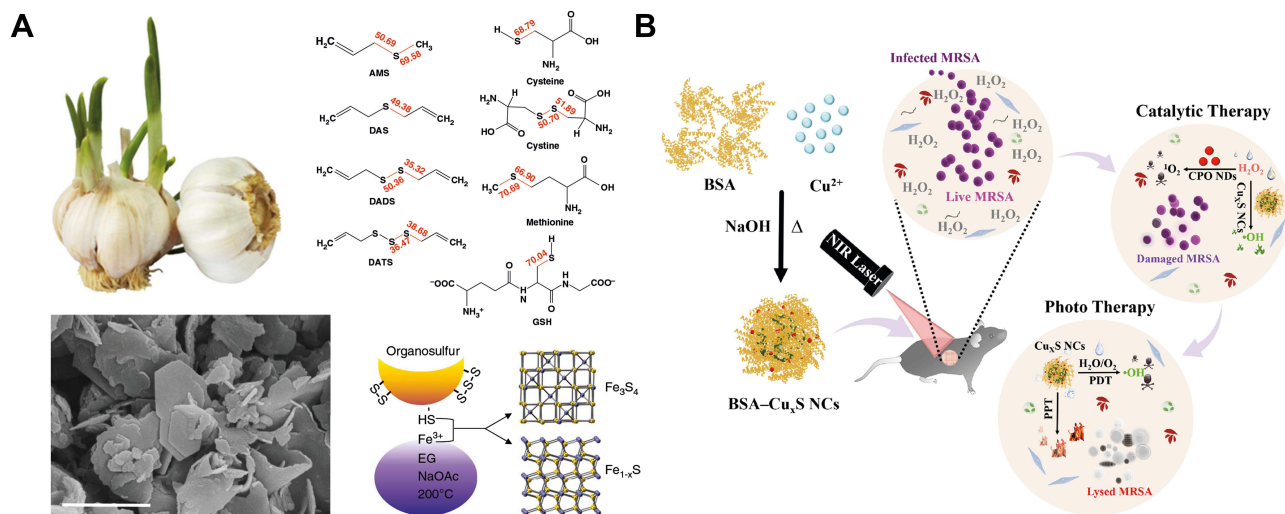


**Figure 9** Chalcogenide-based nanozymes. (A) Converting organosulfur compounds into nano-iron sulfide (nFeS) by solvothermal synthesis. Reprinted with permission from Xu Z, Qiu Z, Liu Q, et al. Converting organosulfur compounds to inorganic polysulfides against resistant bacterial infections. *Nat. Commun.* 2018;9(1):3713. Copyright 2018, Open Access.<sup>241</sup> (B) Schematic representation of the synthesis of the BSA-Cu<sub>x</sub>S NCs and their application for the treatment of bacterial wound infection coupled with NIR laser irradiation. Reprinted with permission from Nain A, Wei SC, Lin YF, et al. Copper Sulfide Nanoassemblies for Catalytic and Photoresponsive Eradication of Bacteria from Infected Wounds. *ACS Appl. Mater. Interfaces.* 2021;13(7):7865–7878. Copyright 2021, American Chemical Society.<sup>249</sup>

properties, and surface functionalization, carbon materials often exhibit intrinsic POD, CAT, hydrolase, and superoxide dismutase activities. The theoretical calculations and experiments helped to reveal that the enzymatic activity of carbon-based materials is derived from the abundant oxygen-containing functional groups on the surface, which has potential application value in the prevention and treatment of infected wounds<sup>253</sup> (Table 3).

CDs are a new type of carbon-based zero-dimensional material with excellent optical properties, stability, and biocompatibility, that have attracted much attention in the development of light-induced sterilization functions.<sup>254,255</sup> Gao et al used *S. cerevisiae* as the precursor-derived fluorescent CDs.<sup>256</sup> Under visible light, photogenerated electrons reacted with oxygen to form superoxide ions, and the bactericidal efficiency against *E. coli* was close to 100% at 120 min. The prepared CD surface is highly negatively charged, capable of selectively staining dead *E. coli* (positively charged) at different excitation wavelengths, and can also be used as a dye for assessing bacterial viability. In addition, the group also prepared novel CDs by a one-pot hydrothermal method using ampicillin as a precursor to generate ROS under visible light irradiation to disrupt the integrity of the cell membrane.<sup>257</sup> Low concentrations (0.7 mg/mL) can also inhibit *Listeria monocytogenes* and *S. aureus*, which are expected to be used in clinical research in infected wounds.

The properties of CDs allow modification of functional groups and doping of different elements.<sup>258,259</sup> Zhang et al synthesized a series of nitrogen-doped CDs related to phosphorescence quantum yield and photooxidative activity, showing higher activity than other carbon nanomaterials, mimicking oxidase production in seconds <sup>1</sup>O<sub>2</sub> with excellent photosensitivity.<sup>260</sup> Under light irradiation conditions, the inhibition efficiency against *E. coli* and *Salmonella enteritidis* (*S. enteritidis*) was 92% and 86%, respectively. Tammina et al used glucosamine as a precursor to synthesize carbon dots (N, Zn-CDs) doped with N and Zn by microwave digestion, which could not only generate ROS under light conditions to kill *E. coli* and *S. aureus*, but also inhibit *E. coli* under dark conditions.<sup>261</sup> In addition, there are nitrogen-doped amorphous carbons (SAF NCs) and nitrogen-doped sponge-like carbon spheres (N-SCS) on bacterial infection, both of which are effective sterilization through POD-like activity synergistic with light effect.<sup>262,263</sup> The anti-infective strategy of synergistic photothermal/photocatalysis with enzymatic activity is currently the main direction in the development of carbon-based nanozymes.<sup>264,265</sup>

The low toxicity of carbon nanotubes (CNTs) makes them exhibit excellent potential in the biomedical field. Using the “competitive inhibition” effect, weakening the noncatalytic sites, and appropriately oxidizing CNTs to enhance the catalytic efficiency are feasible strategies.<sup>266,267</sup> Using pristine carbon nanotubes (p-CNTs) as precursors, Wang et al prepared a series of oxide-rich carbon nanotubes (o-CNTs) by one-pot oxidative reflux method (Figure 10).<sup>268</sup> Through experiments and theoretical calculations, it is found that -OH and -COOH on the surface of o-CNTs act as competing sites and inhibit catalysis, and carbonyl groups act as active sites. Due to the inherent hydrogen bonding interaction and high negative charge, -COOH exhibits stronger inhibitory ability. Therefore, by further preparing 2-bromo-1-acetophenone-modified o-CNTs (o-CNTs-BrPE), after weakening the effect of competitive inhibition, o-CNTs-BrPE in a series of o-CNTs shows the best POD activity. The results of antibacterial experiments showed that o-CNTs not only enhanced the efficiency of ROS generation, but also effectively reduced bacterial-induced purulent inflammation and edema.

Graphene-based nanozymes possess POD-like activity, and their antibacterial properties mainly depend on the number of layers, morphology, size, dispersibility, and electron transport capacity.<sup>269</sup> Notably, studies have shown that graphene quantum dots (GQDs) are less toxic than graphene oxide (GO).<sup>270,271</sup> Sun et al constructed an antibacterial system by combining GQDs and low-concentration H<sub>2</sub>O<sub>2</sub>.<sup>272</sup> During the reaction, the POD-like activity of GQDs converts H<sub>2</sub>O<sub>2</sub> into -OH, which improves the antibacterial properties and avoids unnecessary damage caused by the use of high concentrations of H<sub>2</sub>O<sub>2</sub>. The bacterial experiments showed that the system could significantly inhibit *E. coli* and *S. aureus*. CS functionalization of graphene quantum dots enables synergistic sterilization under light irradiation via multivalent interactions and photothermal, photodynamic, and chemotherapy effects.<sup>273</sup> Furthermore, graphene quantum dots (C60-GQDs) prepared by breaking C60 cages may inherit a nonzero Gaussian curvature, which plays a significant role in association with proteins on bacterial surfaces.<sup>274</sup> Considering reducing toxicity as much as possible, Lin et al prepared tetraaminophthalocyanine-modified graphene oxide nanocomposites by noncovalent functionalization, which can inactivate bacteria at extremely low doses.<sup>275</sup> First, the phthalocyanine photosensitizer generates ROS under 680 nm light irradiation. The second is the physical cleavage of the cell membrane by graphene oxide. Eventually extensive destruction of bacterial morphology occurs, resulting in death.

## MOF-Based Nanozymes

MOFs are highly permeable and crystalline porous coordination polymers formed by assembling organic ligands and metal ions/clusters using the principles of coordination chemistry.<sup>276</sup> MOFs with enzyme-like activity can be obtained by designing organic ligands and metal nodes.<sup>277</sup> As an emerging material, MOFs have emerged as substitutes for enzymes due to their broad coordination capabilities, tunable porosity, mesoporous structure, and customizable cavities and channels.<sup>278,279</sup> In recent years, applications in the fields of gas adsorption/separation, sensing, biomedicine, and catalysis have attracted much attention.<sup>280–284</sup> Compared with traditional antibacterial agents, using MOFs as materials has many advantages. For instance, some metal ions (such as iron ions, gold ions, silver ions, copper ions, zinc ions, and cobalt ions) and nanozymes formed by porphyrin/imidazole can slowly and continuously release toxic metal ions and ROS according to specific conditions (pH, light, temperature, etc.).<sup>285–288</sup> Easily modifiable organic components are beneficial to endow photocatalytic properties and enhance antibacterial ability.<sup>289–291</sup> The high porosity and high specific surface area not only facilitate the surface modification of the material, but also realize the high loading of the contents, and even obtains multieffect antibacterial properties.<sup>292,293</sup> The special structure of MOFs provides a feasible route for the design of more antibacterial agents.<sup>294</sup> In addition, good biocompatibility, dispersibility, and biodegradability are essential for in vivo studies. Numerous advantages have attracted much attention for the design of nanozymes based on MOFs, whose precise framework properties hold a bright future in the treatment of infected wounds<sup>295</sup> (Table 4).

## Natural Enzyme-MOF Composite Nanozymes

The high porosity and surface area of MOFs are good platforms for directly doping natural enzymes. Generally, through the methods of encapsulation, pore penetration, chemical bond connection, and surface adsorption, it can act as an exoskeleton to wrap the natural enzyme and protect it from external stimuli, so the activity of the loaded enzyme can be directly obtained.<sup>296–298</sup> However, the pH of the optimal reaction environment for nanozymes is generally 3–4, and it is often difficult to optimize performance in the microenvironment of infected wounds, which severely limits their application.<sup>299</sup> In general, 2D MOFs have better catalytic activity than 3D MOFs due to their higher specific surface

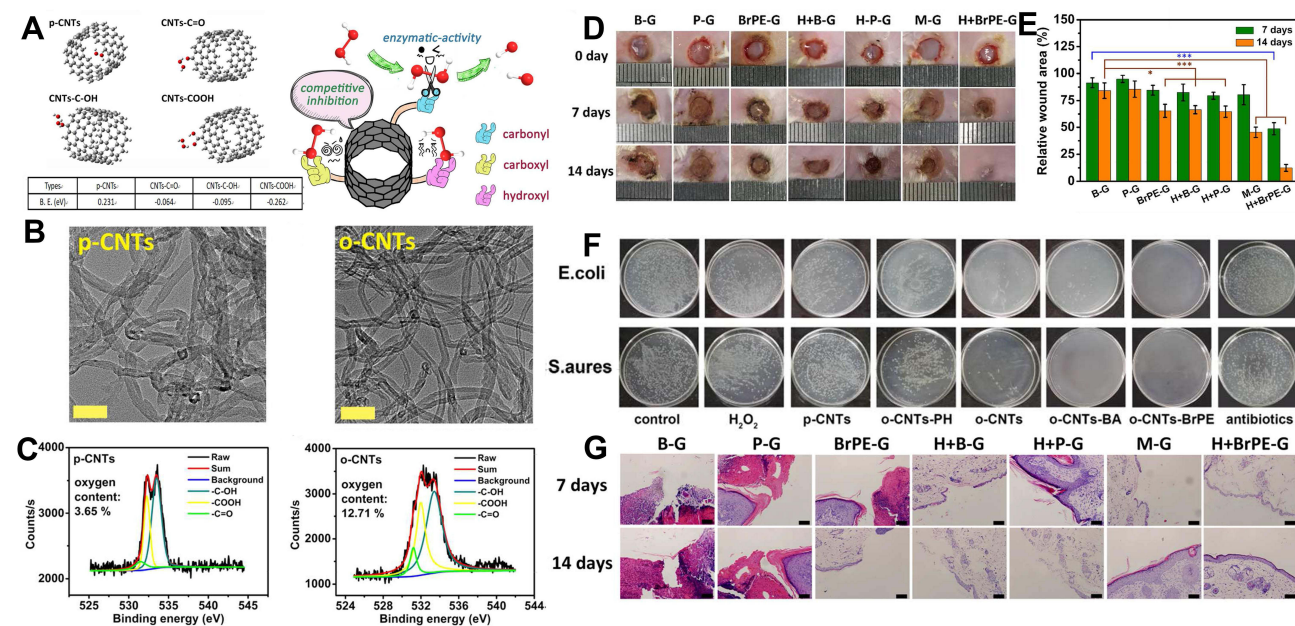


**Figure 10** Carbon-based nanozymes. (A) Binding between  $H_2O_2$  molecule and CNTs. (B) TEM images of p-CNTs and o-CNTs. Scale bars: 50 nm. (C) O1s XPS spectra of p-CNTs and o-CNTs. (D) Time-dependent photographs of wound healing on mouse backs upon different treatments. (E) Quantitative evaluation of wound healing by measuring wound areas. Error bars represent standard deviation from the mean ( $n = 3$ ). Asterisks indicate statistically significant differences ( $*P < 0.05$ ,  $**P < 0.01$ ,  $***P < 0.001$ ). (F) Digital images of the corresponding colonies showed the influence of o-CNTs-based enzymatic activity on the growth of *E. coli* and *S. aureus*. (G) Histological analysis of skin tissues harvested from mice 7 and 14 days post-wounding. Scale bars: 50  $\mu m$ . Reprinted with permission from Wang H, Li P, Yu D, et al. Unraveling the Enzymatic Activity of Oxygenated Carbon Nanotubes and Their Application in the Treatment of Bacterial Infections. *Nano letters*. 2018;18(6):3344–3351. Copyright 2018, American Chemical Society.<sup>268</sup>



**Table 4** MOF-Based Nanozymes for Improving Bacterial Infectious Wound Healing

Type	Nanozymes	Substrate	Synthesis Procedure	Microbial Type	Antibacterial Mechanism	Antimicrobial Activity	Special Characteristics	Ref.
Natural enzyme-MOF	2D Cu-TCPP (Fe)	Glucose, H <sub>2</sub> O <sub>2</sub>	Under mild magnetic stirring	<i>S. aureus</i> , <i>E. coli</i>	Converts glucose to gluconic acid to stimulate POD-like activity, generates ROS	In the presence of glucose, reduce bacterial viability: <i>S. aureus</i> (90%), <i>E. coli</i> (88%), SEM: Bacterial surface roughening and wrinkling	Self-activating cascade system, pH adjustment (3–4)	[172]
	MIL@GOx-MIL NRs	Glucose, O <sub>2</sub> , H <sub>2</sub> O <sub>2</sub>	Water bath	MRSA	Generates ROS, oxidizes glucose to cut off cellular energy supply, inhibits biofilm	Inhibition efficiency>99.9%	Self-activating cascade system, optimum pH = 4 (under 37 °C),	[299]
	GOx-Hb MRs	Glucose (12.5 mM), H <sub>2</sub> O <sub>2</sub>	Co-precipitation process	MRSA	Generates ROS, inhibits biofilm	K <sub>m</sub> and V <sub>max</sub> of GOx-Hb MRs were 2.60 mM and 2.94 × 10 <sup>-8</sup> M s <sup>-1</sup> , respectively	Diabetic wound, action pH = 5	[300]
	I-Arg/GOx@CuBDC	Glucose (10 mM), H <sub>2</sub> O <sub>2</sub>	Package	<i>S. aureus</i> , <i>E. coli</i>	Generates ROS and RNS, Fenton-like effect, decomposition membrane structure	Bacterial inactivation≥97% (38 µg mL <sup>-1</sup> for <i>E. coli</i> and 3.8 µg mL <sup>-1</sup> for <i>S. aureus</i> ), SEM: Bacterial surface roughening and wrinkling	Double-cascade reaction, adhesion properties, multienzyme activity	[305]
Metal-MOF	UsAuNPs/MOFs	H <sub>2</sub> O <sub>2</sub> (100 × 10 <sup>-6</sup> M)	1, Hydrothermal 2, Ultrasonic exfoliation 3, In situ reduction	<i>S. aureus</i> , <i>E. coli</i>	Generates ROS	In the presence of H <sub>2</sub> O <sub>2</sub> , reduce bacterial viability: <i>S. aureus</i> (82%), <i>E. coli</i> (90%), SEM: Bacterial surface roughening and wrinkling	Lower dose of H <sub>2</sub> O <sub>2</sub> , POD-like activity, steady	[310]
	AuNPs/Cu-MOFNs	H <sub>2</sub> O <sub>2</sub>	AuNPs modification	<i>S. aureus</i>	Hot electrons on AuNPs under LSPR excitation activate H <sub>2</sub> O <sub>2</sub> molecules into transition states	Antibacterial effect: close to vancomycin in eight days, SEM: Bacterial surface roughening and wrinkling	Localized surface plasmon resonance, photoexcitation, POD-like activity, the optimum temperature and pH are 60 °C and 6, respectively	[29]
	MOF <sub>-2.5Au-Ce</sub>	H <sub>2</sub> O <sub>2</sub> (0.5 mM), eDNA	1, One-pot hydrothermal method 2, Activated carboxylic acid group	<i>S. aureus</i>	Hydrolyzed eDNA, generates ROS	Complete DNA degradation: 0.5 mg mL <sup>-1</sup> , 3D Confocal Laser Scanning Microscopy: in the Presence of H <sub>2</sub> O <sub>2</sub> , thinner biofilms (<5 µM), SEM: Bacterial surface roughening and wrinkling	Synergy of double enzyme activity, lower dose of H <sub>2</sub> O <sub>2</sub>	[178]

(Continued)

Table 4 (Continued).

Type	Nanozymes	Substrate	Synthesis Procedure	Microbial Type	Antibacterial Mechanism	Antimicrobial Activity	Special Characteristics	Ref.
Derivatives of MOFs	PMCS	H <sub>2</sub> O <sub>2</sub> ((100 μM)	Mesoporous silica protected pyrolysis strategy	<i>P. aeruginosa</i>	Generates ROS	Antibacterial effect: 99.87%	Surface defects, POD-like activity	[25]
	FeN <sub>5</sub> SA/CNF	O <sub>2</sub>	1, Package 2, One-step hydrothermal synthesis	<i>S. aureus</i> , <i>E. coli</i>	Generates ROS	The catalytic rate constant of FeN <sub>5</sub> SA/CNF is 70 times greater than that of the commercial Pt/C	Good stability under strong acid and alkali, OXD-like activity	[322]
	PEG@Zn/Pt-CN	H <sub>2</sub> O <sub>2</sub> (100 μM)	1, Solution coordination 2, Pyrolysis 3, Polyethylene glycol coating treatment	<i>S. aureus</i> , <i>E. coli</i>	Generates ROS, physical cleavage disrupts cell membranes, heat destroys cells	Antibacterial effect: 98.74% ( <i>E. coli</i> ) and 99.63% ( <i>S. aureus</i> ), SEM: Bacterial surface roughening and wrinkling	POD and PTT synergy, optimum pH = 3, photothermal conversion effect = 48%	[325]
Others	V-POD-M	H <sub>2</sub> O <sub>2</sub> (0.1 × 10 <sup>-3</sup> M)	Single-channel oriented assembly method	<i>S. aureus</i> , <i>E. coli</i>	Virus-like spikes disrupt cell membranes, generates ROS, oxidized GSH	MIC ≈ 16 μg mL <sup>-1</sup> MBC = 16 μg mL <sup>-1</sup> , antibacterial effect: close to vancomycin in fifteen days SEM: Bacterial surface roughening and wrinkling	Mesoporous silica-based spike structures trap bacteria, POD-like activity	[315]
	PEG@Zr-Fc MOF	H <sub>2</sub> O <sub>2</sub> (10 × 10 <sup>-4</sup> M)	1, One-pot hydrothermal method 2, Covalent cross-linking	<i>S. aureus</i> , <i>E. coli</i>	Fenton reaction, generates ROS, photothermal effect	Bacterial inactivation: 91.4% ( <i>E. coli</i> ) and 94.7% ( <i>S. aureus</i> ), extinction coefficient at 808nm: 4.60 Lg <sup>-1</sup> cm <sup>-1</sup> , SEM: Bacterial surface roughening and wrinkling	POD and PTT synergy, best temperature: 35 °C	[312]

area. Liu et al encapsulated GOx in an ultrathin 2D MOF (2D Cu-TCPP(Fe)) to form a self-activating cascade employing physical adsorption.<sup>172</sup> In the wound environment, GOx was used to convert glucose into gluconic acid and H<sub>2</sub>O<sub>2</sub> to reduce the pH microenvironment, and coupled with the POD-like activity of Cu-TCPP(Fe), H<sub>2</sub>O<sub>2</sub> was catalyzed to generate highly toxic -OH. While killing bacteria in situ, avoiding the side effects caused by the use of high concentrations of H<sub>2</sub>O<sub>2</sub>, reduces the pH value, greatly improves the catalytic activity of nanozymes, and forms a virtuous cycle. Fluorescence experiments further confirmed the significant enhancement of the catalytic activity of Cu-TCPP(Fe) by gluconic acid, which also has better stability than free GOx. Similarly, Li et al used a coprecipitation method to form a multilayer film on the surface of MnCO<sub>3</sub> with GOx and Hb, and then removed MnCO<sub>3</sub> by slight crosslinking to obtain enzymatic cascade microreactors (GOx-Hb MRs).<sup>300</sup> The Michaelis-Menten constant (K<sub>m</sub>) was 2.60 mM according to by enzyme kinetics theory and method analysis. Compared with other GOx-containing cascade systems,<sup>301,302</sup> the K<sub>m</sub> value of GOx-Hb MRs is lower, which means a better affinity for glucose. Interestingly, GOx-Hb MRs can function in milder acidic environments. Experiments show that pH 5 is not optimal, but the cascade reaction activity remains at approximately 80% of the highest activity, and the intensity of -OH produced is significantly higher than that at pH = 7.4. At a lower concentration (2.4 µg/mL), it can effectively kill MRSA and inhibit the formation of biofilms. It is believed that the high antibacterial efficiency may come from the following two aspects. On the one hand, when bacterial infection occurs and produces mild acidic conditions, GOx-Hb MRs can efficiently catalyze the production of -OH. On the other hand, GOx consumes glucose to reduce the energy supply of bacteria.

Multienzyme nanoassembly is one of the future directions for carrying multiple functions.<sup>303</sup> Inspired by this, Chen et al published the first report of an enzymatic cross-linking reaction for the production of antimicrobial coatings.<sup>304</sup> Using HRP and GOx as catalysts, dendritic polyglycerol (dPG) was cross-linked to the glass surface to form an antibacterial coating l-Arg/GOx@CuBDC. Under extremely low bacterial concentrations (38 µg/L *E. coli*, 3.8 µg/L *S. aureus*), the material can still have an excellent inactivation effect (≥97%). Even with a high bacterial load (OD<sub>540</sub> = 1.0), cell viability can be reduced by more than 40%. Meanwhile, dPG, as a biologically inert polyhydroxy polymer, can reduce bacterial adhesion on the surface of modified objects.<sup>305</sup> The vivo biosafety experiments in mice proved that l-Arg/GOx@CuBDC has low toxicity and can be used in clinical research. The design of these enzymatic-MOFs, especially for targeted therapies, mainly considers the pore size of the MOFs, which affects diffusion and selectivity.<sup>306</sup> Therefore, in addition to maximizing catalytic performance, a fine balance should be considered in the selection of base materials for catalytic systems. In general, the combination of enzymes and MOFs can not only maintain the activity of the enzymes, but also provide high tolerance, enhanced stability under extreme conditions, and reusability, which is an ideal platform for the construction of nanozyme antibacterial agents.<sup>307</sup>

### Metal-MOF Composite Nanozymes

Metal-based nanozymes have superior catalytic activity, but their application is limited by the aggregation phenomenon in the reaction process caused by biosafety and high surface energy.<sup>187</sup> Metals commonly used in the development of MOF antibacterial agents include Cu, Ag, and Ce.<sup>308,309</sup> Hu et al grew ultrasmall gold nanoparticles (UsAuNPs) on ultrathin 2D MOFs by in-situ reduction to prepare nanozyme UsAuNPs/MOFs.<sup>310</sup> Although UsAuNPs have a large surface energy, small diameter, and abundant active sites, they are prone to aggregation, so MOFs can provide an excellent reaction platform for them. UsAuNPs/MOFs have good stability, which can reduce the mass transfer resistance and improve the reaction speed, and play a role in cooperation with Au nanoparticles. The experimental results show that UsAuNPs/MOFs can catalyze the generation of -OH through POD-like activity at a safe dose of H<sub>2</sub>O<sub>2</sub> (100 × 10<sup>-6</sup> M), which can effectively sterilize *E. coli* and *S. aureus*. Metal nanoparticle surfaces have unique localized surface plasmon resonance (LSPR) properties. Yang et al took advantage of the LSPR excitation of AuNPs to enhance the intrinsic POD-like activity of copper metal-organic frameworks (Cu-MOFNs).<sup>29</sup> The prepared AuNPs/Cu-MOFN composite nanozyme effectively promotes the transfer of hot electrons due to the LSPR excitation and matching energy levels, further cleaving the chemical bonds of the substrate, and the reaction kinetics are 1.6 times faster than those under dark excitation. Thus, the enzyme-like activity of the composite material is greatly enhanced.

The use of Ag ions must carefully consider biological safety, and the combination with enzyme-like materials can reduce toxicity hazards to a certain extent. Zhang et al implanted Ag ions into NH<sub>2</sub>-MIL-88B(Fe) material with POD-like

activity to construct  $\text{NH}_2\text{-MIL-88B(Fe)-Ag}$ .<sup>41</sup> In the reaction process, the synthesized material can effectively catalyze  $\text{H}_2\text{O}_2$  to generate  $\text{-OH}$ , and release Ag ions at the same time, avoiding the damage caused by the use of high-concentration Ag ions and  $\text{H}_2\text{O}_2$ . To enable ROS catalyzed by nanozymes to efficiently sterilize, targeting the destruction of biofilms is an effective antibacterial strategy. Liu et al assembled the surface of a Ce nitrilotriacetic acid (NTA) complex and Au-doped MOF MIL-88B(Fe) by a one-pot hydrothermal method to obtain nanozyme MOF-Au-Ce.<sup>178</sup> The Ce center excites the phosphodiester bond after removing the electron from the phosphate, which leads to nucleophilic attack by  $\text{-OH}$ , and finally cleaves the P-O bond of the biofilm DNA. The introduction of Au enhanced the POD-like activity of the pristine MOFs. Different Au doping results in different changes in catalytic ability, among which MOF-2.5Au-Ce has the best catalytic ability. The ROS catalyzed by MOFs synergistically inhibited *S. aureus* by hydrolyzing the biofilm of eDNA by the Ce complex; while attenuating the inflammatory response. Although the current research on antibacterial nanozymes of metal-MOFs is not deep enough, it is expected to play a potential role in the application of infected wounds.

### Other Composite Nanozymes

Targeting is an effective strategy for high-efficiency antibacterial activity. Metabolic biomarker technology can attach chemical functional groups to the surface of bacteria.<sup>311</sup> Mao et al loaded the in vivo metabolic marker molecule 3-azido-D-alanine (D-AzAla) onto MIL-100(Fe)NPs by coupling MOF and metabolic technology.<sup>295</sup> During the reaction, the iron (III) metal center of MIL-100(Fe) can catalyze  $\text{H}_2\text{O}_2$ . The dissociation of MIL-100(Fe) occurs after the coordination cleavage of the melamine acid ligand with iron (III), thereby releasing D-AzAla. Using this principle of action, the material can specifically release D-AzAla in wounds with excessive secretion of  $\text{H}_2\text{O}_2$ , and then selectively integrate into the cell wall of bacteria to achieve metabolic labeling of bacteria in vivo. Animal and fluorescence experiments demonstrate that, with the assistance of MOFs, the synthetic material enables precise bacterial detection and PDT.

The ease of modification of MOF materials facilitates the synthesis of multi-therapeutic-conjugated nanozymes. Wang et al constructed a photothermal-nanozyme-hydrogel synergistic antibacterial platform.<sup>312</sup> First, 2D zirconium-ferrocene metal-organic framework nanosheets (Zr-Fc MOF) with enzymatic activity and photothermal properties were synthesized by a one-pot hydrothermal method, and then polyethylene glycol dicarboxylic acid (COOH-PEG-COOH) was used to functionalize the 2D Zr-Fc MOFs and then intercalate them into carrageenan-based hydrogels to form PEG@Zr-Fc MOF hydrogels. The intercalation of nanozymes modifies the pores of the carbon skeleton supported by carrageenan, and the encapsulation of hydrocolloids avoids the release of metal heteroatoms during the reaction process and reduces biological toxicity. In addition, the photothermal effect of Zr-Fc MOF enhanced the efficiency of catalyzing  $\text{H}_2\text{O}_2$  to generate  $\text{-OH}$ , and wound infection model experiments also confirmed that the hydrogel can efficiently kill *E. coli* and *S. aureus*, and promote rapid tissue recovery. This strategy overcomes the dilemma of single PTT and single MOF catalysis limited by insufficient activity, light irradiation time, wound microenvironment, etc.<sup>313</sup>

Viral phages have spiny tails that enable them to trap and kill bacteria.<sup>314</sup> If artificial nanozymes mimic this behavior, they need to satisfy two structures, mesoporous and pointed; the former is used to load and release bactericidal substances, and the latter is used to trap bacteria. Inspired by this, Ye et al developed a peroxidase mimetic (V-POD-M) with a virus-like structure based on Cu-MOF.<sup>315</sup> The POD-M cascade catalytic center derived from MOF catalyzes the generation of  $\text{-OH}$  from  $\text{H}_2\text{O}_2$  by simulating POD-like activity.<sup>316</sup> Density functional theory (DFT) calculation results show that MOF-supported  $\text{MoO}_3$  acts as a peroxy complex intermediate, which promotes the Fenton-like catalytic activity of Cu (II) and reduces the free energy of catalyzing  $\text{H}_2\text{O}_2$ , thereby enhancing the productivity of ROS. In addition, the synergistic mesoporous silicon-based spiky structure has a nearly 100% inactivation effect at extremely low concentrations (16  $\mu\text{g/mL}$  V-POD-M,  $0.1 \times 10^{-3}$  M  $\text{H}_2\text{O}_2$ ), similar to the antibacterial effect of vancomycin. Biomimetic spiked structures have a promising future in the development of nonantibiotic antibacterial agents. Even for MOF materials with many properties, there are inevitably some inherent defects in exploration. Therefore, MOFs are formed into composites with other components to compensate for defects or even to obtain additional properties for synergistic antimicrobial activity.<sup>317</sup> In the future trend of multifunctional and intelligent treatment modes, MOF composites have bright prospects.

## Derivatives of MOFs

Although nanozymes have catalytic activity comparable to that of natural enzymes, most nanozymes still have limited solubility and intrinsic catalytic activity under physiological conditions. For instance, metal oxide-based ( $\text{Fe}_3\text{O}_4$ ,  $\text{V}_2\text{O}_5$ ,  $\text{CeO}_2$ ) nanozymes have a large number of internal atoms that are inert or cause unnecessary side reactions. Due to the versatility and postsynthesis modifiability of organic ligands and metal node linkages, MOF derivatives are one of the ideal alternatives to solve these difficulties.<sup>182</sup> The porous materials derived after calcination and their uniformly distributed atomic doping not only retain the excellent mesoporous properties of the precursor MOFs, but also the changes in structure and element valence further enhance the catalytic activity.<sup>318</sup>

In the research of antibacterial agents, single-atom nanozymes have become the research frontier because of their abundant active sites and high atom utilization, coupled with a clear definition of the coordination environment and electronic structure, so it is easier to analyze the catalytic mechanism and understand the structural properties.<sup>319–321</sup> Xu et al reported Zn-containing porphyrin-like structure carbon nanospheres (PMCS) derived from zeolite imidazolate framework 8 (ZIF-8) MOFs as precursors through a protective pyrolysis strategy (Figure 11A–D),<sup>25</sup> which not only have photosensitive properties, but also significant POD-like activity. The researchers believe that the coordinative unsaturation of the Zn- $\text{N}_4$  site is the reason for the high POD activity, which catalyzes the decomposition of  $\text{H}_2\text{O}_2$  to generate  $\cdot\text{OH}$  for sterilization. In the mouse wound model, the inhibition rate of *P. aeruginosa* was as high as 99.87%, which significantly promoted wound healing. In addition, Huang et al formed  $\text{FeN}_5\text{SA}/\text{CNF}$  single-atom nanozymes after pyrolysis of MOF-encapsulated iron phthalocyanine (FePc) ( $\text{FePc}@/\text{Zn-MOF}$ ) under  $\text{N}_2$  at 900 °C.<sup>322</sup> During the pyrolysis process, the secondary building blocks of nitrogen-containing organic linkers are transformed into pyridine-

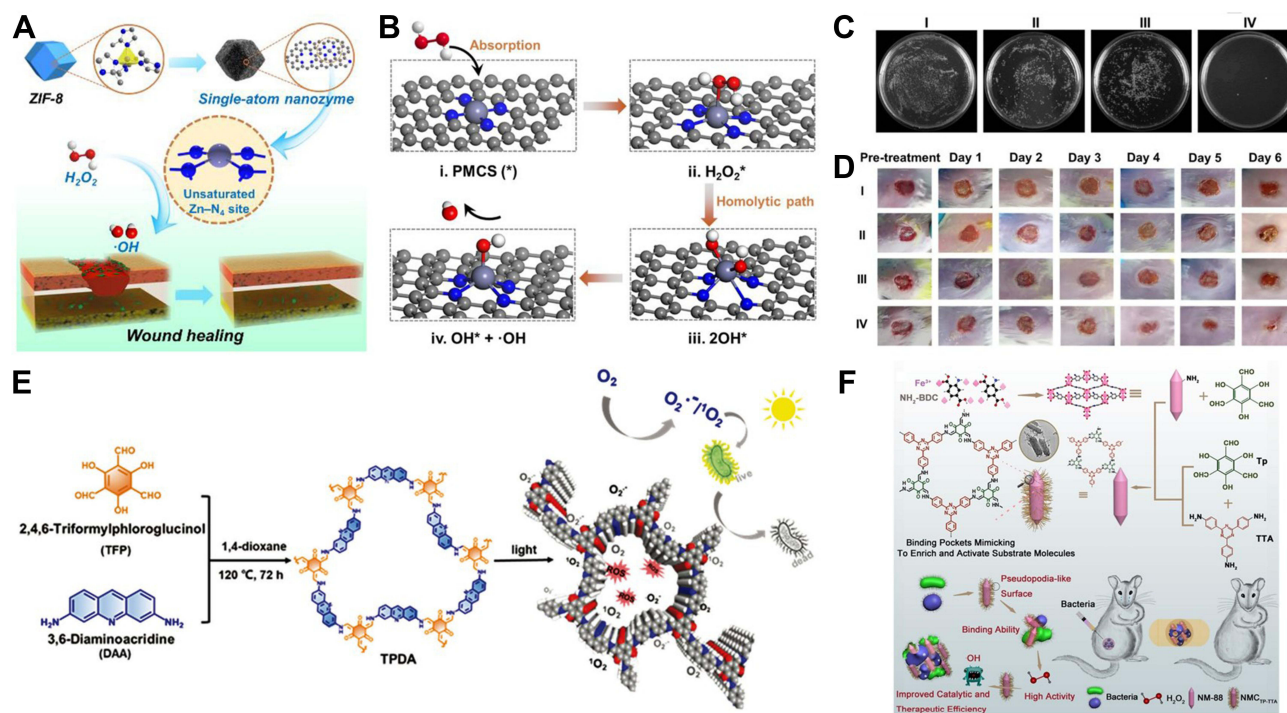


**Figure 11** MOF-based nanozymes and COF-based nanozymes. **(A)** Schematic diagram of PMCS promoting wound healing. **(B)** Schematic diagram of catalytic mechanism. \*Represents the active site on the PMCS (eg,  $\text{H}_2\text{O}_2$  \*Indicates that the  $\text{H}_2\text{O}_2$  molecule binds to the Zn- $\text{N}_4$  active site on the PMCS). **(C)** Photographs of bacterial colonies formed by *P. aeruginosa* after exposed to (I) NaAc buffer, (II) NaAc buffer +  $\text{H}_2\text{O}_2$ , (III) PMCS and (IV) PMCS +  $\text{H}_2\text{O}_2$ , the final working concentrations for NaAc buffer,  $\text{H}_2\text{O}_2$  and PMCS are 0.1 M, 100  $\mu\text{M}$  and 100  $\mu\text{g mL}^{-1}$ , respectively. **(D)** Photographs of *P. aeruginosa* infected wound treated with (I)–(IV) at different days. Reprinted with permission from Wiley, Xu B, Wang H, Wang W, et al. A Single-Atom Nanozyme for Wound Disinfection Applications. *Angew Chem Int Ed Engl.* 2019;58(15):4911–4916. © 2019 Wiley-VCH Verlag GmbH & Co. KGaA, Weinheim.<sup>25</sup> **(E)** Schematic diagram of TPDA preparation and the mechanism of ROS generation. Reprinted with permission from Wiley, Zhang C, Guo J, Zou X, et al. Acridine-Based Covalent Organic Framework Photosensitizer with Broad-Spectrum Light Absorption for Antibacterial Photocatalytic Therapy. *Adv. Healthc. Mater.* 2021;10(19):e2100775. © 2021 Wiley-VCH GmbH.<sup>361</sup> **(F)** The synthesis of NMCTp-TTA hybrid nanozyme and their use for bacterial inhibition. Reprinted with permission from Wiley, Zhang L, Liu Z, Deng Q, et al. Nature-Inspired Construction of MOF@COF Nanozyme with Active Sites in Tailored Microenvironment and Pseudopodia-Like Surface for Enhanced Bacterial Inhibition. *Angew Chem Int Ed Engl.* 2021;60(7):3469–3474. © 2020 Wiley-VCH GmbH.<sup>369</sup>

type N carbon nanoframes and Zn ions after carbonization. The reconstitution sites within the confinement of the pyridine N substrate and the FeN<sub>4</sub> carbon nanoframe coordinate with each other to form FeN<sub>5</sub>/C sites with better thermal stability. Through DFT calculations, the high oxidase catalytic activity is derived from the central metal atom and spatial configuration, and its active site is very similar to the heme coordinated by the axial ligands of natural oxidoreductases. Interestingly, due to the axial N coordination enhancing the catalytic activity, the enzymatic activity of FeN<sub>5</sub>SA/CNF is 17 times higher than that of square-planar Fe-N<sub>4</sub>. Despite the numerous advantages of single-atom nanozymes, the active site relies on a larger support. Therefore, it is easily cleared by the immune system and reduces the antibacterial efficiency in the body. Therefore, adjusting the size of the support and modifying the functional groups is a feasible way to achieve high antibacterial activity and excellent biocompatibility.<sup>323</sup>

As mimic enzymes, metal nanomaterials have unpredictable and nonuniform distributions and uncontrollable aggregation phenomena. When the size of metal atoms in M-N-C nanozymes increases to be similar to that of nanoparticles, MOFs are easily converted into porous carbon after calcination, and the derived metal/carbon nanozymes can prevent the aggregation of isolated MNPs and enhance the catalytic ability.<sup>324</sup> Wang et al constructed a hybrid nanozyme PEG@Zn/Pt-CN with photothermal, “nanoknife” and enzymatic catalysis through an MOF-derived strategy.<sup>325</sup> By effectively preventing the aggregation of Pt nanoparticles, the kinetic mass transfer resistance of the reaction process and the inhibition of photoelectron-hole complexation were reduced, which ultimately led to the improvement of the peroxidase-like catalytic and photothermal conversion performance of PEG@Zn/Pt-CN. The experimental results show that under the condition of a low concentration of H<sub>2</sub>O<sub>2</sub>, PEG@Zn/Pt-CN can generate a large amount of -OH and increase the permeability of the biofilm. In addition, when the NIR laser is introduced, it can also exert the effect of a “nano-knife” to physically damage bacteria. The bactericidal efficiencies against *E. coli* and *S. aureus* were 98.74% and 99.63%, respectively.

Metal oxide/carbon nanostructures constructed by immobilizing metal oxides on carbonaceous structures have stronger catalytic performance and make up for some shortcomings of traditional metal oxide nanoparticles, such as irregular distribution of active sites and aggregation.<sup>326,327</sup> Fan et al reported a MOF-derived 2D carbon nanosheet for anti-infective therapy.<sup>328</sup> The 2D nanomaterials (TRB-ZnO@G) were formed by anchoring carbon on MOF-derived ZnO-doped graphene (ZnO@G) with a phase-change thermally responsive brush via in-situ polymerization. The high photothermal activity and Zn ion release ability is synergistically antibacterial, and the sterilization rate is close to 100% under short time and low concentration conditions. The controllable porosity, good physical/chemical stability, high electrical conductivity, and high catalytic activity of MOF derivatives make them strong candidates for multifunctional materials. Simultaneously, it is also difficult to effectively control the properties (morphology, surface area, and composition) of calcined MOF materials due to various factors during the synthesis process. Achieving an effective controllable design in the development of antibacterial nanozymes is a future challenge.<sup>33,318,329,330</sup>

## COF-Based Nanozymes

COFs are nontoxic, stable, green, low-cost, and tunable emerging porous crystalline materials.<sup>331–334</sup> The monomer design of COFs exploits the principles of directional bonding established by coordination polymers and supramolecular assemblies.<sup>335,336</sup> COF-based nanomaterials have a wide range of applied research in the medical field, including acting as carrier/ligand for antibiotics, tumor therapy, photodetectors, aptasensors, photodynamics, and photocatalysis.<sup>337–341</sup> Although there are few studies on the use of COFs to construct nanozymes for the treatment of bacterial infectious wounds, COFs have many characteristics that are suitable for designing nanozymes (Table 5). First, it is highly adjustable and can be used as a platform.<sup>342–345</sup> Second, structural ordering is conducive to catalysis, membrane construction, and material characterization.<sup>346</sup> Then, with high porosity and low density, COFs with uniform void distribution and composed of light elements are a potential basis for loaded drugs for targeted therapy and high gravimetric performance.<sup>347–349</sup> Finally, the stability is excellent. COFs linked by stable covalent bonds maintain a high degree of morphology in extreme pH, temperature, and solvent, with higher stability than most MOFs.<sup>350–354</sup>

Photosensitive fungicides have been studied in silver nanoparticles, copper, oxides, porphyrin derivatives, and phthalocyanines.<sup>249,355–358</sup> The key question is how to solve, and improve the absorption range of the spectrum, toxicity, and photostability.<sup>359</sup> In contrast, the rich pore structure and conjugated structure of COFs provide a possibility for the

**Table 5** COF-Based Nanozymes for Improving Bacterial Infectious Wound Healing

Materials	Substrate	Synthesis Procedure	Microbial Type	Antibacterial Mechanism	Antimicrobial Activity	Special Characteristics	Ref.
GFeF	Glucose (15 mM), H <sub>2</sub> O <sub>2</sub>	1, Fe chelation 2, GOx loading	<i>E. coli</i> , <i>S. aureus</i>	Generates ROS	SEM: Bacterial surface roughening and wrinkling	Cascade reaction, optimum pH = 4, electrostatic adsorption	[364]
NMC <sub>TP</sub> -TTA	H <sub>2</sub> O <sub>2</sub> (10 mM)	Sequential growth	<i>E. coli</i> , MRSA	Generates ROS, surface pseudopodia tear at cell walls and deform structures	SEM: Bacterial surface roughening and wrinkling	Binding pocket structure to strengthen catalysis, COF pseudopodia surface catches bacteria, POD-like activity, in situ generations of -OH	[369]

design of antibacterial agents.<sup>360</sup> Zhang et al synthesized a photosensitizer (TPDA) with multiple active sites by condensing 2,4,4-triformylphloroglucinol (TFP) and 3,6-diaminoacridine (DAA) with Schiff bases (Figure 11E).<sup>361</sup> Due to the excellent light-harvesting ability of DAA and the increased conjugation effect brought by the COF framework, the light-converting ability of TPDA has been improved, and the high specific surface area exposes more active sites, which can be used in a short time (10 minutes) of light. This result showed the high killing effect of *S. aureus* and *E. coli* under irradiation. In addition, the abundant pore structure can facilitate the rapid arrival of ROS to the infection site. Although fish skin was selected for animal experiments, the good biocompatibility of TPDA makes it potentially applicable to humans.

The hyperglycemic microenvironment of diabetic wounds is an important factor leading to angiogenesis dysfunction and bacterial proliferation, and GOx is used to degrade excess glucose.<sup>362,363</sup> Li et al prepared an ionic COF nanozyme (GFeF) that indirectly generates H<sub>2</sub>O<sub>2</sub> by a three-step method.<sup>364</sup> The loaded GOx produces gluconic acid and H<sub>2</sub>O<sub>2</sub> in the wound, and then mimics the indirect production of H<sub>2</sub>O<sub>2</sub> catalyzed by POD activity. Simultaneously, the positive charge characteristic of the composite material improves the adhesion of the synthetic material to the bacterial membrane and realizes the in-situ catalytic release of -OH. Therefore, the H<sub>2</sub>O<sub>2</sub> indirectly generated by the cascade reaction triggered by glucose in the wound not only avoids direct damage to normal cells, but also has good antibacterial properties. Notably, the nanozyme can also be incorporated into injectable thermals to synergistically promote the healing of infected wounds. The same principle has also been studied in MOF-based nanozymes.<sup>365</sup>

The structure of the natural enzyme binding pocket can provide a friendly reaction microenvironment for the active center, which is beneficial to improve the catalytic efficiency.<sup>366,367</sup> Then COFs or MOFs can be used as the main framework, and then the functional groups on the surface can be adjusted to surround the active site to form a customized microenvironment.<sup>333,368</sup> Zhang et al constructed the MOF@COF nanozyme (NMCTP-TTA) for the first time (Figure 11F).<sup>369</sup> Surface COFTP-TTA was formed using ligands of phenol (weak acid) and triazine (basic functional) groups on amino-functionalized POD-like NH<sub>2</sub>-MIL-88B(Fe)(NM-88) modified. Then, the COFTP-TTA-grown custom hierarchical nanocavities were used as enzyme-binding pockets to form pore microenvironments around the metal active sites of the MOF. The binding pocket structure enables the collection of substrate molecules for catalysis through noncovalent interactions. In addition, the pseudopod-like structures on the surface of COFs can effectively capture bacteria and kill them by in situ generated ROS, showing excellent antibacterial effects in antibacterial and animal experiments. The design of such multifunctional enzymes may provide new ideas for the treatment of infected wounds.

Currently, the antibacterial research of COF-based materials is more focused on photoexcitation and drug delivery, such as porphyrin-based and triazine-based materials, among which conjugation modulation is one of the new strategies to enhance photosensitivity.<sup>370–374</sup> However, the design of nanozymes is scarce, and it is expected that more antimicrobial agents can be derived by exploiting the advantages of COF.

## Conclusion, Challenges, and Outlook

Wound healing is one of the great challenges facing modern medicine. Insufficient knowledge of pathophysiology and histiocyte recovery has limited the availability of medicinal materials for clinical infectious wound treatment. This means that new approaches are needed to make improvements to current treatment strategies. Currently, a series of artificial nanozymes is being developed with the advancement of biotechnology and nanotechnology. As potentially useful enzyme activity mimics, nanozymes not only show excellent performance in sensing, pollutant treatment, cancer treatment, ROS scavenging, and biopharmaceuticals, but also have the advantage of replacing antibiotic therapy in the clinical treatment of infected wounds. In this review, we address the pathophysiology of wound healing and the pitfalls of therapeutic approaches. The antibacterial advantages and antibacterial mechanisms of nanozymes and the research progress in the field of infected wounds are summarized. Current research on nanozymes has overcome many limitations of natural enzymes, such as complex preparation and storage, and poor stability. From our perspective, there are still challenges and obstacles that cannot be underestimated in future research.

1. Compared with most natural enzymes, the preparation price, stability, and reproducibility of nanozymes are well optimized. However, large-scale fabrication applications, such as the development of alternatives to noble metal nanozymes and further improving the physiological stability of pristine MOFs, should be considered. Simultaneously, antibacterial properties should be guaranteed.
2. At present, because of the lack of substrate specificity of nanozymes, their further application in wound healing is limited. Researchers have identified many factors that influence catalytic performance by positive and negative charge interactions, pH, GSH, and laser to confer the ability to target bacteria or biofilms with nanozymes. However, the complex composition of bacterial colonies and biofilms may attenuate these abilities. How to achieve substrate specificity and precise control of external conditions for multienzyme active nanozymes should receive more attention in the future.
3. In recent years of rapid development, research on nanozyme antimicrobial agents has been more focused on synthesis, treatment and application. The catalytic mechanism is fundamental to understanding the catalytic reactions of nanozymes, especially the relationship between catalytic performance and microstructure from the whole material to the atomic to the electronic structure. In contrast, in-depth studies and targeted mechanistic research strategies involving the mechanism of action are less available.
4. The pH of the optimal action environment for most nanozymes is acidic, which is not favorable for practical applications. It is worth exploring the physiological environment that can be stimulated in infected wounds to maintain excellent catalytic activity.
5. In the field of antimicrobial activity, POD-like nanozymes have received extensive attention. Therefore, other oxidoreductases (eg, OXD, CAT, SOD, GSH-Px) should also be promoted for utilization.
6. Due to the complex structure of nanozymes, some work affects the overall material properties only through the material surface. Other works precisely control the atomic distribution, content and structure of nanomaterials by adjusting the synthesis strategy. For example, MOFs with desirable catalytic activity are synthesized by the rational design of organic linkers and metal nodes to mimic the coordination environment of metal cofactors in natural enzymes. Currently, most MOF-derived nanozymes start from the ZIF series. Therefore, the development of other synthetic strategies and the discovery of other starting materials can provide new opportunities for nanozyme applications.
7. The long-term in vivo toxicity of nanozymes cannot be ignored in clinical applications. Although most nanozyme research involves biocompatibility, there is a lack of toxicity mechanism explanations and corresponding solutions. Attention should be paid to potential metabolic accumulation impairment and carcinogenicity, especially nanozymes that require in vivo administration and may favor accumulation in the liver and spleen. First, we can try to design nanomaterials of smaller sizes that can be metabolized through the kidneys and reduce retention. Second, nanozymes that can degrade in physiological environments should be constructed. Since there are currently few studies on renal metabolism and biodegradability, it would be valuable to conduct more in-depth studies.



8. Currently, there is no report of bacterial resistance to ROS. Considering the sustainability of the practical application of nanozymes, long-term observation of changes in this aspect is necessary. In this rapidly developing field, it is highly expected that the use of nanozymes in infected wounds will enable dazzling advances in medical antimicrobials.

## Abbreviations

ROS, reactive oxygen species; H<sub>2</sub>O<sub>2</sub>, hydrogen peroxide; PMNs, polymorphonuclear neutrophils; NADPH, nicotinamide adenine dinucleotide phosphate; *S. aureus*, Staphylococcus aureus; *P. aeruginosa*, Pseudomonas aeruginosa; QS, dendritic cells; AMPs, antimicrobial peptides; CS, chitosan; *E. coli*, Escherichia coli; HA, hyaluronic acid; MOF, metal-organic framework; COF, covalent-organic framework; POD, peroxidase; -OH, hydroxyl radical; <sup>1</sup>O<sub>2</sub>, singlet oxygen; GOx, glucose oxidase; eDNA, environmental DNA; BME, biofilm microenvironment; GSH, glutathione; MRSA, methicillin-resistant Staphylococcus aureus; MNPs, metal nanoparticles; AA, ascorbic acid; NRs, nanorods; ATP, adenosine triphosphate; *B. subtilis*, Bacillus subtilis; O<sup>2-</sup>, superoxide anion radical; PTT, photothermal therapy; PDT, photodynamic therapy; XPS, X-ray photoelectron spectroscopy; CAT, catalase; BSA, bovine serum albumin; NIR, near infrared; CDs, carbon dots; *S. enteritidis*, Salmonella enteritidis; CNTs, carbon nanotubes; p-CNTs, pristine carbon nanotubes; o-CNTs, oxide-rich carbon nanotubes; GQDs, graphene quantum dots; GO, graphene oxide; MRs, microreactors; Km, Michaelis-Menten constant; dPG, dendritic polyglycerol; LSPR, localized surface plasmon resonance; NTA, nitrilotriacetic acid; D-AzAla, 3-azido-D-alanine; DFT, density functional theory; ZIF-8, zeolite imidazolate framework 8; TFP, 2,4,4-trifluoromethylphloroglucinol; DAA, 3,6-diaminoacridine.

## Ethics Approval and Consent to Participate

This manuscript is a review article that does not require prior approval.

## Acknowledgments

This work was supported by the National Natural Science Foundation of China (82003710), the Natural Science Foundation of Guangdong Province (2020A1515010075), the Project of Educational Commission of Guangdong Province (2021ZDZX2012, 2021KCXTD056), the National Key Clinical Specialty Construction Project (Clinical Pharmacy), and High-Level Clinical Key Specialty (Clinical Pharmacy) in Guangdong Province.

## Disclosure

The authors declare that they have no known competing financial interests or personal relationships that could have appeared to influence the work reported in this paper.

## References

1. Dickson K, Lehmann C. Inflammatory response to different toxins in experimental sepsis models. *Int J Mol Sci*. 2019;20(18):4341. doi:10.3390/ijms20184341
2. Serra R, Grande R, Butrico L, et al. Chronic wound infections: the role of Pseudomonas aeruginosa and Staphylococcus aureus. *Expert Review of Anti-Infective Therapy*. 2015;13(5):605–613. doi:10.1586/14787210.2015.1023291
3. Byrd AL, Belkaid Y, Segre JA. The human skin microbiome. *Nat Rev Microbiol*. 2018;16(3):143–155. doi:10.1038/nrmicro.2017.157
4. Gurtner GC, Werner S, Barrandon Y, et al. Wound repair and regeneration. *Nature*. 2008;453(7193):314–321. doi:10.1038/nature07039
5. Natarajan S, Williamson D, Stiltz AJ, et al. Advances in wound care and healing technology. *Am J Clin Dermatol*. 2000;1(5):269–275. doi:10.2165/00128071-200001050-00002
6. Gould L, Abadir P, Brem H, et al. Chronic wound repair and healing in older adults: current status and future research. *J Am Geriatr Soc*. 2015;63(3):427–438. doi:10.1111/jgs.13332
7. Morton LM, Phillips TJ. Wound healing and treating wounds: differential diagnosis and evaluation of chronic wounds. *J Am Acad Dermatol*. 2016;74(4):589–605. doi:10.1016/j.jaad.2015.08.068
8. Lipsky BA, Berendt AR, Cornia PB, et al. 2012 Infectious Diseases Society of America clinical practice guideline for the diagnosis and treatment of diabetic foot infections. *Clin Infect Dis*. 2012;54(12):E132–E173. doi:10.1093/cid/cis346
9. Corl KA, Zeba F, Caffrey AR, et al. Delay in antibiotic administration is associated with mortality among septic shock patients with Staphylococcus aureus bacteremia. *Crit Care Med*. 2020;48(4):525–532. doi:10.1097/ccm.0000000000004212
10. Zhao RL, Liang HLN, Clarke E, et al. Inflammation in chronic wounds. *Int J Mol Sci*. 2016;17(12):2085. doi:10.3390/ijms17122085

11. Powers JG, Higham C, Broussard K, et al. Wound healing and treating wounds: chronic wound care and management. *J Am Acad Dermatol*. 2016;74(4):607–625. doi:10.1016/j.jaad.2015.08.070
12. Cohen ML. Changing patterns of infectious disease. *Nature*. 2000;406(6797):762–767. doi:10.1038/35021206
13. Zhu X, Radovic-Moreno AF, Wu J, et al. Nanomedicine in the management of microbial infection – overview and perspectives. *Nano Today*. 2014;9(4):478–498. doi:10.1016/j.nantod.2014.06.003
14. Blair JMA, Webber MA, Baylay AJ, et al. Molecular mechanisms of antibiotic resistance. *Nat Rev Microbiol*. 2015;13(1):42–51. doi:10.1038/nrmicro3380
15. Boateng J, Catanzano O. Advanced therapeutic dressings for effective wound healing—a review. *J Pharm Sci*. 2015;104(11):3653–3680. doi:10.1002/jps.24610
16. Giono-Cerezo S, Santos-Preciado JI, Morfin-Otero MDR, et al. Antimicrobial resistance. Its importance and efforts to control it. *Gaceta medica de Mexico*. 2020;156(2):171–178. doi:10.24875/gmm.m20000358
17. Sharifi S, Hajipour MJ, Gould L, et al. Nanomedicine in healing chronic wounds: opportunities and challenges. *Mol Pharmaceutics*. 2021;18(2):550–575. doi:10.1021/acs.molpharmaceut.0c00346
18. Fan X, Yang F, Nie C, et al. Mussel-inspired synthesis of NIR-responsive and biocompatible Ag–graphene 2D nanoagents for versatile bacterial disinfections. *ACS Appl Mater Interfaces*. 2018;10(1):296–307. doi:10.1021/acsami.7b16283
19. Wang G, Feng H, Hu L, et al. An antibacterial platform based on capacitive carbon-doped TiO<sub>2</sub> nanotubes after direct or alternating current charging. *Nat Commun*. 2018;9(1):2055. doi:10.1038/s41467-018-04317-2
20. Qu Z, Xu H, Xu P, et al. Ultrasensitive ELISA using enzyme-loaded nanospherical brushes as labels. *Anal Chem*. 2014;86(19):9367–9371. doi:10.1021/ac502522b
21. Chen LJ, Wang N, Wang XD, et al. Protein-directed in situ synthesis of platinum nanoparticles with superior peroxidase-like activity, and their use for photometric determination of hydrogen peroxide. *Microchim Acta*. 2013;180(15–16):1517–1522. doi:10.1007/s00604-013-1068-6
22. Vatansever F, de Melo WCMA, Avci P, et al. Antimicrobial strategies centered around reactive oxygen species – bactericidal antibiotics, photodynamic therapy, and beyond. *FEMS Microbiology Reviews*. 2013;37(6):955–989. doi:10.1111/1574-6976.12026
23. Sun D, Pang X, Cheng Y, et al. Ultrasound-switchable nanozyme augments sonodynamic therapy against multidrug-resistant bacterial infection. *ACS nano*. 2020;14(2):2063–2076. doi:10.1021/acsnano.9b08667
24. Wei F, Cui XY, Wang Z, et al. Recoverable peroxidase-like Fe<sub>3</sub>O<sub>4</sub>@MoS<sub>2</sub>-Ag nanozyme with enhanced antibacterial ability. *Chem Eng J*. 2021;408:127240. doi:10.1016/j.cej.2020.127240
25. Xu B, Wang H, Wang W, et al. A single-atom nanozyme for wound disinfection applications. *Angewandte Chemie*. 2019;58(15):4911–4916. doi:10.1002/anie.201813994
26. Li YQ, Liu JW. Nanozyme’s catching up: activity, specificity, reaction conditions and reaction types. *Mater Horiz*. 2021;8(2):336–350. doi:10.1039/d0mh01393e
27. Fan S, Zhao M, Ding L, et al. Preparation of Co(3)O(4)/crumpled graphene microsphere as peroxidase mimetic for colorimetric assay of ascorbic acid. *Biosens Bioelectron*. 2017;89(Pt2):846–852. doi:10.1016/j.bios.2016.09.108
28. Zhu XF, Chen X, Jia Z, et al. Cationic chitosan@Ruthenium dioxide hybrid nanozymes for photothermal therapy enhancing ROS-mediated eradicating multidrug resistant bacterial infection. *J Colloid Interface Sci*. 2021;603:615–632. doi:10.1016/j.jcis.2021.06.073
29. Liao X, Xu Q, Sun H, et al. Plasmonic nanozymes: localized surface plasmonic resonance regulates reaction kinetics and antibacterial performance. *J Phys Chem Lett*. 2022;13(1):312–323. doi:10.1021/acs.jpcclett.1c03804
30. Chen QM, Li SQ, Liu Y, et al. Size-controllable Fe-N/C single-atom nanozyme with exceptional oxidase-like activity for sensitive detection of alkaline phosphatase. *Sensor Actuat B-Chem*. 2020;305:127511. doi:10.1016/j.snb.2019.127511
31. Bhagat S, Vallabani NVS, Shutthanandan V, et al. Gold core/ceria shell-based redox active nanozyme mimicking the biological multienzyme complex phenomenon. *J Colloid Interface Sci*. 2018;513:831–842. doi:10.1016/j.jcis.2017.11.064
32. Song W, Zhao B, Wang C, et al. Functional nanomaterials with unique enzyme-like characteristics for sensing applications. *J Mater Chem B*. 2019;7(6):850–875. doi:10.1039/c8tb02878h
33. Zou KY, Li ZX. Controllable syntheses of MOF-derived materials. *Chemistry*. 2018;24(25):6506–6518. doi:10.1002/chem.201705415
34. Li N, Zhao P, Astruc D. Anisotropic gold nanoparticles: synthesis, properties, applications, and toxicity. *Angewandte Chemie*. 2014;53(7):1756–1789. doi:10.1002/anie.201300441
35. Rycenga M, Cobley CM, Zeng J, et al. Controlling the synthesis and assembly of silver nanostructures for plasmonic applications. *Chem Rev*. 2011;111(6):3669–3712. doi:10.1021/cr100275d
36. Zhang H, Jin M, Xiong Y, et al. Shape-controlled synthesis of Pd nanocrystals and their catalytic applications. *Acc Chem Res*. 2013;46(8):1783–1794. doi:10.1021/ar300209w
37. Dong C, Feng W, Xu W, et al. The coppery age: copper (Cu)-involved nanotheranostics. *Adv Sci*. 2020;7(21):2001549. doi:10.1002/advs.202001549
38. Ferrando R, Jellinek J, Johnston RL. Nanoalloys: from theory to applications of alloy clusters and nanoparticles. *Chem Rev*. 2008;108(3):845–910. doi:10.1021/cr040090g
39. Avnir D. Recent progress in the study of molecularly doped metals. *Adv Mater*. 2018;30(41):1706804. doi:10.1002/adma.201706804
40. Liu B, Wang Y, Chen Y, et al. Biomimetic two-dimensional nanozymes: synthesis, hybridization, functional tailoring, and biosensor applications. *J Mater Chem B*. 2020;8(44):10065–10086. doi:10.1039/d0tb02051f
41. Zhang WT, Ren XY, Shi S, et al. Ionic silver-infused peroxidase-like metal-organic frameworks as versatile “antibiotic” for enhanced bacterial elimination. *Nanoscale*. 2020;12(30):16330–16338. doi:10.1039/d0nr01471k
42. Walkey C, Das S, Seal S, et al. Catalytic properties and biomedical applications of cerium oxide nanoparticles. *Environ Sci Nano*. 2015;2(1):33–53. doi:10.1039/c4en00138a
43. Safarik I, Prochazkova J, Schroer MA, et al. Cotton textile/iron oxide nanozyme composites with peroxidase-like activity: preparation, characterization, and application. *ACS Appl Mater Interfaces*. 2021;13(20):23627–23637. doi:10.1021/acsami.1c02154
44. Tarn D, Ashley CE, Xue M, et al. Mesoporous silica nanoparticle nanocarriers: biofunctionality and biocompatibility. *Acc Chem Res*. 2013;46(3):792–801. doi:10.1021/ar3000986

45. Reddy LH, Arias JL, Nicolas J, et al. Magnetic nanoparticles: design and characterization, toxicity and biocompatibility, Pharmaceutical and biomedical applications. *Chem Rev.* 2012;112(11):5818–5878. doi:10.1021/cr300068p
46. Yang K, Feng L, Shi X, et al. Nano-graphene in biomedicine: theranostic applications. *Chem Soc Rev.* 2013;42(2):530–547. doi:10.1039/c2cs35342c
47. Heister E, Brunner EW, Dieckmann GR, et al. Are carbon nanotubes a natural solution? Applications in biology and medicine. *ACS Appl Mater Interfaces.* 2013;5(6):1870–1891. doi:10.1021/am302902d
48. Azizi-Lalabadi M, Hashemi H, Feng J, et al. Carbon nanomaterials against pathogens; the antimicrobial activity of carbon nanotubes, graphene/graphene oxide, fullerenes, and their nanocomposites. *Adv Colloid Interface Sci.* 2020;284:102250. doi:10.1016/j.cis.2020.102250
49. Takeo M, Lee W, Ito M. Wound healing and skin regeneration. *Cold Spring Harb Perspect Med.* 2015;5(1):a023267. doi:10.1101/cshperspect.a023267
50. Martin P, Nunan R. Cellular and molecular mechanisms of repair in acute and chronic wound healing. *Br J Dermatol.* 2015;173(2):370–378. doi:10.1111/bjd.13954
51. Smith F, Sharp A. Undertaking a person-centred assessment of patients with chronic wounds. *Nurs Stand.* 2019;34(10):77–82. doi:10.7748/ns.2019.e11305
52. Fabian TC. Damage control in trauma: laparotomy wound management acute to chronic. *Surg Clin N Am.* 2007;87(1):73–93. doi:10.1016/j.suc.2006.09.011
53. Yang A, Yassin M, Phan T. *Vibrio mimicus* wound infection in a burn patient. *Radiol Case Rep.* 2021;16(6):1348–1351. doi:10.1016/j.radcr.2021.03.021
54. Boodhoo K, Vlok M, Tabb DL, et al. Dysregulated healing responses in diabetic wounds occur in the early stages postinjury. *J Mol Endocrinol.* 2021;66(2):141–155. doi:10.1530/jme-20-0256
55. Izadi K, Ganchi P. Chronic wounds. *Clin Plast Surg.* 2005;32(2):209–222. doi:10.1016/j.cps.2004.11.011
56. Furtado KAX, Infante P, Sobral A, et al. Prevalence of acute and chronic wounds - with emphasis on pressure ulcers - in integrated continuing care units in Alentejo, Portugal. *Int Wound J.* 2020;17(4):1002–1010. doi:10.1111/iwj.13364
57. Fu RH, Weinstein AL, Chang MM, et al. Risk factors of infected sternal wounds versus sterile wound dehiscence. *J Surg Res.* 2016;200(1):400–407. doi:10.1016/j.jss.2015.07.045
58. Razyieva K, Kim Y, Zharkinkbekov Z, et al. Immunology of acute and chronic wound healing. *Biomolecules.* 2021;11(5):700. doi:10.3390/biom11050700
59. Li M, Hou Q, Zhong L, et al. Macrophage related chronic inflammation in non-healing wounds. *Front Immunol.* 2021;12:681710. doi:10.3389/fimmu.2021.681710
60. Eming SA, Martin P, Tomic-Canic M. Wound repair and regeneration: mechanisms, signaling, and translation. *Sci Transl Med.* 2014;6(265):265sr6. doi:10.1126/scitranslmed.3009337
61. Bowler PG, Davies BJ. The microbiology of acute and chronic wounds. *Wounds.* 1999;11(4):72–78.
62. Swaney MH, Kalan LR. Living in your skin: microbes, molecules, and mechanisms. *Infect Immun.* 2021;89(4):e00695–20. doi:10.1128/iai.00695-20
63. Lindley LE, Stojadinovic O, Pastar I, et al. Biology and biomarkers for wound healing. *Plast Reconstr Surg.* 2016;138:18S–28S. doi:10.1097/prs.0000000000002682
64. Opneja A, Kapoor S, Stavrou EX. Contribution of platelets, the coagulation and fibrinolytic systems to cutaneous wound healing. *Thromb Res.* 2019;179:56–63. doi:10.1016/j.thromres.2019.05.001
65. Velnar T, Bailey T, Smrkoli V. The wound healing process: an overview of the cellular and molecular mechanisms. *J Int Med Res.* 2009;37(5):1528–1542. doi:10.1177/147323000903700531
66. Krzyszczyk P, Schloss R, Palmer A, et al. The role of macrophages in acute and chronic wound healing and interventions to promote pro-wound healing phenotypes. *Front Physiol.* 2018;9:419. doi:10.3389/fphys.2018.00419
67. McDaniel JC, Roy S, Wilgus TA. Neutrophil activity in chronic venous leg ulcers—a target for therapy? *Wound Repair Regen.* 2013;21(3):339–351. doi:10.1111/wrr.12036
68. Lord JM, Midwinter MJ, Chen YF, et al. The systemic immune response to trauma: an overview of pathophysiology and treatment. *Lancet.* 2014;384(9952):1455–1465. doi:10.1016/s0140-6736(14)
69. Mahdavian Delavary B, van der Veer WM, van Egmond M, et al. Macrophages in skin injury and repair. *Immunobiology.* 2011;216(7):753–762. doi:10.1016/j.imbio.2011.01.001
70. Egozi EI, Ferreira AM, Burns AL, et al. Mast cells modulate the inflammatory but not the proliferative response in healing wounds. *Wound Repair Regen.* 2003;11(1):46–54. doi:10.1046/j.1524-475X.2003.11108.x
71. Tanaka S, Furuta K. Roles of IgE and histamine in mast cell maturation. *Cells.* 2021;10(8):2170. doi:10.3390/cells10082170
72. Kolaczowska E, Kubes P. Neutrophil recruitment and function in health and inflammation. *Nat Rev Immunol.* 2013;13(3):159–175. doi:10.1038/nri3399
73. Visan I. Wound healing. *Nat Immunol.* 2019;20(9):1089. doi:10.1038/s41590-019-0484-0
74. El-Benna J, Hurtado-Nedelec M, Marzaioli V, et al. Priming of the neutrophil respiratory burst: role in host defense and inflammation. *Immunol Rev.* 2016;273(1):180–193. doi:10.1111/imr.12447
75. Segel GB, Halterman MW, Lichtman MA. The paradox of the neutrophil's role in tissue injury. *J Leukocyte Biol.* 2011;89(3):359–372. doi:10.1189/jlb.0910538
76. Brinkmann V, Reichard U, Goosmann C, et al. Neutrophil extracellular traps kill bacteria. *Science.* 2004;303(5663):1532–1535. doi:10.1126/science.1092385
77. Rahim K, Saleha S, Zhu X, et al. Bacterial Contribution in Chronicity of Wounds. *Microb Ecol.* 2017;73(3):710–721. doi:10.1007/s00248-016-0867-9
78. Bowler PG, Duerden BI, Armstrong DG. Wound microbiology and associated approaches to wound management. *Clin Microbiol Rev.* 2001;14(2):244–269. doi:10.1128/cmr.14.2.244-269.2001
79. Pastar I, Nusbaum AG, Gil J, et al. Interactions of methicillin resistant *Staphylococcus aureus* USA300 and *Pseudomonas aeruginosa* in polymicrobial wound infection. *PLoS One.* 2013;8(2):e56846. doi:10.1371/journal.pone.0056846

80. Guo S, DiPietro LA. Factors affecting wound healing. *J Dent Res*. 2010;89(3):219–229. doi:10.1177/0022034509359125
81. Anderson K, Hamm RL. Factors that impair wound healing. *J Am Coll Clin Wound Spec*. 2012;4(4):84–91. doi:10.1016/j.jccw.2014.03.001
82. Sender R, Fuchs S, Milo R. Are we really vastly outnumbered? Revisiting the ratio of bacterial to host cells in humans. *Cell*. 2016;164(3):337–340. doi:10.1016/j.cell.2016.01.013
83. Ursell LK, Haiser HJ, Van Treuren W, et al. The intestinal metabolome: an intersection between microbiota and host. *Gastroenterology*. 2014;146(6):1470–1476. doi:10.1053/j.gastro.2014.03.001
84. Hasan N, Yang H. Factors affecting the composition of the gut microbiota, and its modulation. *PeerJ*. 2019;7:e7502. doi:10.7717/peerj.7502
85. Gardner SE, Frantz RA. Wound bioburden and infection-related complications in diabetic foot ulcers. *Biol Res Nurs*. 2008;10(1):44–53. doi:10.1177/1099800408319056
86. Edwards R, Harding KG. Bacteria and wound healing. *Curr Opin Infect Dis*. 2004;17(2):91–96. doi:10.1097/00001432-200404000-00004
87. Percival SL, Thomas JG, Williams DW. Biofilms and bacterial imbalances in chronic wounds: anti-Koch. *Int Wound J*. 2010;7(3):169–175. doi:10.1111/j.1742-481X.2010.00668.x
88. Negut I, Grumezescu V, Grumezescu AM. Treatment strategies for infected wounds. *Molecules*. 2018;23(9):2392. doi:10.3390/molecules23092392
89. Frieri M, Kumar K, Boutin A. Antibiotic resistance. *J Infect Public Health*. 2017;10(4):369–378. doi:10.1016/j.jiph.2016.08.007
90. Hoiby N, Bjarnsholt T, Moser C, et al. ESCMID\* guideline for the diagnosis and treatment of biofilm infections 2014. *Clin Microbiol Infect*. 2015;21:S1–S25. doi:10.1016/j.cmi.2014.10.024
91. Hoiby N, Bjarnsholt T, Givskov M, et al. Antibiotic resistance of bacterial biofilms. *Int J Antimicrob Agents*. 2010;35(4):322–332. doi:10.1016/j.ijantimicag.2009.12.011
92. Percival SL, Hill KE, Williams DW, et al. A review of the scientific evidence for biofilms in wounds. *Wound Repair Regener*. 2012;20(5):647–657. doi:10.1111/j.1524-475X.2012.00836.x
93. Hall CW, Mah T-F. Molecular mechanisms of biofilm-based antibiotic resistance and tolerance in pathogenic bacteria. *Fems Microbiol Rev*. 2017;41(3):276–301. doi:10.1093/femsre/fux010
94. Moser C, Jensen PO, Thomsen K, et al. Immune responses to *Pseudomonas aeruginosa* biofilm infections. *Front Immunol*. 2021;12:625597. doi:10.3389/fimmu.2021.625597
95. Moser C, Pedersen HT, Lerche CJ, et al. Biofilms and host response - helpful or harmful. *APMIS Suppl*. 2017;125(4):320–338. doi:10.1111/apm.12674
96. Banachereau J, Steinman RM. Dendritic cells and the control of immunity. *Nature*. 1998;392(6673):245–252. doi:10.1038/32588
97. Trostrup H, Holstein P, Christophersen L, et al. S100A8/A9 is an important host defence mediator in neuropathic foot ulcers in patients with type 2 diabetes mellitus. *Arch Dermatol Res*. 2016;308(5):347–355. doi:10.1007/s00403-016-1646-7
98. Trostrup H, Lundquist R, Christensen LH, et al. S100A8/A9 deficiency in nonhealing venous leg ulcers uncovered by multiplexed antibody microarray profiling. *Br J Dermatol*. 2011;165(2):292–301. doi:10.1111/j.1365-2133.2011.10384.x
99. Thorey IS, Roth J, Regenbogen J, et al. The Ca<sup>2+</sup>-binding proteins S100A8 and S100A9 are encoded by novel injury-regulated genes. *J Biol Chem*. 2001;276(38):35818–35825. doi:10.1074/jbc.M104871200
100. Jensen PO, Bjarnsholt T, Phipps R, et al. Rapid necrotic killing of polymorphonuclear leukocytes is caused by quorum-sensing-controlled production of rhamnolipid by *Pseudomonas aeruginosa*. *Microbiol-Sgm*. 2007;153:1329–1338. doi:10.1099/mic.0.2006/003863-0
101. Alhede M, Bjarnsholt T, Jensen PO, et al. *Pseudomonas aeruginosa* recognizes and responds aggressively to the presence of polymorphonuclear leukocytes. *Microbiol-Sgm*. 2009;155:3500–3508. doi:10.1099/mic.0.031443-0
102. Nguyen KT, Seth AK, Hong SJ, et al. Deficient cytokine expression and neutrophil oxidative burst contribute to impaired cutaneous wound healing in diabetic, biofilm-containing chronic wounds. *Wound Repair Regener*. 2013;21(6):833–841. doi:10.1111/wrr.12109
103. Pereira RF, Barrias CC, Granja PL, et al. Advanced biofabrication strategies for skin regeneration and repair. *Nanomedicine*. 2013;8(4):603–621. doi:10.2217/nmm.13.50
104. Eming SA, Wynn P, Martin P. Inflammation and metabolism in tissue repair and regeneration. *Science*. 2017;356(6342):1026–1030. doi:10.1126/science.aam7928
105. Zimmermann C, Troeltzsch D, Gimenez-Rivera VA, et al. Mast cells are critical for controlling the bacterial burden and the healing of infected wounds. *Proc Natl Acad Sci USA*. 2019;116(41):20500–20504. doi:10.1073/pnas.1908816116
106. Pereira RF, Bartolo PJ. Traditional therapies for skin wound healing. *Adv Wound Care*. 2016;5(5):208–229. doi:10.1089/wound.2013.0506
107. Bodeker GC, Ryan TJ, Ong CK. Traditional approaches to wound healing. *Clin Dermatol*. 1999;17(1):93–98. doi:10.1016/s0738-081x(98)00056-x
108. Ribeiro Neto JA, Pimenta Taroco BR, Dos Santos HB, et al. Using the plants of Brazilian Cerrado for wound healing: from traditional use to scientific approach. *J Ethnopharmacol*. 2020;260:112547. doi:10.1016/j.jep.2020.112547
109. Vujanovic S, Vujanovic J. Bioresources in the pharmacotherapy and healing of burns: a mini-review. *Burns*. 2013;39(6):1031–1038. doi:10.1016/j.burns.2013.03.016
110. Upadhyay NK, Kumar R, Mandotra SK, et al. Safety and healing efficacy of Sea buckthorn (*Hippophae rhamnoides* L.) seed oil on burn wounds in rats. *Food Chem Toxicol*. 2009;47(6):1146–1153. doi:10.1016/j.fct.2009.02.002
111. Gupta A, Kumar R, Pal K, et al. A preclinical study of the effects of seabuckthorn (*Hippophae rhamnoides* L.) leaf extract on cutaneous wound healing in albino rats. *Int J Low Extrem Wounds*. 2005;4(2):88–92. doi:10.1177/1534734605277401
112. Tameshloo M, Norouzian M, Zarein-Dolab S, et al. Aloe vera gel and thyroid hormone cream may improve wound healing in Wistar rats. *Anat Cell Biol*. 2012;45(3):170–177. doi:10.5115/acb.2012.45.3.170
113. Eshghi F, Hosseinimehr SJ, Rahmani N, et al. Effects of aloe vera cream on post hemorrhoidectomy pain and wound healing: results of a randomized, blind, placebo-control study. *J Altern Complement Med*. 2010;16(6):647–650. doi:10.1089/acm.2009.0428
114. Takzare N, Hosseini M-J, Hasanzadeh G, et al. Influence of aloe vera gel on dermal wound healing process in rat. *Toxicol Mech Methods*. 2009;19(1):73–77. doi:10.1080/15376510802442444
115. Hsiao C-Y, Hung C-Y, Tsai T-H, et al. A study of the wound healing mechanism of a traditional Chinese medicine, angelica sinensis, using a proteomic approach. *Evid Based Complement Alternat Med*. 2012;2012:467531. doi:10.1155/2012/467531

116. Nayak BS, Pinto Pereira LM. Catharanthus roseus flower extract has wound-healing activity in Sprague Dawley rats. *BMC Complementary Altern Med*. 2006;6:41. doi:10.1186/1472-6882-6-41
117. Boudreau MD, Beland FA. An evaluation of the biological and toxicological properties of Aloe barbadensis (Miller), Aloe vera. *J Environ Sci Heal C*. 2006;24(1):103–154. doi:10.1080/10590500600614303
118. Hamman JH. Composition and applications of Aloe vera leaf gel. *Molecules*. 2008;13(8):1599–1616. doi:10.3390/molecules13081599
119. Mashreghi M, Bazaz MR, Shahri NM, et al. Topical effects of frog “Rana ridibunda” skin secretions on wound healing and reduction of wound microbial load. *J Ethnopharmacol*. 2013;145(3):793–797. doi:10.1016/j.jep.2012.12.016
120. Liu H, Mu L, Tang J, et al. A potential wound healing-promoting peptide from frog skin. *Int J Biochem Cell Biol*. 2014;49:32–41. doi:10.1016/j.biocel.2014.01.010
121. Majtan J. Honey: an immunomodulator in wound healing. *Wound Repair Regen*. 2014;22(2):187–192. doi:10.1111/wrr.12117
122. Martinotti S, Ranzato E. Propolis: a new frontier for wound healing? *Burns Trauma*. 2015;3:9. doi:10.1186/s41038-015-0010-z
123. Zaidi SMA, Jameel SS, Zaman F, et al. A systematic overview of the medicinal importance of sanguivorous leeches. *Altern Med Rev*. 2011;16(1):59–65.
124. Iqbal A, Jan A, Wajid MA, et al. Management of chronic non-healing wounds by hirudotherapy. *World J Plast Surg*. 2017;6(1):9–17.
125. Percival SL, Thomas J, Linton S, et al. The antimicrobial efficacy of silver on antibiotic-resistant bacteria isolated from burn wounds. *Int Wound J*. 2012;9(5):488–493. doi:10.1111/j.1742-481X.2011.00903.x
126. Percival SL, Salisbury A-M, Chen R. Silver, biofilms and wounds: resistance revisited. *Crit Rev Microbiol*. 2019;45(2):223–237. doi:10.1080/1040841x.2019.1573803
127. Percival SL, Bowler PG, Russell D. Bacterial resistance to silver in wound care. *J Hosp Infect*. 2005;60(1):1–7. doi:10.1016/j.jhin.2004.11.014
128. Rustad KC, Gurtner GC. Mesenchymal stem cells home to sites of injury and inflammation. *Adv Wound Care*. 2012;1(4):147–152. doi:10.1089/wound.2011.0314
129. Fleck CA, Simman R. Modern collagen wound dressings: function and purpose. *The Journal of the American College of Certified Wound Specialists*. 2010;2(3):50–54. doi:10.1016/j.jcws.2010.12.003
130. Jimi S, Jaguparov A, Nurkesh A, et al. Sequential delivery of cryogel released growth factors and cytokines accelerates wound healing and improves tissue regeneration. *Front Bioeng Biotechnol*. 2020;8:345. doi:10.3389/fbioe.2020.00345
131. Nardini M, Perteghella S, Mastracci L, et al. Growth factors delivery system for skin regeneration: an advanced wound dressing. *Pharmaceutics*. 2020;12(2):120. doi:10.3390/pharmaceutics12020120
132. Dai C, Shih S, Khachemoune A. Skin substitutes for acute and chronic wound healing: an updated review. *J Dermatol Treat*. 2020;31(6):639–648. doi:10.1080/09546634.2018.1530443
133. Wang T, Zhu X-K, Xue X-T, et al. Hydrogel sheets of chitosan, honey and gelatin as burn wound dressings. *Carbohydr Polym*. 2012;88(1):75–83. doi:10.1016/j.carbpol.2011.11.069
134. Yan W, Banerjee P, Liu Y, et al. Development of thermosensitive hydrogel wound dressing containing Acinetobacter baumannii phage against wound infections. *Int J Pharm*. 2021;602:120508. doi:10.1016/j.ijpharm.2021.120508
135. Singh D, Chopra K, Sabino J, et al. Practical things you should know about wound healing and vacuum-assisted closure management. *Plast Reconstr Surg*. 2020;145(4):839e–854e. doi:10.1097/prs.0000000000006652
136. Leach RM, Rees PJ, Wilmshurst P. ABC of oxygen: hyperbaric oxygen therapy. *BMJ*. 1998;317(7166):1140–1143. doi:10.1136/bmj.317.7166.1140
137. Lam G, Fontaine R, Ross FL, et al. Hyperbaric oxygen therapy: exploring the clinical evidence. *Adv Skin Wound Care*. 2017;30(4):181–190. doi:10.1097/01.ASW.0000513089.75457.22
138. Schreml S, Szeimies RM, Prantl L, et al. Oxygen in acute and chronic wound healing. *Br J Dermatol*. 2010;163(2):257–268. doi:10.1111/j.1365-2133.2010.09804.x
139. Han G, Ceilley R. Chronic wound healing: a review of current management and treatments. *Adv Ther*. 2017;34(3):599–610. doi:10.1007/s12325-017-0478-y
140. Ke Q, Costa M. Hypoxia-inducible factor-1 (HIF-1). *Mol Pharmacol*. 2006;70(5):1469–1480. doi:10.1124/mol.106.027029
141. Wahid F, Zhao X-J, Zhao X-Q, et al. Fabrication of bacterial cellulose-based dressings for promoting infected wound healing. *ACS Appl Mater Interfaces*. 2021;13(28):32716–32728. doi:10.1021/acsami.1c06986
142. Shiekh PA, Singh A, Kumar A. Exosome laden oxygen releasing antioxidant and antibacterial cryogel wound dressing OxOBand alleviate diabetic and infectious wound healing. *Biomaterials*. 2020;249:120020. doi:10.1016/j.biomaterials.2020.120020
143. Shilo S, Roth S, Amzel T, et al. Cutaneous wound healing after treatment with plant-derived human recombinant collagen flowable gel. *Tissue Eng Part A*. 2013;19(13–14):1519–1526. doi:10.1089/ten.tea.2012.0345
144. Silvestro I, Lopreiato M, Scotto d’Abusco A, et al. Hyaluronic acid reduces bacterial fouling and promotes fibroblasts’ adhesion onto chitosan 2D-wound dressings. *Int J Mol Sci*. 2020;21(6):2070. doi:10.3390/ijms21062070
145. Ong S-Y, Wu J, Moochhala SM, et al. Development of a chitosan-based wound dressing with improved hemostatic and antimicrobial properties. *Biomaterials*. 2008;29(32):4323–4332. doi:10.1016/j.biomaterials.2008.07.034
146. Goh CH, Heng PWS, Chan LW. Alginates as a useful natural polymer for microencapsulation and therapeutic applications. *Carbohydr Polym*. 2012;88(1):1–12. doi:10.1016/j.carbpol.2011.11.012
147. Varaprasad K, Jayaramudu T, Kanikireddy V, et al. Alginate-based composite materials for wound dressing application: A mini review. *Carbohydr Polym*. 2020;236:116025. doi:10.1016/j.carbpol.2020.116025
148. Abdelhamid HN, Mathew AP. Cellulose-metal organic frameworks (CelloMOFs) hybrid materials and their multifaceted Applications: a review. *Coord Chem Rev*. 2022;451:214263. doi:10.1016/j.ccr.2021.214263
149. Boukraa L, Sulaiman SA. Honey use in burn management: potentials and limitations. *Forsch Komplementmed*. 2010;17(2):74–80. doi:10.1159/000297213
150. Carter MJ. Cost-effectiveness research in wound care: definitions, approaches, and limitations. *Ostomy Wound Manage*. 2010;56(11):48–59.
151. Al-Waili NS, Salom K, Butler G, et al. Honey and microbial infections: a review supporting the use of honey for microbial control. *J Med Food*. 2011;14(10):1079–1096. doi:10.1089/jmf.2010.0161

152. Kwakman PHS, Velde AAT, de Boer L, et al. Two major medicinal honeys have different mechanisms of bactericidal activity. *PLoS One*. 2011;6(3):e17709. doi:10.1371/journal.pone.0017709
153. Schacke H. Mechanisms involved in the side effects of glucocorticoids. *Pharmacol Ther*. 2002;96(1):23–43. doi:10.1016/S0163-7258(02)00297-8
154. Lachiewicz AM, Hauck CG, Weber DJ, et al. Bacterial infections after burn injuries: impact of multidrug resistance. *Clin Infect Dis*. 2017;65(12):2130–2136. doi:10.1093/cid/cix682
155. Durão P, Balbontin R, Gordo I. Evolutionary mechanisms shaping the maintenance of antibiotic resistance. *Trends Microbiol*. 2018;26(8):677–691. doi:10.1016/j.tim.2018.01.005
156. Mc Carlie S, Boucher CE, Bragg RR. Molecular basis of bacterial disinfectant resistance. *Drug Resist Updat*. 2020;48:100672. doi:10.1016/j.drup.2019.100672
157. Gao F, Shao T, Yu Y, et al. Surface-bound reactive oxygen species generating nanozymes for selective antibacterial action. *Nat Commun*. 2021;12(1):745. doi:10.1038/s41467-021-20965-3
158. Niu JS, Sun YH, Wang FM, et al. Photomodulated nanozyme used for a gram-selective antimicrobial. *Chem Mater*. 2018;30(20):7027–7033. doi:10.1021/acs.chemmater.8b02365
159. Wang Q, Jiang J, Gao L. Catalytic antimicrobial therapy using nanozymes. *Wiley Interdiscip Rev Nanomed Nanobiotechnol*. 2022;14(2):e1769. doi:10.1002/wnan.1769
160. Komkova MA, Karyakina EE, Karyakin AA. Catalytically synthesized Prussian blue nanoparticles defeating natural enzyme peroxidase. *J Am Chem Soc*. 2018;140(36):11302–11307. doi:10.1021/jacs.8b05223
161. Gao L, Fan K, Yan X. Iron oxide nanozyme: a multifunctional enzyme mimetic for biomedical applications. *Theranostics*. 2017;7(13):3207–3227. doi:10.7150/thno.19738
162. He WW, Wu XC, Liu JB, et al. Design of AgM bimetallic alloy nanostructures (M = Au, Pd, Pt) with tunable morphology and peroxidase-like activity. *Chem Mater*. 2010;22(9):2988–2994. doi:10.1021/cm100393v
163. Wu J, Qin K, Yuan D, et al. Rational design of Au@Pt multibranch nanostructures as bifunctional nanozymes. *ACS Appl Mater Interfaces*. 2018;10(15):12954–12959. doi:10.1021/acsami.7b17945
164. Li Y, Fu R, Duan Z, et al. Adaptive hydrogels based on nanozyme with dual-enhanced triple enzyme-like activities for wound disinfection and mimicking antioxidant defense system. *Adv Healthc Mater*. 2022;11(2):e2101849. doi:10.1002/adhm.202101849
165. Liu X, Gao Y, Chandrawati R, et al. Therapeutic applications of multifunctional nanozymes. *Nanoscale*. 2019;11(44):21046–21060. doi:10.1039/c9nr06596b
166. Wu J, Li S, Wei H. Integrated nanozymes: facile preparation and biomedical applications. *Chem Commun*. 2018;54(50):6520–6530. doi:10.1039/c8cc01202d
167. Yang B, Chen Y, Shi J. Reactive oxygen species (ROS)-based nanomedicine. *Chem Rev*. 2019;119(8):4881–4985. doi:10.1021/acs.chemrev.8b00626
168. Yin W, Yu J, Lv F, et al. Functionalized Nano-MoS<sub>2</sub> with peroxidase catalytic and near-infrared photothermal activities for safe and synergetic wound antibacterial applications. *ACS nano*. 2016;10(12):11000–11011. doi:10.1021/acsnano.6b05810
169. Dharmaraja AT. Role of Reactive Oxygen Species (ROS) in therapeutics and drug resistance in cancer and bacteria. *J Med Chem*. 2017;60(8):3221–3240. doi:10.1021/acs.jmedchem.6b01243
170. Murphy EC, Friedman AJ. Hydrogen peroxide and cutaneous biology: translational applications, benefits, and risks. *J Am Acad Dermatol*. 2019;81(6):1379–1386. doi:10.1016/j.jaad.2019.05.030
171. Natalio F, André R, Hartog AF, et al. Vanadium pentoxide nanoparticles mimic vanadium haloperoxidases and thwart biofilm formation. *Nat Nanotechnol*. 2012;7(8):530–535. doi:10.1038/nnano.2012.91
172. Liu X, Yan Z, Zhang Y, et al. Two-dimensional metal–organic framework/enzyme hybrid nanocatalyst as a benign and self-activated cascade reagent for in vivo wound healing. *ACS Nano*. 2019;13(5):5222–5230. doi:10.1021/acsnano.8b09501
173. Liang M, Zhang M, Yu S, et al. Silver-laden black phosphorus nanosheets for an efficient in vivo antimicrobial application. *Small*. 2020;16(13):e1905938. doi:10.1002/sml.201905938
174. Lin Y, Liu X, Liu Z, et al. Visible-light-driven photocatalysis-enhanced nanozyme of TiO<sub>2</sub> Nanotubes@MoS<sub>2</sub> nanoflowers for efficient wound healing infected with multidrug-resistant bacteria. *Small*. 2021;17(39):e2103348. doi:10.1002/sml.202103348
175. Lu J, Yang J, Carvalho A, et al. Light–matter interactions in phosphorene. *Acc Chem Res*. 2016;49(9):1806–1815. doi:10.1021/acs.accounts.6b00266
176. Mao C, Xiang Y, Liu X, et al. Repeatable photodynamic therapy with triggered signaling pathways of fibroblast cell proliferation and differentiation to promote bacteria-accompanied wound healing. *ACS Nano*. 2018;12(2):1747–1759. doi:10.1021/acsnano.7b08500
177. Jiao L, Wang Y, Jiang H-L, et al. Metal-organic frameworks as platforms for catalytic applications. *Adv Mater*. 2018;30(37):e1703663. doi:10.1002/adma.201703663
178. Liu Z, Wang F, Ren J, et al. A series of MOF/Ce-based nanozymes with dual enzyme-like activity disrupting biofilms and hindering recolonization of bacteria. *Biomaterials*. 2019;208:21–31. doi:10.1016/j.biomaterials.2019.04.007
179. Chen Z, Wang Z, Ren J, et al. Enzyme mimicry for combating bacteria and biofilms. *Acc Chem Res*. 2018;51(3):789–799. doi:10.1021/acs.accounts.8b00011
180. Gupta A, Das R, Yesilbag Tonga G, et al. Charge-switchable nanozymes for bioorthogonal imaging of biofilm-associated infections. *ACS Nano*. 2018;12(1):89–94. doi:10.1021/acsnano.7b07496
181. Gao Y, Wang J, Chai M, et al. Size and charge adaptive clustered nanoparticles targeting the biofilm microenvironment for chronic lung infection management. *ACS Nano*. 2020;14(5):5686–5699. doi:10.1021/acsnano.0c00269
182. Wang D, Jana D, Zhao Y. Metal–organic framework derived nanozymes in biomedicine. *Acc Chem Res*. 2020;53(7):1389–1400. doi:10.1021/acs.accounts.0c00268
183. Unnikrishnan B, Lien C-W, Chu H-W, et al. A review on metal nanozyme-based sensing of heavy metal ions: challenges and future perspectives. *J Hazard Mater*. 2021;401:123397. doi:10.1016/j.jhazmat.2020.123397
184. Chen W, Li S, Wang J, et al. Metal and metal-oxide nanozymes: bioenzymatic characteristics, catalytic mechanism, and eco-environmental applications. *Nanoscale*. 2019;11(34):15783–15793. doi:10.1039/c9nr04771a

185. Jin L, Sun Y, Shi L, et al. PdPt bimetallic nanowires with efficient oxidase mimic activity for the colorimetric detection of acid phosphatase in acidic media. *J Mater Chem B*. 2019;7(29):4561–4567. doi:10.1039/c9tb00730j
186. Niu X, Shi Q, Zhu W, et al. Unprecedented peroxidase-mimicking activity of single-atom nanozyme with atomically dispersed Fe–Nx moieties hosted by MOF derived porous carbon. *Biosens Bioelectron*. 2019;142:111495. doi:10.1016/j.bios.2019.111495
187. Liu Q, Zhang A, Wang R, et al. A review on metal- and metal oxide-based nanozymes: properties, mechanisms, and applications. *Nano-Micro Lett*. 2021;13(1):154. doi:10.1007/s40820-021-00674-8
188. Lin C, Guo X, Chen L, et al. Ultrathin trimetallic metal–organic framework nanosheets for accelerating bacteria-infected wound healing. *J Colloid Interface Sci*. 2022;628(Pt B):731–744. doi:10.1016/j.jcis.2022.08.073
189. Lou-Franco J, Das B, Elliott C, et al. Gold nanozymes: from concept to biomedical applications. *Nano-Micro Lett*. 2020;13(1):10. doi:10.1007/s40820-020-00532-z
190. Saint-Lager MC, Laoufi I, Bailly A, et al. Catalytic properties of supported gold nanoparticles: new insights into the size-activity relationship gained from in operando measurements. *Faraday Discuss*. 2011;1522:53–65; discussion 293–306. doi:10.1039/c1fd00028d
191. Zhou X, Xu W, Liu G, et al. Size-dependent catalytic activity and dynamics of gold nanoparticles at the single-molecule level. *J Am Chem Soc*. 2010;132(1):138–146. doi:10.1021/ja904307n
192. McVey C, Logan N, Thanh NTK, et al. Unusual switchable peroxidase-mimicking nanozyme for the determination of proteolytic biomarker. *Nano Res*. 2019;12(3):509–516. doi:10.1007/s12274-018-2241-3
193. Biswas S, Tripathi P, Kumar N, et al. Gold nanorods as peroxidase mimetics and its application for colorimetric biosensing of malathion. *Sensors and Actuators B: Chemical*. 2016;231:584–592. doi:10.1016/j.snb.2016.03.066
194. Ong W-J, Tan -L-L, Ng YH, et al. Graphitic carbon nitride (g-C 3 N 4)-based photocatalysts for artificial photosynthesis and environmental remediation: are we a step closer to achieving sustainability? *Chem Rev*. 2016;116(12):7159–7329. doi:10.1021/acs.chemrev.6b00075
195. Zhang X, Xie X, Wang H, et al. Enhanced photoresponsive ultrathin graphitic-phase C 3 N 4 nanosheets for bioimaging. *J Am Chem Soc*. 2013;135(1):18–21. doi:10.1021/ja308249k
196. Jun Y-S, Park J, Lee SU, et al. Three-dimensional macroscopic assemblies of low-dimensional carbon nitrides for enhanced hydrogen evolution. *Angewandte Chemie*. 2013;52(42):11083–11087. doi:10.1002/anie.201304034
197. Kang Y, Yang Y, Yin L-C, et al. An amorphous carbon nitride photocatalyst with greatly extended visible-light-responsive range for photocatalytic hydrogen generation. *Adv Mater*. 2015;27(31):4572–4577. doi:10.1002/adma.201501939
198. Wang X, Maeda K, Thomas A, et al. A metal-free polymeric photocatalyst for hydrogen production from water under visible light. *Nat Mater*. 2009;8(1):76–80. doi:10.1038/nmat2317
199. Liu H, Lv X, Qian J, et al. Graphitic carbon nitride quantum dots embedded in carbon nanosheets for near-infrared imaging-guided combined photo-chemotherapy. *ACS nano*. 2020;14(10):13304–13315. doi:10.1021/acsnano.0c05143
200. Wang Z, Dong K, Liu Z, et al. Activation of biologically relevant levels of reactive oxygen species by Au/g-C3N4 hybrid nanozyme for bacteria killing and wound disinfection. *Biomaterials*. 2017;113:145–157. doi:10.1016/j.biomaterials.2016.10.041
201. Zhang Q, Chen S, Wang H, et al. Exquisite enzyme-Fenton biomimetic catalysts for hydroxyl radical production by mimicking an enzyme cascade. *ACS Appl Mater Interfaces*. 2018;10(10):8666–8675. doi:10.1021/acsami.7b18690
202. Sun L, Zhang Q, Li GG, et al. Multifaceted Gold–palladium bimetallic nanorods and their geometric, compositional, and catalytic tunabilities. *ACS nano*. 2017;11(3):3213–3228. doi:10.1021/acsnano.7b00264
203. Zhang Q, Zhou Y, Villarreal E, et al. Faceted gold nanorods: nanocuboids, convex nanocuboids, and concave nanocuboids. *Nano Lett*. 2015;15(6):4161–4169. doi:10.1021/acs.nanolett.5b01286
204. Xi J, Wei G, An L, et al. Copper/carbon hybrid nanozyme: tuning catalytic activity by the copper state for antibacterial therapy. *Nano Lett*. 2019;19(11):7645–7654. doi:10.1021/acs.nanolett.9b02242
205. Conner SD, Schmid SL. Regulated portals of entry into the cell. *Nature*. 2003;422(6927):37–44. doi:10.1038/nature01451
206. Ivask A, Elbadawy A, Kaweeteerawat C, et al. Toxicity mechanisms in Escherichia coli vary for silver nanoparticles and differ from ionic silver. *ACS nano*. 2014;8(1):374–386. doi:10.1021/nn4044047
207. Lv H, Cui S, Yang Q, et al. AgNPs-incorporated nanofiber mats: relationship between AgNPs size/content, silver release, cytotoxicity, and antibacterial activity. *Mater Sci Eng C Mater Biol Appl*. 2021;118:111331. doi:10.1016/j.msec.2020.111331
208. Rezvani E, Rafferty A, McGuinness C, et al. Adverse effects of nanosilver on human health and the environment. *Acta biomaterialia*. 2019;94:145–159. doi:10.1016/j.actbio.2019.05.042
209. Guebitz GM, Nyanhongo GS. Enzymes as green catalysts and interactive biomolecules in wound dressing hydrogels. *Trends Biotechnol*. 2018;36(10):1040–1053. doi:10.1016/j.tibtech.2018.05.006
210. Zhao X, Wu H, Guo B, et al. Antibacterial anti-oxidant electroactive injectable hydrogel as self-healing wound dressing with hemostasis and adhesiveness for cutaneous wound healing. *Biomaterials*. 2017;122:34–47. doi:10.1016/j.biomaterials.2017.01.011
211. Dimatteo R, Darling NJ, Segura T. In situ forming injectable hydrogels for drug delivery and wound repair. *Adv Drug Deliv Rev*. 2018;127:167–184. doi:10.1016/j.addr.2018.03.007
212. Eivazzadeh-Keihan R, Khalili F, Khosropour N, et al. Hybrid bionanocomposite containing magnesium hydroxide nanoparticles embedded in a carboxymethyl cellulose hydrogel plus silk fibroin as a scaffold for wound dressing applications. *ACS Appl Mater Interfaces*. 2021;13(29):33840–33849. doi:10.1021/acscami.1c07285
213. Eivazzadeh-Keihan R, Moghim Aliabadi HA, Radinekiyan F, et al. Investigation of the biological activity, mechanical properties and wound healing application of a novel scaffold based on lignin–agarose hydrogel and silk fibroin embedded zinc chromite nanoparticles. *RSC Adv*. 2021;11(29):17914–17923. doi:10.1039/d1ra01300a
214. Eivazzadeh-Keihan R, Khalili F, Aliabadi HAM, et al. Alginate hydrogel-polyvinyl alcohol/silk fibroin/magnesium hydroxide nanorods: a novel scaffold with biological and antibacterial activity and improved mechanical properties. *Int J Biol Macromol*. 2020;162:1959–1971. doi:10.1016/j.ijbiomac.2020.08.090
215. Eivazzadeh-Keihan R, Radinekiyan F, Maleki A, et al. A novel biocompatible core-shell magnetic nanocomposite based on cross-linked chitosan hydrogels for in vitro hyperthermia of cancer therapy. *Int J Biol Macromol*. 2019;140:407–414. doi:10.1016/j.ijbiomac.2019.08.031
216. Jia Z, Lv X, Hou Y, et al. Mussel-inspired nanozyme catalyzed conductive and self-setting hydrogel for adhesive and antibacterial bioelectronics. *Bioact Mater*. 2021;6(9):2676–2687. doi:10.1016/j.bioactmat.2021.01.033

217. Yang J, Bai R, Suo Z. Topological adhesion of wet materials. *Adv Mater*. 2018;30(25):e1800671. doi:10.1002/adma.201800671
218. Cui C, Fan C, Wu Y, et al. Water-triggered hyperbranched polymer universal adhesives: from strong underwater adhesion to rapid sealing hemostasis. *Adv Mater*. 2019;31(49):e1905761. doi:10.1002/adma.201905761
219. Afewerki S, Wang X, Ruiz-Esparza GU, et al. Combined catalysis for engineering bioinspired, lignin-based, long-lasting, adhesive, self-mending, antimicrobial hydrogels. *ACS Nano*. 2020;14(12):17004–17017. doi:10.1021/acsnano.0c06346
220. Oun AA, Shankar S, Rhim J-W. Multifunctional nanocellulose/metal and metal oxide nanoparticle hybrid nanomaterials. *Crit Rev Food Sci Nutr*. 2020;60(3):435–460. doi:10.1080/10408398.2018.1536966
221. Kannan K, Radhika D, Sadasivuni KK, et al. Nanostructured metal oxides and its hybrids for photocatalytic and biomedical applications. *Adv Colloid Interface Sci*. 2020;281:102178. doi:10.1016/j.cis.2020.102178
222. Shi S, Wu S, Shen Y, et al. Iron oxide nanozyme suppresses intracellular Salmonella Enteritidis growth and alleviates infection in vivo. *Theranostics*. 2018;8(22):6149–6162. doi:10.7150/thno.29303
223. Ji H, Dong K, Yan Z, et al. Bacterial hyaluronidase self-triggered prodrug release for chemo-photothermal synergistic treatment of bacterial infection. *Small*. 2016;12(45):6200–6206. doi:10.1002/smll.201601729
224. Karim MN, Singh M, Weerathung P, et al. Visible-light-triggered reactive-oxygen-species-mediated antibacterial activity of peroxidase-mimic CuO nanorods. *ACS Appl Nano Mater*. 2018;1(4):1694–1704. doi:10.1021/acsnm.8b00153
225. Matter MT, Furer LA, Starsich FHL, et al. Engineering the bioactivity of flame-made ceria and ceria/bioglass hybrid nanoparticles. *ACS Appl Mater Interfaces*. 2019;11(3):2830–2839. doi:10.1021/acsnami.8b18778
226. Ma W, Zhang T, Li R, et al. Bienzymatic synergism of vanadium oxide nanodots to efficiently eradicate drug-resistant bacteria during wound healing in vivo. *J Colloid Interface Sci*. 2020;559:313–323. doi:10.1016/j.jcis.2019.09.040
227. Zhang Y, Li D, Tan J, et al. Near-infrared regulated nanozymatic/photothermal/photodynamic triple-therapy for combating multidrug-resistant bacterial infections via oxygen-vacancy molybdenum trioxide nanodots. *Small*. 2021;17(1):e2005739. doi:10.1002/smll.202005739
228. Yalcinkaya Y, Komarek K. Polyvinyl butyral (PVB) nanofiber/nanoparticle-covered yarns for antibacterial textile surfaces. *Int J Mol Sci*. 2019;20(17):4317. doi:10.3390/ijms20174317
229. Li C, Sun Y, Li X, et al. Bactericidal effects and accelerated wound healing using Tb4O7 nanoparticles with intrinsic oxidase-like activity. *J Nanobiotechnol*. 2019;17(1):54. doi:10.1186/s12951-019-0487-x
230. Zhong L, Yun K. Graphene oxide-modified ZnO particles: synthesis, characterization, and antibacterial properties. *Int J Nanomed*. 2015;10:79–92. doi:10.2147/ijn.s88319
231. Gao L, Giglio KM, Nelson JL, et al. Ferromagnetic nanoparticles with peroxidase-like activity enhance the cleavage of biological macromolecules for biofilm elimination. *Nanoscale*. 2014;6(5):2588–2593. doi:10.1039/c3nr05422e
232. Velema WA, van der Berg JP, Hansen MJ, et al. Optical control of antibacterial activity. *Nat Chem*. 2013;5(11):924–928. doi:10.1038/nchem.1750
233. Jiang D, Ni D, Rosenkrans ZT, et al. Nanozyme: new horizons for responsive biomedical applications. *Chem Soc Rev*. 2019;48(14):3683–3704. doi:10.1039/c8cs00718g
234. Stefan L, Denat F, Monchaud D. Insights into how nucleotide supplements enhance the peroxidase-mimicking DNAzyme activity of the G-quadruplex/hemin system. *Nucleic Acids Res*. 2012;40(17):8759–8772. doi:10.1093/nar/gks581
235. Vallabani NVS, Vinu A, Singh S, et al. Tuning the ATP-triggered pro-oxidant activity of iron oxide-based nanozyme towards an efficient antibacterial strategy. *J Colloid Interface Sci*. 2020;567:154–164. doi:10.1016/j.jcis.2020.01.099
236. Roy I, Shetty D, Hota R, et al. A multifunctional subphthalocyanine nanosphere for targeting, labeling, and killing of antibiotic-resistant bacteria. *Angewandte Chemie*. 2015;54(50):15152–15155. doi:10.1002/anie.201507140
237. Zhang Y, Wang F, Liu C, et al. Nanozyme decorated metal–organic frameworks for enhanced photodynamic therapy. *ACS Nano*. 2018;12(1):651–661. doi:10.1021/acsnano.7b07746
238. Xu J-W, Yao K, Xu Z-K. Nanomaterials with a photothermal effect for antibacterial activities: an overview. *Nanoscale*. 2019;11(18):8680–8691. doi:10.1039/c9nr01833f
239. Xu Z, Lu J, Zheng X, et al. A critical review on the applications and potential risks of emerging MoS<sub>2</sub> nanomaterials. *J Hazard Mater*. 2020;399:123057. doi:10.1016/j.jhazmat.2020.123057
240. Xu J, Cai R, Zhang Y, et al. Molybdenum disulfide-based materials with enzyme-like characteristics for biological applications. *Colloids Surf B Biointerfaces*. 2021;200:111575. doi:10.1016/j.colsurfb.2021.111575
241. Xu Z, Qiu Z, Liu Q, et al. Converting organosulfur compounds to inorganic polysulfides against resistant bacterial infections. *Nat Commun*. 2018;9(1):3713. doi:10.1038/s41467-018-06164-7
242. Feng Z, Liu X, Tan L, et al. Electrophoretic deposited stable Chitosan@MoS<sub>2</sub> coating with rapid in situ bacteria-killing ability under dual-light irradiation. *Small*. 2018;14(21):e1704347. doi:10.1002/smll.201704347
243. Liao Z-Y, Xia Y-M, Zuo J-M, et al. Metal–organic framework modified MoS<sub>2</sub> nanozyme for synergetic combating drug-resistant bacterial infections via photothermal effect and photodynamic modulated peroxidase-mimic activity. *Adv Healthc Mater*. 2022;11(1):e2101698. doi:10.1002/adhm.202101698
244. Lee K, Mazare A, Schmuki P. One-dimensional titanium dioxide nanomaterials: nanotubes. *Chem Rev*. 2014;114(19):9385–9454. doi:10.1021/cr500061m
245. Li Y, Fu R, Duan Z, et al. Construction of multifunctional hydrogel based on the tannic acid-metal coating decorated MoS<sub>2</sub> dual nanozyme for bacteria-infected wound healing. *Bioact Mater*. 2022;9:461–474. doi:10.1016/j.bioactmat.2021.07.023
246. Cao F, Zhang L, Wang H, et al. Defect-rich adhesive nanozymes as efficient antibiotics for enhanced bacterial inhibition. *Angewandte Chemie*. 2019;58(45):16236–16242. doi:10.1002/anie.201908289
247. Wang T, Zhang X, Mei L, et al. A two-step gas/liquid strategy for the production of N-doped defect-rich transition metal dichalcogenide nanosheets and their antibacterial applications. *Nanoscale*. 2020;12(15):8415–8424. doi:10.1039/d0nr00192a
248. Bhatwalkar SB, Mondal R, Krishna SBN, et al. Antibacterial properties of organosulfur compounds of garlic (*Allium sativum*). *Front Microbiol*. 2021;12:613077. doi:10.1111/j.1742-481X.2011.00903.x
249. Nain A, Wei SC, Lin YF, et al. Copper sulfide nanoassemblies for catalytic and photoresponsive eradication of bacteria from infected wounds. *ACS Appl Mater Interfaces*. 2021;13(7):7865–7878. doi:10.1021/acsnami.0c18999



250. Han H, Yang J, Li X, et al. Shining light on transition metal sulfides: new choices as highly efficient antibacterial agents. *Nano Res.* **2021**;14:2512–2534. doi:10.1007/s12274-021-3293-3
251. Lopez-Cantu DO, González-González RB, Melchor-Martínez EM, et al. Enzyme-mimicking capacities of carbon-dots nanozymes: properties, catalytic mechanism, and applications - a review. *Int J Biol Macromol.* **2022**;194:676–687. doi:10.1016/j.ijbiomac.2021.11.112
252. Zhang Q, He X, Han A, et al. Artificial hydrolase based on carbon nanotubes conjugated with peptides. *Nanoscale.* **2016**;8(38):16851–16856. doi:10.1039/c6nr05015h
253. Sun H, Zhou Y, Ren J, et al. Carbon nanozymes: enzymatic properties, catalytic mechanism, and applications. *Angewandte Chemie.* **2018**;57(30):9224–9237. doi:10.1002/anie.201712469
254. Dong X, Liang W, Mezziani MJ, et al. Carbon dots as potent antimicrobial agents. *Theranostics.* **2020**;10(2):671–686. doi:10.7150/thno.39863
255. Maruthapandi M, Saravanan A, Das P, et al. Microbial inhibition and biosensing with multifunctional carbon dots: progress and perspectives. *Biotechnol Adv.* **2021**;53:107843. doi:10.1016/j.biotechadv.2021.107843
256. Gao Z, Zhao CX, Li YY, et al. Beer yeast-derived fluorescent carbon dots for photoinduced bactericidal functions and multicolor imaging of bacteria. *Appl Microbiol Biotechnol.* **2019**;103(11):4585–4593. doi:10.1007/s00253-019-09782-3
257. Gao Z, Yang D, Wan Y, et al. One-step synthesis of carbon dots for selective bacterial inactivation and bacterial differentiation. *Anal Bioanal Chem.* **2020**;412(4):871–880. doi:10.1007/s00216-019-02293-0
258. Qian Z, Shan X, Chai L, et al. Si-doped carbon quantum dots: a facile and general preparation strategy, bioimaging application, and multifunctional sensor. *ACS Appl Mater Interfaces.* **2014**;6(9):6797–6805. doi:10.1021/am500403n
259. Zhu D, Zhang M, Pu L, et al. Nitrogen-enriched conjugated polymer enabled metal-free carbon nanozymes with efficient oxidase-like activity. *Small.* **2022**;18(3):e2104993. doi:10.1002/smll.202104993
260. Zhang J, Lu X, Tang D, et al. Phosphorescent carbon dots for highly efficient oxygen photosensitization and as photo-oxidative nanozymes. *ACS Appl Mater Interfaces.* **2018**;10(47):40808–40814. doi:10.1021/acsami.8b15318
261. Tammina SK, Wan Y, Li Y, et al. Synthesis of N, Zn-doped carbon dots for the detection of Fe(3+) ions and bactericidal activity against Escherichia coli and Staphylococcus aureus. *J Photochem Photobiol B.* **2020**;202:111734. doi:10.1016/j.jphotobiol.2019.111734
262. Xi J, Wei G, Wu Q, et al. Light-enhanced sponge-like carbon nanozyme used for synergetic antibacterial therapy. *Biomater Sci.* **2019**;7(10):4131–4141. doi:10.1039/c9bm00705a
263. Huo M, Wang L, Zhang H, et al. Construction of single-iron-atom nanocatalysts for highly efficient catalytic antibiotics. *Small.* **2019**;15(31):e1901834. doi:10.1002/smll.201901834
264. Wang X, Lu Y, Hua K, et al. Iodine-doped carbon dots with inherent peroxidase catalytic activity for photocatalytic antibacterial and wound disinfection. *Anal Bioanal Chem.* **2021**;413(5):1373–1382. doi:10.1007/s00216-020-03100-x
265. Wang X, Shi Q, Zha Z, et al. Copper single-atom catalysts with photothermal performance and enhanced nanozyme activity for bacteria-infected wound therapy. *Bioact Mater.* **2021**;6(12):4389–4401. doi:10.1016/j.bioactmat.2021.04.024
266. Feng Y, Qin J, Zhou Y, et al. Spherical mesoporous Fe-N-C single-atom nanozyme for photothermal and catalytic synergistic antibacterial therapy. *J Colloid Interface Sci.* **2022**;606(Pt 1):826–836. doi:10.1016/j.jcis.2021.08.054
267. Mocan T, Matea CT, Pop T, et al. Carbon nanotubes as anti-bacterial agents. *Cell Mol Life Sci.* **2017**;74(19):3467–3479. doi:10.1007/s00018-017-2532-y
268. Wang H, Li P, Yu D, et al. Unraveling the enzymatic activity of oxygenated carbon nanotubes and their application in the treatment of bacterial infections. *Nano Lett.* **2018**;18(6):3344–3351. doi:10.1021/acs.nanolett.7b05095
269. Zou X, Zhang L, Wang Z, et al. Mechanisms of the antimicrobial activities of graphene materials. *J Am Chem Soc.* **2016**;138(7):2064–2077. doi:10.1021/jacs.5b11411
270. Palmieri V, Perini G, De Spirito M, et al. Graphene oxide touches blood: in vivo interactions of bio-coronated 2D materials. *Nanoscale Horizons.* **2019**;4(2):273–290. doi:10.1039/c8nh00318a
271. Anand A, Unnikrishnan B, Wei SC, et al. Graphene oxide and carbon dots as broad-spectrum antimicrobial agents - a minireview. *Nanoscale Horizons.* **2019**;4(1):117–137. doi:10.1039/c8nh00174j
272. Sun H, Gao N, Dong K, et al. Graphene quantum dots-band-aids used for wound disinfection. *ACS nano.* **2014**;8(6):6202–6210. doi:10.1021/nn501640q
273. Mei L, Gao X, Shi Y, et al. Augmented graphene quantum dot-light irradiation therapy for bacteria-infected wounds. *ACS Appl Mater Interfaces.* **2020**;12(36):40153–40162. doi:10.1021/acsami.0c13237
274. Hui L, Huang J, Chen G, et al. Antibacterial property of graphene quantum dots (both source material and bacterial shape matter). *ACS Appl Mater Interfaces.* **2016**;8(1):20–25. doi:10.1021/acsami.5b10132
275. Mei L, Shi Y, Miao Z, et al. Photo-initiated enhanced antibacterial therapy using a non-covalent functionalized graphene oxide nanoplateform. *Dalton Transact.* **2021**;50(24):8404–8412. doi:10.1039/d1dt00642h
276. Li B, Wen HM, Cui Y, et al. Emerging multifunctional metal-organic framework materials. *Adv Mater.* **2016**;28(40):8819–8860. doi:10.1002/adma.201601133
277. Wang Y, Zhao M, Ping J, et al. Bioinspired design of ultrathin 2d bimetallic metal-organic-framework nanosheets used as biomimetic enzymes. *Adv Mater.* **2016**;28(21):4149–4155. doi:10.1002/adma.201600108
278. Zhou HC, Long JR, Yaghi OM. Introduction to metal-organic frameworks. *Chem Rev.* **2012**;112(2):673–674. doi:10.1021/cr300014x
279. Nong W, Wu J, Ghiladi RA, et al. The structural appeal of metal-organic frameworks in antimicrobial applications. *Coord Chem Rev.* **2021**;442:214007. doi:10.1016/j.ccr.2021.214007
280. He L, Liu Y, Liu J, et al. Core-shell noble-metal@metal-organic-framework nanoparticles with highly selective sensing property. *Angewandte Chemie.* **2013**;52(13):3741–3745. doi:10.1002/anie.201209903
281. Lian X, Fang Y, Joseph E, et al. Enzyme-MOF (metal-organic framework) composites. *Chem Soc Rev.* **2017**;46(11):3386–3401. doi:10.1039/c7cs00058h
282. Quan Y, Song Y, Shi W, et al. Metal-organic framework with dual active sites in engineered mesopores for bioinspired synergistic catalysis. *J Am Chem Soc.* **2020**;142(19):8602–8607. doi:10.1021/jacs.0c02966
283. Qian Q, Asinger PA, Lee MJ, et al. MOF-based membranes for gas separations. *Chem Rev.* **2020**;120(16):8161–8266. doi:10.1021/acs.chemrev.0c00119

284. Zeng MH, Yin Z, Tan YX, et al. Nanoporous cobalt(II) MOF exhibiting four magnetic ground states and changes in gas sorption upon post-synthetic modification. *J Am Chem Soc.* 2014;136(12):4680–4688. doi:10.1021/ja500191r
285. Kitagawa S, Kitaura R, Noro S. Functional porous coordination polymers. *Angewandte Chemie.* 2004;43(18):2334–2375. doi:10.1002/anie.200300610
286. Lin S, Liu X, Tan L, et al. Porous iron-carboxylate metal-organic framework: a novel bioplatfrom with sustained antibacterial efficacy and nontoxicity. *ACS Appl Mater Interfaces.* 2017;9(22):19248–19257. doi:10.1021/acsami.7b04810
287. Cai W, Wang J, Chu C, et al. Metal-organic framework-based stimuli-responsive systems for drug delivery. *Adv Sci.* 2019;6(1):1801526. doi:10.1002/advs.201801526
288. Zhang Y, Sun P, Zhang L, et al. Silver-infused porphyrinic metal-organic framework: surface-adaptive, on-demand nanoplatfrom for synergistic bacteria killing and wound disinfection. *Adv Funct Mater.* 2019;29(11):1808594. doi:10.1002/adfm.201808594
289. Gong M, Xiao S, Yu X, et al. Research progress of photocatalytic sterilization over semiconductors. *RSC Adv.* 2019;9(34):19278–19284. doi:10.1039/c9ra01826c
290. Zhao X-L, Sun W-Y. The organic ligands with mixed N-/O-donors used in construction of functional metal-organic frameworks. *Crystengcomm.* 2014;16(16):3247–3258. doi:10.1039/c3ce41791c
291. Abednatanzi S, Derakhshandeh PG, Depauw H, et al. Mixed-metal metal-organic frameworks. *Chem Soc Rev.* 2019;48(9):2535–2565. doi:10.1039/c8cs00337h
292. Yang Q, Xu Q, Jiang H-L. Metal-organic frameworks meet metal nanoparticles: synergistic effect for enhanced catalysis. *Chem Soc Rev.* 2017;46(15):4774–4808. doi:10.1039/c6cs00724d
293. Liang S, Wu X-L, Xiong J, et al. Metal-organic frameworks as novel matrices for efficient enzyme immobilization: an update review. *Coord Chem Rev.* 2020;406:213149. doi:10.1016/j.ccr.2019.213149
294. Chen S, Lu J, You T, et al. Metal-organic frameworks for improving wound healing. *Coord Chem Rev.* 2021;439:213929. doi:10.1016/j.ccr.2021.213929
295. Mao D, Hu F, Kong D, Liu B. Metal-organic-framework-assisted in vivo bacterial metabolic labeling and precise antibacterial therapy. *Adv Mater.* 2018;30(18):e1706831. doi:10.1002/adma.201706831
296. Huang S, Kou X, Shen J, et al. "Armor-plating" enzymes with metal-organic frameworks (MOFs). *Angewandte Chemie.* 2020;59(23):8786–8798. doi:10.1002/anie.201916474
297. Liang W, Wied P, Carraro F, et al. Metal-organic framework-based enzyme biocomposites. *Chem Rev.* 2021;121(3):1077–1129. doi:10.1021/acs.chemrev.0c01029
298. Zhao XD, Zheng MQ, Gao XL, et al. The application of MOFs-based materials for antibacterials adsorption. *Coord Chem Rev.* 2021;440:213970. doi:10.1016/j.ccr.2021.213970
299. Li T, Qiu H, Liu N, et al. Construction of self-activated cascade metal-organic framework/enzyme hybrid nanoreactors as antibacterial agents. *Colloids Surf B Biointerfaces.* 2020;191:111001. doi:10.1016/j.colsurfb.2020.111001
300. Li T, Li J, Pang Q, et al. Construction of microreactors for cascade reaction and their potential applications as antibacterial agents. *ACS Appl Mater Interfaces.* 2019;11(7):6789–6795. doi:10.1021/acsami.8b20069
301. Huo M, Wang L, Chen Y, et al. Tumor-selective catalytic nanomedicine by nanocatalyst delivery. *Nat Commun.* 2017;8(1):357. doi:10.1038/s41467-017-00424-8
302. Jo SM, Wurm FR, Landfester K. Biomimetic cascade network between interactive multicompartments organized by enzyme-loaded silica nanoreactors. *ACS Appl Mater Interfaces.* 2018;10(40):34230–34237. doi:10.1021/acsami.8b11198
303. Giannakopoulou A, Gkantzou E, Polydera A, et al. Multienzymatic nanoassemblies: recent progress and applications. *Trends Biotechnol.* 2020;38(2):202–216. doi:10.1016/j.tibtech.2019.07.010
304. Cheng X, Zhang S, Liu H, et al. Biomimetic metal-organic framework composite-mediated cascade catalysis for synergistic bacteria killing. *ACS Appl Mater Interfaces.* 2020;12(33):36996–37005. doi:10.1021/acsami.0c12159
305. Calderón M, Quadri MA, Sharma SK, et al. Dendritic polyglycerols for biomedical applications. *Adv Mater.* 2010;22(2):190–218. doi:10.1002/adma.200902144
306. Bayne L, Ulijn RV, Halling PJ. Effect of pore size on the performance of immobilised enzymes. *Chem Soc Rev.* 2013;42(23):9000–9010. doi:10.1039/c3cs60270b
307. Wang C, Liao K. Recent advances in emerging metal- and covalent-organic frameworks for enzyme encapsulation. *ACS Appl Mater Interfaces.* 2021;13(48):56752–56776. doi:10.1021/acsami.1c13408
308. Pettinari C, Pettinari R, Di Nicola C, et al. Antimicrobial MOFs. *Coord Chem Rev.* 2021;446:214121. doi:10.1016/j.ccr.2021.214121
309. Dutta P, Wang B. Zeolite-supported silver as antimicrobial agents. *Coord Chem Rev.* 2019;383:1–29. doi:10.1016/j.ccr.2018.12.014
310. Hu WC, Younis MR, Zhou Y, et al. In situ fabrication of ultrasmall gold nanoparticles/2D MOFs hybrid as nanozyme for antibacterial therapy. *Small.* 2020;16(23):2000553. doi:10.1002/sml.202000553
311. Kuru E, Tekkam S, Hall E, et al. Synthesis of fluorescent D-amino acids and their use for probing peptidoglycan synthesis and bacterial growth in situ. *Nat Protoc.* 2015;10(1):33–52. doi:10.1038/nprot.2014.197
312. Wang X, Sun X, Bu T, et al. Construction of a photothermal hydrogel platform with two-dimensional PEG@zirconium-ferrocene MOF nanozymes for rapid tissue repair of bacteria-infected wounds. *Acta biomaterialia.* 2021;135:342–355. doi:10.1016/j.actbio.2021.08.022
313. Chen Y, Gao Y, Chen Y, et al. Nanomaterials-based photothermal therapy and its potentials in antibacterial treatment. *J Control Release.* 2020;328:251–262. doi:10.1016/j.jconrel.2020.08.055
314. Harada LK, Silva EC, Campos WF, et al. Biotechnological applications of bacteriophages: state of the art. *Microbiol Res.* 2018;212:38–58. doi:10.1016/j.micres.2018.04.007
315. Yang Y, Wu X, Ma L, et al. Bioinspired spiky peroxidase-mimics for localized bacterial capture and synergistic catalytic sterilization. *Adv Mater.* 2021;33(8):e2005477. doi:10.1002/adma.202005477
316. Yang B, Chen Y, Shi J. Nanocatalytic medicine. *Adv Mater.* 2019;31(39):e1901778. doi:10.1002/adma.201901778
317. Chen G, Huang S, Kou X, et al. Embedding functional biomacromolecules within peptide-directed Metal-Organic Framework (MOF) nanoarchitectures enables activity enhancement. *Angewandte Chemie.* 2020;59(33):13947–13954. doi:10.1002/anie.202005529

318. Liu D, Wan J, Pang G, et al. Hollow metal-organic-framework micro/nanostructures and their derivatives: emerging multifunctional materials. *Adv Mater.* 2019;31(38):e1803291. doi:10.1002/adma.201803291
319. Tang C, Jiao Y, Shi B, et al. Coordination tunes selectivity: two-electron oxygen reduction on high-loading molybdenum single-atom catalysts. *Angewandte Chemie.* 2020;59(23):9171–9176. doi:10.1002/anie.202003842
320. Zhang H, Lu XF, Wu ZP, et al. Emerging multifunctional single-atom catalysts/nanozymes. *ACS Cent Sci.* 2020;6(8):1288–1301. doi:10.1021/acscentsci.0c00512
321. Zhang XL, Li GL, Chen G, et al. Single-atom nanozymes: a rising star for biosensing and biomedicine. *Coord Chem Rev.* 2020;418:213376. doi:10.1016/j.ccr.2020.213376
322. Huang L, Chen J, Gan L, et al. Single-atom nanozymes. *Sci Adv.* 2019;5(5):eaav5490. doi:10.1126/sciadv.aav5490
323. Jiao L, Yan H, Wu Y, et al. When nanozymes meet single-atom catalysis. *Angewandte Chemie.* 2020;59(7):2565–2576. doi:10.1002/anie.201905645
324. Jagadeesh RV, Murugesan K, Alshammari AS, et al. MOF-derived cobalt nanoparticles catalyze a general synthesis of amines. *Science.* 2017;358(6361):326–332. doi:10.1126/science.aan6245
325. Wang X, Sun XY, Bu T, et al. In situ fabrication of metal-organic framework derived hybrid nanozymes for enhanced nanozyme-photothermal therapy of bacteria-infected wounds. *Composites Part B.* 2022;229:109465. doi:10.1016/j.compositesb.2021.109465
326. Huang Y, Ren J, Qu X. Nanozymes: classification, catalytic mechanisms, activity regulation, and applications. *Chem Rev.* 2019;119(6):4357–4412. doi:10.1021/acs.chemrev.8b00672
327. Zhang F, Liu Y, Lei J, et al. Metal-organic-framework-derived carbon nanostructures for site-specific dual-modality photothermal/photodynamic thrombus therapy. *Adv Sci.* 2019;6(17):1901378. doi:10.1002/advs.201901378
328. Fan X, Yang F, Huang J, et al. Metal-organic-framework-derived 2D carbon nanosheets for localized multiple bacterial eradication and augmented anti-infective therapy. *Nano Lett.* 2019;19(9):5885–5896. doi:10.1021/acs.nanolett.9b01400
329. Marpaung F, Kim M, Khan JH, et al. Metal-Organic Framework (MOF)-derived nanoporous carbon materials. *Chem Asian J.* 2019;14(9):1331–1343. doi:10.1002/asia.201900026
330. Mai HD, Rafiq K, Yoo H. Nano metal-organic framework-derived inorganic hybrid nanomaterials: synthetic strategies and applications. *Chemistry.* 2017;23(24):5631–5651. doi:10.1002/chem.201604703
331. Zou L, Sun Y, Che S, et al. Porous organic polymers for post-combustion carbon capture. *Adv Mater.* 2017;29(37):1700229. doi:10.1002/adma.201700229
332. Wang X, Chen L, Chong SY, et al. Sulfone-containing covalent organic frameworks for photocatalytic hydrogen evolution from water. *Nat Chem.* 2018;10(12):1180–1189. doi:10.1038/s41557-018-0141-5
333. Sun Q, Fu CW, Aguila B, et al. Pore environment control and enhanced performance of enzymes infiltrated in covalent organic frameworks. *J Am Chem Soc.* 2018;140(3):984–992. doi:10.1021/jacs.7b10642
334. Esrafil A, Wagner A, Inamdar S, et al. Covalent organic frameworks for biomedical applications. *Adv Healthc Mater.* 2021;10(6):e2002090. doi:10.1002/adhm.202002090
335. Wuest JD. Engineering crystals by the strategy of molecular tectonics. *Chem Commun.* 2005;47(47):5830–5837. doi:10.1039/b512641j
336. Chakrabarty R, Mukherjee PS, Stang PJ. Supramolecular coordination: self-assembly of finite two- and three-dimensional ensembles. *Chem Rev.* 2011;111(11):6810–6918. doi:10.1021/cr200077m
337. Li D, Fang Y, Zhang X. Bacterial detection and elimination using a dual-functional porphyrin-based porous organic polymer with peroxidase-like and high near-infrared-light-enhanced antibacterial activity. *ACS Appl Mater Interfaces.* 2020;12(8):8989–8999. doi:10.1021/acscami.9b20102
338. Rengaraj A, Puthiaraj P, Haldorai Y, et al. Porous covalent triazine polymer as a potential nanocargo for cancer therapy and imaging. *ACS Appl Mater Interfaces.* 2016;8(14):8947–8955. doi:10.1021/acscami.6b00284
339. Zhang L, Wang S, Zhou Y, et al. Covalent organic frameworks as favorable constructs for photodynamic therapy. *Angewandte Chemie.* 2019;58(40):14213–14218. doi:10.1002/anie.201909020
340. Xiong Y, Liao Q, Huang Z, et al. Ultrahigh responsivity photodetectors of 2D covalent organic frameworks integrated on graphene. *Adv Mater.* 2020;32(9):e1907242. doi:10.1002/adma.201907242
341. Zhou N, Ma Y, Hu B, et al. Construction of Ce-MOF@COF hybrid nanostructure: label-free aptasensor for the ultrasensitive detection of oxytetracycline residues in aqueous solution environments. *Biosens Bioelectron.* 2019;127:92–100. doi:10.1016/j.bios.2018.12.024
342. Spitler EL, Colson JW, Uribe-Romo FJ, et al. Lattice expansion of highly oriented 2D phthalocyanine covalent organic framework films. *Angewandte Chemie.* 2012;51(11):2623–2627. doi:10.1002/anie.201107070
343. Yang H, Du Y, Wan S, et al. Mesoporous 2D covalent organic frameworks based on shape-persistent arylene-ethynylene macrocycles. *Chem Sci.* 2015;6(7):4049–4053. doi:10.1039/c5sc00894h
344. Zhu Y, Wan S, Jin Y, et al. Desymmetrized vertex design for the synthesis of covalent organic frameworks with periodically heterogeneous pore structures. *J Am Chem Soc.* 2015;137(43):13772–13775. doi:10.1021/jacs.5b09487
345. Huang N, Zhai L, Couprie DE, et al. Multiple-component covalent organic frameworks. *Nat Commun.* 2016;7:12325. doi:10.1038/ncomms12325
346. Vyas VS, Haase F, Stegbauer L, et al. A tunable azine covalent organic framework platform for visible light-induced hydrogen generation. *Nat Commun.* 2015;6:8508. doi:10.1038/ncomms9508
347. Baldwin LA, Crowe JW, Pyles DA, et al. Metalation of a mesoporous three-dimensional covalent organic framework. *J Am Chem Soc.* 2016;138(46):15134–15137. doi:10.1021/jacs.6b10316
348. Xu F, Xu H, Chen X, et al. Radical covalent organic frameworks: a general strategy to immobilize open-accessible polyradicals for high-performance capacitive energy storage. *Angewandte Chemie.* 2015;54(23):6814–6818. doi:10.1002/anie.201501706
349. Huang N, Krishna R, Jiang D. Tailor-made pore surface engineering in covalent organic frameworks: systematic functionalization for performance screening. *J Am Chem Soc.* 2015;137(22):7079–7082. doi:10.1021/jacs.5b04300
350. El-Kaderi HM, Hunt JR, Mendoza-Cortés JL, et al. Designed synthesis of 3D covalent organic frameworks. *Science.* 2007;316(5822):268–272. doi:10.1126/science.1139915

351. Uribe-Romo FJ, Doonan CJ, Furukawa H, et al. Crystalline covalent organic frameworks with hydrazone linkages. *J Am Chem Soc.* 2011;133(30):11478–11481. doi:10.1021/ja204728y
352. Du Y, Yang H, Whiteley JM, et al. Ionic covalent organic frameworks with spiroborate linkage. *Angewandte Chemie.* 2016;55(5):1737–1741. doi:10.1002/anie.201509014
353. Waller PJ, Lyle SJ, Osborn Popp TM, et al. Chemical conversion of linkages in covalent organic frameworks. *J Am Chem Soc.* 2016;138(48):15519–15522. doi:10.1021/jacs.6b08377
354. Xu H, Gao J, Jiang D. Stable, crystalline, porous, covalent organic frameworks as a platform for chiral organocatalysts. *Nat Chem.* 2015;7(11):905–912. doi:10.1038/nchem.2352
355. Mao C, Xiang Y, Liu X, et al. Photo-inspired antibacterial activity and wound healing acceleration by hydrogel embedded with Ag/Ag@AgCl/ZnO nanostructures. *ACS nano.* 2017;11(9):9010–9021. doi:10.1021/acsnano.7b03513
356. Wang D, Niu L, Qiao ZY, et al. Synthesis of self-assembled porphyrin nanoparticle photosensitizers. *ACS Nano.* 2018;12(4):3796–3803. doi:10.1021/acsnano.8b01010
357. Chen L, Bai H, Xu JF, et al. Supramolecular porphyrin photosensitizers: controllable disguise and photoinduced activation of antibacterial behavior. *ACS Appl Mater Interfaces.* 2017;9(16):13950–13957. doi:10.1021/acsmi.7b02611
358. Galstyan A, Schiller R, Dobrindt U. Boronic acid functionalized photosensitizers: a strategy to target the surface of bacteria and implement active agents in polymer coatings. *Angewandte Chemie.* 2017;56(35):10362–10366. doi:10.1002/anie.201703398
359. Jia Q, Song Q, Li P, et al. Rejuvenated photodynamic therapy for bacterial infections. *Adv Healthc Mater.* 2019;8(14):e1900608. doi:10.1002/adhm.201900608
360. Yang Y, Deng D, Zhang S, et al. Porous organic frameworks featured by distinct confining fields for the selective hydrogenation of biomass-derived ketones. *Adv Mater.* 2020;32(22):e1908243. doi:10.1002/adma.201908243
361. Zhang C, Guo J, Zou X, et al. Acridine-based covalent organic framework photosensitizer with broad-spectrum light absorption for antibacterial photocatalytic therapy. *Adv Healthc Mater.* 2021;10(19):e2100775. doi:10.1002/adhm.202100775
362. Hu SC, Lan CE. High-glucose environment disturbs the physiologic functions of keratinocytes: focusing on diabetic wound healing. *J Dermatol Sci.* 2016;84(2):121–127. doi:10.1016/j.jdermsci.2016.07.008
363. Wong SL, Demers M, Martinod K, et al. Diabetes primes neutrophils to undergo NETosis, which impairs wound healing. *Nat Med.* 2015;21(7):815–819. doi:10.1038/nm.3887
364. Li Y, Wang L, Liu H, et al. Ionic covalent-organic framework nanozyme as effective cascade catalyst against bacterial wound infection. *Small.* 2021;17(32):e2100756. doi:10.1002/sml.202100756
365. Li D, Chen T, Zhang Y, et al. Synergistical starvation and chemo-dynamic therapy for combating multidrug-resistant bacteria and accelerating diabetic wound healing. *Adv Healthc Mater.* 2021;10(18):e2100716. doi:10.1002/adhm.202100716
366. Liao JJ. Molecular recognition of protein kinase binding pockets for design of potent and selective kinase inhibitors. *J Med Chem.* 2007;50(3):409–424. doi:10.1021/jm0608107
367. Sun Z, Lonsdale R, Kong XD, et al. Reshaping an enzyme binding pocket for enhanced and inverted stereoselectivity: use of smallest amino acid alphabets in directed evolution. *Angewandte Chemie.* 2015;54(42):12410–12415. doi:10.1002/anie.201501809
368. Li M, Qiao S, Zheng Y, et al. Fabricating covalent organic framework capsules with commodious microenvironment for enzymes. *J Am Chem Soc.* 2020;142(14):6675–6681. doi:10.1021/jacs.0c00285
369. Zhang L, Liu Z, Deng Q, et al. Nature-inspired construction of MOF@COF nanozyme with active sites in tailored microenvironment and pseudopodia-like surface for enhanced bacterial inhibition. *Angewandte Chemie.* 2021;60(7):3469–3474. doi:10.1002/anie.202012487
370. Ding LG, Wang S, Yao BJ, et al. Synergistic antibacterial and anti-inflammatory effects of a drug-loaded self-standing porphyrin-COF membrane for efficient skin wound healing. *Adv Healthc Mater.* 2021;10(8):e2001821. doi:10.1002/adhm.202001821
371. Liu T, Hu X, Wang Y, et al. Triazine-based covalent organic frameworks for photodynamic inactivation of bacteria as type-II photosensitizers. *J Photochem Photobiol B.* 2017;175:156–162. doi:10.1016/j.jphotobiol.2017.07.013
372. Hynek J, Zelenka J, Rathouský J, et al. Designing porphyrinic covalent organic frameworks for the photodynamic inactivation of bacteria. *ACS Appl Mater Interfaces.* 2018;10(10):8527–8535. doi:10.1021/acsmi.7b19835
373. Li C, Chen C, Zhao J, et al. Electrospun fibrous membrane containing a cyclodextrin covalent organic framework with antibacterial properties for accelerating wound healing. *ACS Biomater Sci Eng.* 2021;7(8):3898–3907. doi:10.1021/acsbmaterials.1c00648
374. Meng FL, Qian HL, Yan XP. Conjugation-regulating synthesis of high photosensitizing activity porphyrin-based covalent organic frameworks for photodynamic inactivation of bacteria. *Talanta.* 2021;233:122536. doi:10.1016/j.talanta.2021.122536
375. Liao ZY, Xia YM, Zuo JM, et al. Metal-organic framework modified MoS<sub>2</sub> nanozyme for synergetic combating drug-resistant bacterial infections via photothermal effect and photodynamic modulated peroxidase-mimic activity. *Adv Healthcare Mater.* 2022;11(1):e2101698. doi:10.1002/adhm.202101698

International Journal of Nanomedicine

Dovepress

Publish your work in this journal

The International Journal of Nanomedicine is an international, peer-reviewed journal focusing on the application of nanotechnology in diagnostics, therapeutics, and drug delivery systems throughout the biomedical field. This journal is indexed on PubMed Central, MedLine, CAS, SciSearch®, Current Contents®/Clinical Medicine, Journal Citation Reports/Science Edition, EMBase, Scopus and the Elsevier Bibliographic databases. The manuscript management system is completely online and includes a very quick and fair peer-review system, which is all easy to use. Visit <http://www.dovepress.com/testimonials.php> to read real quotes from published authors.

Submit your manuscript here: <https://www.dovepress.com/international-journal-of-nanomedicine-journal>